CHARACTERIZING THE WEATHER BAND VARIABILITY OF THE TEXAS COASTAL CURRENT

A Thesis

by

HEATHER M. ZIMMERLE

Submitted to the Office of Graduate and Professional Studies of
Texas A&M University
in partial fulfillment of the requirements for the degree of

MASTER OF SCIENCE

Chair of Committee,	Steven F. DiMarco
Committee Members,	Norman L. Guinasso, Jr.
	Courtney Schumacher
Head of Department,	Debbie Thomas

August 2014

Major Subject: Oceanography

ABSTRACT

Current velocities from 21 years (1992-2012) of near-continuous observations are used to investigate the Texas Coastal Current on the western Texas-Louisiana continental shelf in the northwestern Gulf of Mexico. Observations were made using the moored current meters deployed as part of the Texas Automated Buoy System (TABS) and historical current meter data. The general coastal circulation is known to be deterministic, with downcoast flow (westward) in the non-summer months (September-May) and a reversal to upcoast (eastward) flow in the summertime (June-August). This study focuses on characterizing features of the Texas Coastal Current that include the onset, frequency, magnitude, and persistence of current reversals along with the upcoast transport that occurs during reversals. The determined interannual variability of the Texas Coastal Current is imperative for understanding the surface transport of water and mitigating associated coastal hazards, including oil, harmful algal blooms, and hypoxia.

Results show the onset of the upcoast reversal during the summer with a mostly downcoast flow during the non-summer at upper Texas coastal locations. More persistent currents are observed during the non-summer in the downcoast direction within the weather band frequencies (2-15 days). Currents with longer persistence are found to be relatively slow, generally below 10 cm s^{-1}. Fast currents (> 50 cm s^{-1}) tend to be short-lived, typically lasting less than 72 hours. Maximum upcoast transport is observed along the upper coast during the summer, reaching a minimum in the winter

and fall. A relationship between the along-shore wind stress and along-shore current velocity is indicated, signaling that the Texas Coastal Current is mostly wind-driven.

Spatial variability is present along the southern Texas coast. Current flow is directed downcoast during the summer and slightly downcoast during the non-summer at buoy J, the southernmost location. Currents near the coastal bend tend to be upcoast during the non-summer and slightly downcoast during the summer. Longer persistence is observed at the southern location in the downcoast direction during the summer, with several currents lasting longer than 15 days. Maximum upcoast transport is present during the winter along the southern Texas Coast, reaching a minimum during the summer. Some evidence of a relationship between the along-shore wind stress and along-shore current flow are present, indicating some wind-driven forcing on the current flow.

Less seasonal variability is present at offshore locations. Locations on the outer shelf display a general upcoast flow regardless of season. Longer persistence is observed in the upcoast direction on the outer shelf during the summer and non-summer. Maximum upcoast transport is present during the non-summer at all offshore locations. Little correlation is found between seasonal winds and along-shore current flow, meaning mesoscale features, such as Loop Current eddies, provide offshore current forcing.

DEDICATION

This thesis is dedicated to my mom, Kathy Zimmerle, who always believed in me and never let me stop pursuing my dreams.

ACKNOWLEDGEMENTS

I would like to thank my committee chair, Dr. Steve DiMarco, and my committee members, Dr. Norman Guinasso Jr. and Dr. Courtney Schumacher, for their guidance and support throughout my research. I would like to thank Dr. DiMarco for his patience as well as for his specific guidance and advising and for helping me learn how to "love my data". I would also like to thank Dr. Guinasso for his useful comments and insightful discussions about ocean observing. Finally, I would like to thank Dr. Schumacher for her challenging comments and valuable discussions.

I would also like to thank my mom, Kathy, my sisters, Holly and Melissa, my brother, Michael, and my numerous friends who have supported me through both the ups and downs of graduate school. I cannot thank you enough for your love and encouragement. It truly has meant the world to me.

TABLE OF CONTENTS

LIST OF FIGURES

FIGURE Page

LIST OF TABLES

TABLE Page

1. INTRODUCTION

1.1 General circulation on Texas-Louisiana Shelf

The Texas-Louisiana shelf is located in the northwest quadrant of the Gulf of Mexico, extending from the Rio Grande to the Mississippi Delta and bounded by the Texas-Louisiana coastline from the north and west. The depth of the shelf increases gradually from the shore to the shelf break, with the contours remaining mostly parallel from the coastline out to the shelf break at about 200 meters depth. The width of the shelf ranges from about 100 km near the Rio Grande to more than 200 km near Cameron, Louisiana (Garrison and Martin, 1973).

Throughout the continental shelf area, the circulation flow is dominated by different forcing mechanisms at different locations. Nowlin et al. (2005) suggested that the circulation patterns on the Texas-Louisiana shelf be divided into two categories, the outer shelf (depth>50 meters) and inner shelf (depth<50 meters). While currents in the outer shelf are predominately driven by mesoscale features such as eddies, the inner shelf currents are driven by winds in the weather band (frequency band of 2-15 days). Previous studies have found that the low-frequency circulation over the inner shelf is primarily downcoast, meaning the flow moves westward from Louisiana towards Mexico, during the non-summer months (September to May) and upcoast, with the flow moving eastward from Mexico to Louisiana, during the summer months (June to August) (Cho et al., 1998; Chu et al., 2005; Cochrane and Kelly, 1986; Li et al., 1997; Smith, 1980; Wang et al., 1998). However, the frequency of frontal passages varies

throughout the year, which can result in seasonal variations in the low-frequency circulation of inner shelf currents (Chu et al., 2005).

1.2 Coastal currents

Within the inner shelf, there are two specific currents that have been documented in previous studies. Both coastal currents are shown in Figure 1. The Louisiana Coastal Current flows on the eastern part of the Texas-Louisiana shelf and is formed by buoyancy fluxes caused by the discharge of freshwater from the Mississippi and Atchafalaya Rivers mixing with the salty shelf waters (Li et al., 1996; Jarosz and Murray, 2005; Wiseman and Kelly, 1994). However, this study focuses on the other coastal current on the continental shelf, the Texas Coastal Current. Flowing along the Texas coast, the main forcing mechanism for the direction and strength of the current flow is generally driven by along-shore winds (Li et al., 1996; Zhang and Hetland, 2012). During the non-summer months, dominant winds toward the west lead to a downcoast flow (De Velasco and Winant, 1996). In the summer months, the prevailing winds shift toward the north-northeast, leading to an upcoast flow (Cochrane and Kelly, 1986; Cho et al., 1998; De Velasco and Winant, 1996; Nowlin et al., 2005; Smith, 1975; Zhang and Hetland, 2012). The flow of the coastal current can also be influenced by frontal passages and movements of air masses. These events create winds that cause a series of along-shore flow reversals to occur near the coast, particularly during the non-summer months (Smith, 1978; Wang et al., 1998; Vastano and Barron, 1994; Vastano et al., 1995).

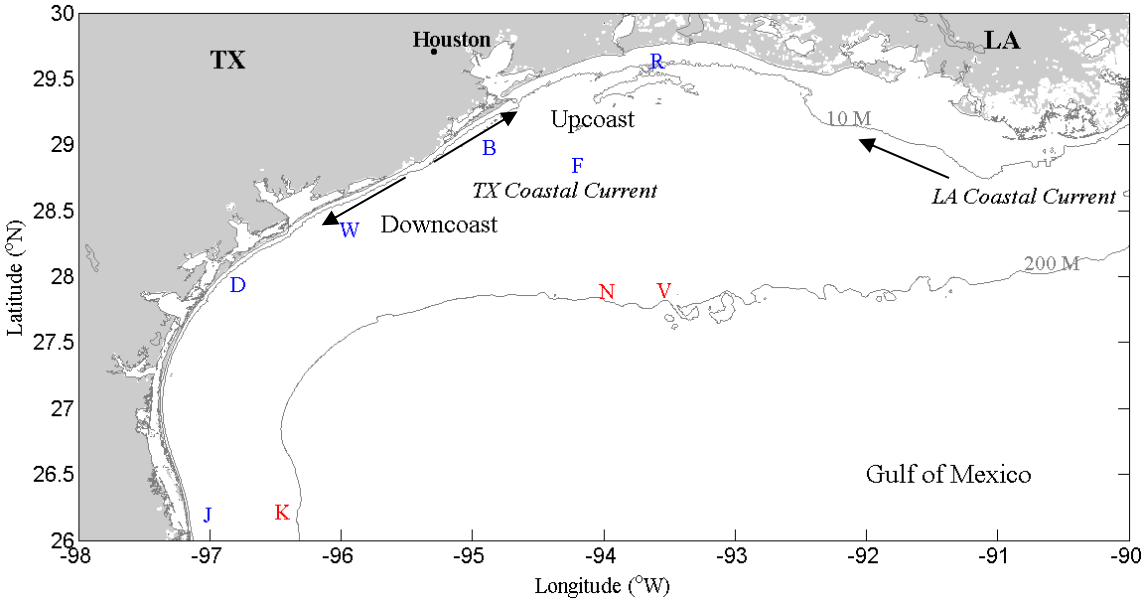

Figure 1. Map of coastal currents on Texas-Louisiana Shelf. The map shows that an upcoast reversal flows along the Texas coast to the east while a downcoast reversal flows to the west. The two known coastal currents on the shelf are also highlighted: the buoyancy-driven Louisiana Coastal Current and the wind-driven Texas Coastal Current.

1.3 Importance of study

Determining the temporal and spatial variability of the coastal current is important for understanding surface transport of water and coastal hazards, particularly oil. While the 2010 Deepwater Horizon oil spill occurred in the deep waters off the coast of Louisiana, the threat to coastal regions was considered high due to the surface transport of oil by nearshore currents into coastal bays, estuaries, and wetlands. With the high presence of oil and gas drilling platforms on the shelf, knowing the interannual variability of the Texas Coastal Current allows stakeholders (e.g. government, academia,

and industry) to make decisions regarding the mitigation of such coastal hazards (Bender et al., 2007; Walpert et al., 2011). In addition, the coastal current impacts the horizontal distribution of surface freshwater along the shelf, and therefore, influences water quality and oxygen ventilation on the Texas-Louisiana Shelf (DiMarco et al., 2012).

1.4 Study questions

The focus of this study is to characterize the seasonal variability within the weather band frequency of the Texas Coastal Current. Specifically, this study determines the interannual variability that is present within the current using moored current meters, utilizing 21 years of observations from 1992 through 2012. Different current features are assessed: the magnitude of the current velocity along with the persistence of the current flow in each direction (upcoast and downcoast), the upcoast transport that occurs during reversals in addition to the onset and frequency of current reversals.

In order to characterize the interannual variability of the Texas Coastal Current, the following questions will be evaluated:

1.4.1 Are there statistically significant seasonal differences in the frequency and duration of reversals in the Texas Coastal Current?

To determine if there are seasonal differences in current reversals, the persistence and frequency of reversals at each study site are separately quantified. Each parameter is separated into non-summer (September 1 through May 31) occurrences and summer (June 1 through August 31) occurrences for analysis to determine whether distinguishable seasonal differences between the number of reversals and the duration of the current reversals are present.

1.4.2 Are there spatial differences in the frequency and duration of reversals in the Texas Coastal Current?

The frequency and persistence of reversals at selected site locations are compared in various ways to investigate whether there are spatial differences in current reversals. Different sites along the Texas coastline are compared, including the upper Texas coast (TABS buoys R, F, B, and W) and locations off the southern Texas coast (TABS buoys D and J). In addition, coastal sites (those previously listed) will be compared to locations further offshore (TABS buoy K) and those closer to the continental shelf break (TABS buoys N and V) to determine if there are differences in current flow characteristics of nearshore observations compared to offshore observations.

2. DATA AND METHODS

2.1 Data

2.1.1 TABS data

Current meter velocity data used in this study are principally from the Texas Automated Buoy System (TABS), funded by the Texas General Land Office (TGLO) and operated and maintained by the Geochemical and Environmental Research Group (GERG). Since the system went operational in April 1995, a total of 19 buoys have been deployed through the present, as shown in Figure 2 (Walpert et al., 2011). Figure 3 shows the length of current data available from each of the 19 buoys. There are seven permanent buoy locations positioned along the coast between the Texas-Louisiana border and the United States-Mexico border. Two additional buoys (N and V) are located at the Flower Garden Banks National Marine Sanctuary and are funded by an oil industry consortium (Walpert et al., 2011). Other buoy locations were either discontinued or were funded by different government agencies (e.g. National Oceanographic Partnership Program and by the Mineral Management Service through Louisiana State University) and were only deployed for the timespan of the funded projects, but were still considered part of the TABS program (Bender et al., 2007).

Each buoy records water temperature and salinity along with five-minute vector-averaged current velocity (Kelly et al., 1998) and direction at 1.8 meters below the water surface. Data are recorded every 30 minutes and transmitted via the Globalstar satellite network back to GERG, where the data are subject to quality control before being

processed and presented on the TABS webpage (http://tabs.gerg.tamu.edu/tglo) and in real time on the National Data Buoy Center's (NDBC) website (http://ndbc.noaa.gov) through the National Oceanic and Atmospheric Administration (NOAA) (Guinasso Jr. et al., 2001; Walpert et al., 2011).

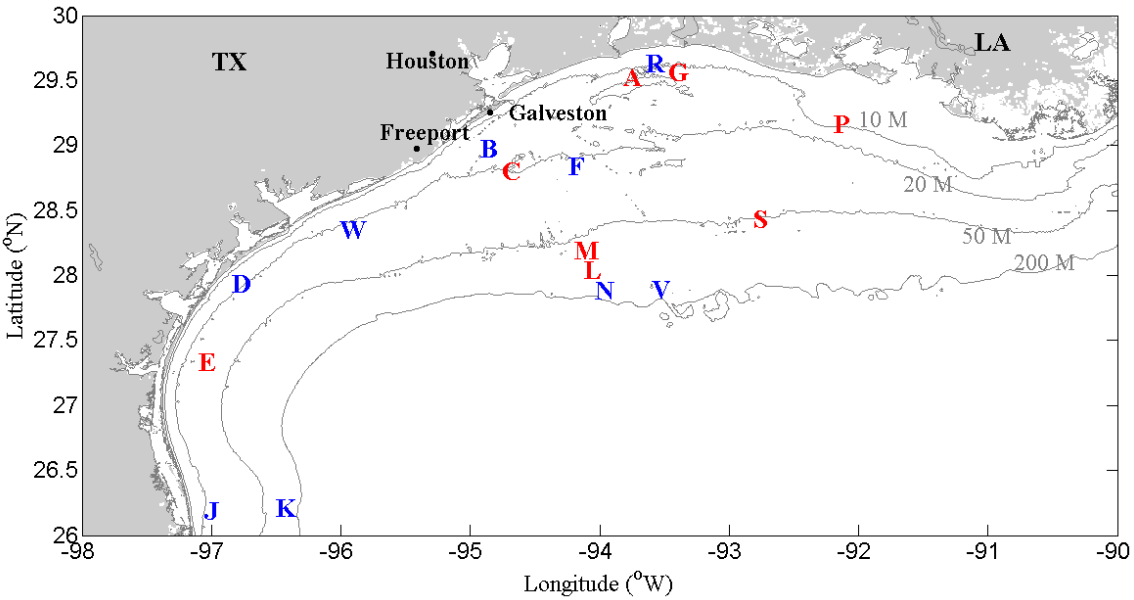

Figure 2. Basemap of TABS buoys in the Northwest Gulf of Mexico. Each of the 19 buoy locations are marked by the name of the buoy. Red letters are buoys that have been discontinued and blue letters are buoys that are currently in operation. Bathymetry lines are shown at 10 m, 20 m, 50 m, and 200 m.

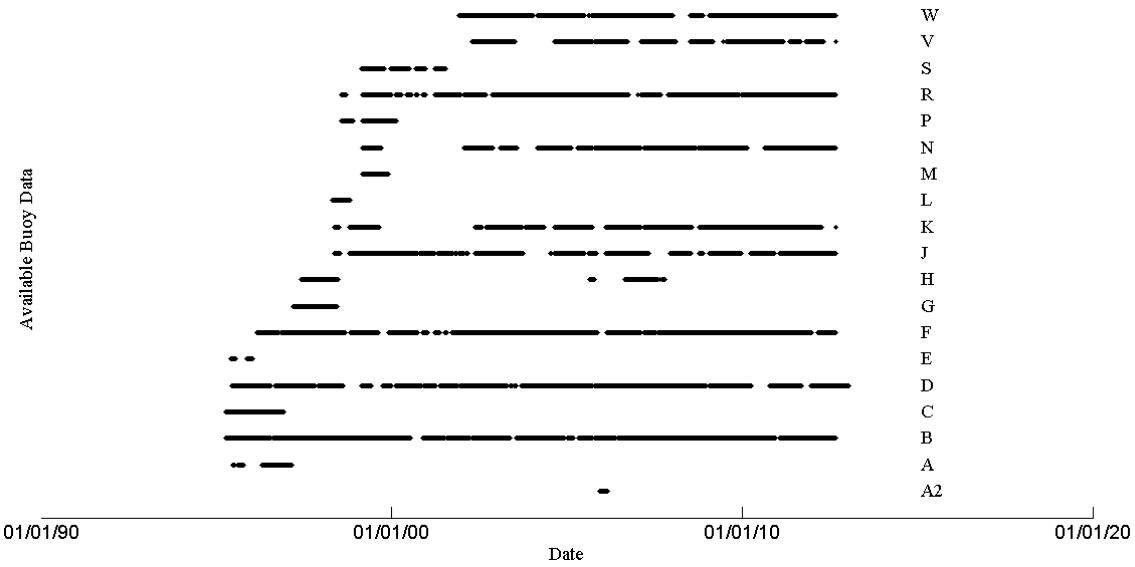

Figure 3. Data timeline for TABS buoys. The black lines in the data timeline show the available current data at each of the 19 TABS buoy locations. Space between the black lines represents gaps in the current data.

2.1.2 Historical current meter data (LATEX)

In addition to the TABS current velocity data, measurements are used from the field component of the Texas-Louisiana Shelf Circulation and Transport Process Study (LATEX), a project funded by the Minerals Management Service of the U.S. Department of the Interior (DiMarco et al., 1997). From April 1992 to December 1994, 81 current meters were placed at 31 locations on the Texas-Louisiana Shelf. Each mooring was positioned along bathymetric contours at the 10 m, 20 m, 50 m, and 200 m isobaths from Corpus Christi, TX to the Mississippi River Delta (Nowlin et al., 1998). Each mooring recorded velocity, salinity, and temperature in varying time steps, but

most were recorded in 30 minute increments (DiMarco et al., 1997). From the LATEX project, only Mooring 21 is formally used in this study because there are no gaps present in the dataset. The data from this mooring was obtained from April 13, 1992 through November 30, 1994 from a current mooring located 14 meters below the water surface. This mooring was located along the 20 m isobaths, as shown in Figure 4, and was placed close to where TABS buoy F is currently located (NOAA's National Oceanographic Data Center (NODC) Accession #9500056).

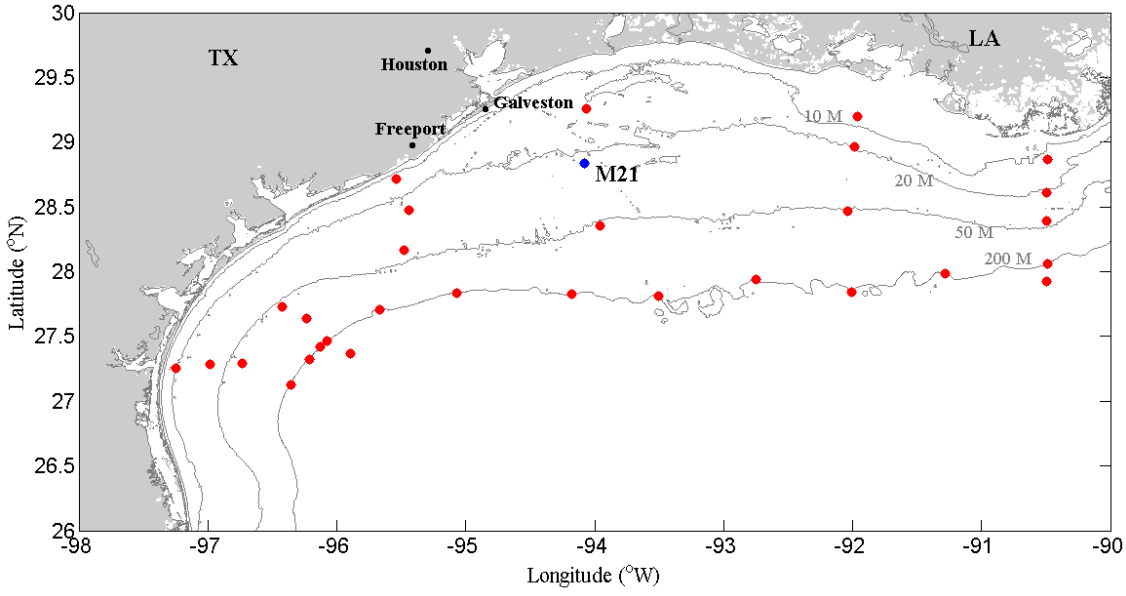

Figure 4. Basemap of LATEX moorings. The map shows the locations of all the LATEX moorings used throughout the program from 1992 to 1994. The mooring used for this study is represented by the blue dot, showing Mooring 21. The red dots indicate the other locations of LATEX moorings, but were not used during this study.

2.1.3 Wind data

Direct observations are recorded at six of the TABS buoys equipped with meteorological packages that measure wind speed and direction, along with air temperature, relative humidity, and atmospheric pressure. These parameters are recorded every half hour at 3.4 meters above the water surface on buoys B, H, J, K, N, and V (Bender et al., 2007; Walpert et al., 2011). In addition to TABS, direct wind observations are also evaluated from buoys deployed by the NDBC along the Texas coast. NDBC stations with meteorological packages collect wind speed and direction, relative humidity, atmospheric pressure as well as air and dew point temperatures among other measurements. These parameters are measured at 5 meters above the sea surface when measured on buoys and at 14.9 meters above sea level when measured at Coastal-Marine Automated Network (C-MAN) stations, located on land along the coast. The TABS meteorological data that are used in this study are from buoys B, K, and N and the NDBC station selected for use in this study is Station PTAT2, all shown on Figure 5. The PTAT2 station is located in Port Aransas, Texas and is positioned near TABS buoy D.

2.1.4 Sea surface height data

Sea surface height (SSH) anomaly is obtained from the Colorado Center for Astrodynamics Research (http://eddy.colorado.edu/ccar/ssh/hist_gom_grid_viewer). Data are compiled from Jason-1, Geosat Follow-On (GFO), ERS-2, Envisat and TOPEX/POSEIDON (T/P) satellites and height variability is calculated with the respect

to the mean according to methods presented in Leben (2005). SSH images are chosen to correspond with select persistent periods of upcoast flow at offshore locations (TABS buoys N and V) to show dominant mesoscale forcing on the current flow at the edge of the shelf.

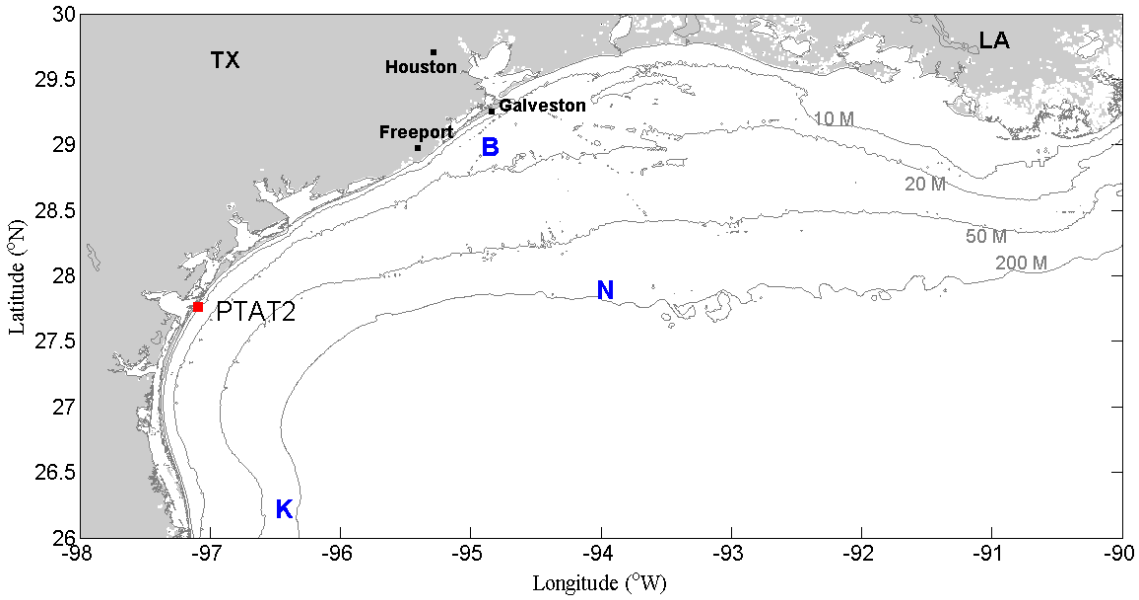

Figure 5. Basemap of wind stations. The basemap above shows locations where wind data is used during this study. TABS buoys with meteorological packages are shown in blue while the NDBC stations used are represented by red dots.

2.2 Methods

2.2.1 Definitions

2.2.1.1 Current reversal

A current reversal is defined when the along-shore velocity switches from negative to positive and crosses two designated thresholds. The thresholds are set at -1 cm s^{-1} and +1 cm s^{-1}. The along-shore velocity must cross both thresholds before it qualifies as a reversal. The current velocity is classified in terms of 40-hour low-pass data. At this location, principally diurnal tides are present (DiMarco and Reid, 1998) and the local inertial period is 24 hours (Chen et al., 1996), meaning the reversal data does not include tide and inertial oscillations.

2.2.1.2 Persistence

Persistence of a current is defined as the duration of the current flow during reversals. It is evaluated in terms of the frequency of occurrence of velocity classes along-shore for each velocity class. The current persistence is in terms of 40-hour low-pass data, meaning the persistence only includes low-frequency (non-tidal/inertial) flow.

2.2.2 Data filtering and rotation

The data used in the time series analysis are filtered using a cosine-Lanczos filter. This filter applies a weighted sine function (Duchon, 1979) to the time series current velocity data in order to obtain a 40-hour low-passed data sequence. Applying this low-frequency filter to the data removes oscillations caused by tidal and sea breeze

effects (Chu et al., 2005) as well as inertial oscillations. In addition to filtering the data, each independent time series is rotated about its principle axis specific to each time series. Rotating transforms the data into along-shore and cross-shore coordinates. This results in positive along-shore currents that flow upcoast towards Louisiana and negative along-shore currents that flow downcoast towards the United States-Mexico border. For the cross-shore components, positive currents would indicate onshore flow towards the coast while negative currents would mean offshore flow away from the coast.

2.2.3 Persistence

The quantification of persistent currents are determined and subdivided into u-velocity and duration classes. In addition, the u-velocity data are partitioned into positive and negative u-velocities in order to estimate the current persistence in upcoast and downcoast direction. Velocity classes are spaced by 5 cm s^{-1}, a value arbitrarily chosen for consistency. The velocity classes vary for each buoy, but tend to fall within the range of 0 cm s^{-1} to 95 cm s^{-1}. Fourteen duration classes are used and are spaced every 24 hours, starting at 48 hours and ending at 360 hours. This coordinates with the weather band frequencies in order to evaluate the persistence of currents on the timescale of 2-15 days. In addition, general duration statistics (e.g. duration total, maximum, mean, and standard deviation) are calculated for each velocity class.

2.2.4 Reversals

The numbers of current reversals that occur in the u-velocity are examined. Reversals are examined throughout the length of each buoy record, and divided into

seasons. Before being quantified, reversal numbers are normalized. For mean reversal numbers, data are normalized by the number of seasons with data present in order to account for records with season-wide gaps. For variance analysis, reversal numbers are normalized by the number of observations in each season and presented in terms of the number of reversals that occur per month for each season. For each reversal that occurs, the reversal start date, and general statistics (e.g. duration of reversal, maximum velocity, mean velocity, and standard deviation of velocity) are recorded for further analysis.

2.2.5 Spectra

Spectral analysis is useful in time series studies for partitioning the variance based on frequency into different spectral bands. For the current velocity, the spectral band that is of interest for this study is the weather band (2-15 day frequency). For each time series, the data are divided into seasons and normalized by the number of data points in each season. The spectral analysis is performed using the Fast Fourier Transform (FFT) (Emery and Thomson, 2001). The running mean is applied to smooth the data using a window length of 5. For spectral band amplitude comparisons, the spectral variance present in each year is summed to determine if there are seasonal differences in the weather band frequencies at different buoy locations.

2.2.6 Wavelet analysis

Wavelet analysis is used to determine how frequency powers vary locally as well as if there are seasonal frequency peaks present within each time series. The analysis

uses a wavelike structure to locate frequency peaks within the dataset. The wavelet is first scaled by certain parameters in order to adequately sample frequencies present within each time series. Two days is selected as the smallest wavelet that can be resolved. Periods of 2, 4, 8, and 16 days are selected as the scale periods. The wavelet is then transformed and convoluted in order to segment the data into different frequency ranges (Torrence and Compo, 1998). The wavelet transform shows time-frequency decomposition, displaying when frequencies peaks occur in the dataset (Pearce, 2011). The frequency peaks of interest in this study are in the weather band timescale. In order to get better resolution, each time series is divided into 2-3 segments and the wavelet analysis is performed on each segment to determine when variance occurs. Data gaps are masked out and ignored for analysis. The wavelet analysis package is used to perform wavelet transforms on the current velocity records. Torrence and Compo (1998) describe the wavelet analysis software package, which can be found at http://paos.colorado.edu/research/wavelets/. In addition, corrections are applied to the analysis package in order to rectify a bias for low-frequency data records, as discussed in Liu et al. (2007).

2.2.7 Coherency

Coherency analysis displays the correlation of spectral estimates of independent datasets. Because coherency is useful for determining if two datasets have similar spectral properties, it is suitable for analyzing whether frequency peaks are present in the current velocity at spatially close buoys (Emery and Thomson, 2001). After the velocity

data are filtered, a running mean is used in order to smooth the data, using a window length of 25. The data points within the weather band frequencies are then averaged to get an average coherency value. In order to determine if the coherence estimates are reliable, the following equation from RORY Thompson (1979) is used to find a 95% confidence level:

$$\gamma^2 = 1-\alpha^{[2/(DOF-2)]}$$

Coherency amplitudes that fall below this 95% confidence level were not analyzed. For this study, buoys that are spatially close to each other are evaluated for coherency. These include TABS buoys B and F as well as N and V. Weather band frequencies are focused on for analysis.

2.2.8 Analysis of variance

An analysis of variance, or ANOVA, is a method of testing for differences between datasets. Results from ANOVAs can be used to determine whether the amount of variability between independent datasets is due to chance or if the variability present is due to specific causes and effects (Emery and Thomson, 2001). Current velocity data from different buoys are analyzed using ANOVAs in various ways. Basic statistics are calculated for each buoy in both the upcoast and downcoast flows and input into a one-way ANOVA to determine if seasonal and/or spatial variability is present. Variability analysis in the normalized number of reversals and the duration of reversals is also performed for each season and compared between buoy locations.

2.2.9 Time series analysis

Time series analysis is beneficial for characterizing a dataset, determining patterns, and extracting important statistics. In this study, time series analysis is used for both current and wind velocity data. For each dataset selected for time series analysis, sections of data are selected that contain the fewest gaps, resulting in the analysis of data with a general timespan of 2-3 years. TABS wind data are rotated by the theta used to rotate the current velocity collected at each buoy. The PTAT2 station wind data are rotated by the theta used to rotate the current velocity collected at the TABS buoy D location. After rotation, the wind velocity data are converted into wind stress (τ), using the following equation:

$$\tau = C_D * \rho * u^2$$

where ρ is air density, C_D is a drag coefficient, and u^2 is the velocity data. The air density value used in the equation is 1.22 kg m^{-2} and .0013 is used as the drag coefficient, a dimensionless number. Wind stress is then compared to the along-shore current velocity to determine if there is a relationship between the two variables at different locations on the Texas-Louisiana shelf.

3. RESULTS

3.1 Seasonal differences

Basic statistics, as displayed in Table 1, reveal generally negative mean u-velocity values during the non-summer, indicating a downcoast flow is present. This is particularly true along the inner shelf at coastal buoy locations. A relatively strong average downcoast flow is present along the Texas-Louisiana border, with mean u-velocities of -14.7 and -14 cm s^{-1} at buoys A and R, respectively. Further west along the coast, a downcoast flow is still present, with respective mean u-velocities of -9.3, -5.2, -7.6, and -13.4 cm s^{-1} observed at buoys F, C, B, and W. Along the bend in the Texas coast, an upcoast flow is found, with mean u-velocities of 1.1 and 5.2 cm s^{-1} at buoys D and E, respectively. Near the southern Texas coast, negative mean u-velocities indicate a downcoast flow is present, with a mean of -2.9 cm s^{-1} recorded at buoy J. On the southern outer shelf, a downcoast flow is still present, with a mean u-velocity of -1.9 cm s^{-1} at buoy K. On the outer shelf, an upcoast flow is observed, with positive u-velocity means of 1.1, 9.4, and 6.4 cm s^{-1} recorded at buoys M, N, and V. Figure 6 shows the overall flow trends on the Texas-Louisiana Shelf during the non-summer, with a downcoast flow present along most of the inner shelf and an upcoast flow observed on the outer shelf.

Table 1. Basic statistics for TABS buoys by seasons.

Winter

Buoy	Latitude	Longitude	U_{mean}	V_{mean}	U_{STD}	V_{STD}	U_{max}	V_{max}	U_{max}	V_{max}	$Speed_{max}$	$Speed_{mean}$	$Velocity_{mean}$
	°N	°W	cm/s	cm/s	cm/s	cm/s	cm/s	cm/s	cm/s	cm/s	cm/s	cm/s	cm/s
							Upcoast		Downcoast				
A	29.5325	93.8122	-16.5	-17.7	20.6	18.1	55.4	25.3	68.9	79.5	102.0	31.4	24.2
B	28.9818	94.9186	-6.7	-15.2	14.4	23.7	78.3	95.0	87.2	99.8	107.7	27.0	16.6
C	28.8092	94.7521	1.5	-3.4	6.0	6.7	23.9	11.8	21.0	36.0	41.6	7.8	3.7
D	27.9396	96.8429	2.1	-18.7	6.2	26.0	42.8	82.1	55.6	77.5	84.0	27.7	18.8
E	27.3383	97.1	12.7	-4.2	20.7	13.8	61.0	34.4	35.9	36.9	70.2	22.7	13.4
F	28.8425	94.2416	-8.1	-3.8	12.1	7.3	48.4	20.4	71.0	38.7	78.4	13.3	8.9
G	29.5664	93.4683	-3.3	2.6	8.3	9.5	14.6	26.3	26.8	22.3	31.1	11.6	4.2
J	26.1914	97.0507	8.1	0.8	25.7	11.7	99.0	50.2	71.2	88.6	101.7	24.2	8.1
K	26.2168	96.4998	-1.5	1.8	15.6	12.1	60.2	51.4	51.5	44.8	66.1	16.5	2.3
L	28.0417	94.1167											
M	28.1921	94.1914											
N	27.8903	94.0367	7.7	-1.3	16.5	9.6	74.2	33.5	58.5	39.3	81.4	17.0	7.8
P	29.1662	92.1914	-1.2	-5.5	7.4	8.6	18.4	17.9	18.6	27.3	29.4	11.1	5.6
R	29.635	93.6417	-10.5	-5.0	14.4	8.1	52.3	28.5	66.1	37.5	72.5	16.6	11.6
S	28.4364	92.8112	-5.7	-14.2	11.5	15.7	20.7	13.4	38.5	52.3	61.8	20.4	15.3
V	27.8966	93.5973	5.3	0.8	14.2	9.4	78.9	46.7	44.9	33.5	87.4	14.6	5.3
W	28.3507	96.0058	-14.1	-20.8	16.9	22.4	57.6	48.8	65.8	90.8	105.4	31.6	25.1

Table 1 continued

Spring

Buoy	Latitude	Longitude	U_{mean}	V_{mean}	U_{STD}	V_{STD}	U_{max}	V_{max}	U_{max}	V_{max}	$Speed_{max}$	$Speed_{mean}$	$Velocity_{mean}$
	°N	°W	cm/s	cm/s	cm/s	cm/s	cm/s	cm/s	cm/s	cm/s	cm/s	cm/s	cm/s
							Upcoast		Downcoast				
A	29.5325	93.8122	-6.5	-6.8	18.8	17.8	27.1	25.5	48.3	63.1	77.8	22.4	9.4
B	28.9818	94.9186	-7.7	-16.3	17.0	27.9	61.2	96.5	78.8	139.7	149.4	31.4	18.0
C	28.8092	94.7521	-8.1	-12.0	11.4	12.5	26.3	30.4	42.9	55.5	57.0	19.0	14.5
D	27.9396	96.8429	2.1	-13.7	6.4	25.2	56.6	70.8	36.7	78.0	78.1	24.2	13.9
E	27.3383	97.1											
F	28.8425	94.2416	-8.9	-2.9	13.0	9.2	68.1	38.9	77.8	48.0	84.5	15.1	9.3
G	29.5664	93.4683	-10.5	0.8	19.7	12.4	33.9	36.6	68.3	30.4	68.5	21.3	10.6
J	26.1914	97.0507	-9.1	-0.3	25.1	10.0	106.0	62.8	94.5	72.1	106.1	24.0	9.2
K	26.2168	96.4998	-2.5	4.4	14.7	11.8	58.4	45.0	55.7	40.2	66.6	16.6	5.0
L	28.0417	94.1167	-1.1	10.8	15.9	12.5	29.5	43.4	40.6	16.8	52.2	20.4	10.9
M	28.1921	94.1914	1.1	2.0	12.5	8.2	30.4	19.7	36.0	28.4	37.7	13.1	2.3
N	27.8903	94.0367	11.0	0.4	12.9	9.2	82.1	32.9	32.5	39.9	86.4	16.3	11.0
P	29.1662	92.1914	-5.6	-4.7	12.1	11.3	37.7	22.2	41.2	40.9	51.3	14.7	7.3
R	29.635	93.6417	-15.0	-6.5	21.2	11.9	56.5	27.5	84.5	46.5	92.2	24.4	16.4
S	28.4364	92.8112	-4.0	-6.3	11.6	29.7	37.6	112.7	52.5	74.7	112.8	25.5	7.4
V	27.8966	93.5973	7.2	2.5	12.0	9.2	66.6	41.3	38.4	40.3	67.8	14.2	7.6
W	28.3507	96.0058	-11.7	-13.4	18.4	24.0	87.2	62.0	66.0	83.2	105.1	30.0	17.7

Table 1 Continued

Fall

Buoy	Latitude	Longitude	U_{mean}	V_{mean}	U_{STD}	V_{STD}	U_{max}	V_{max}	U_{max}	V_{max}	$Speed_{max}$	$Speed_{mean}$	$Velocity_{mean}$
	°N	°W	cm/s	cm/s	cm/s	cm/s	cm/s	cm/s	cm/s	cm/s	cm/s	cm/s	cm/s
							Upcoast		Downcoast				
A	29.5325	93.8122	-13.5	-11.7	19.0	15.0	39.8	49.4	69.1	50.5	80.0	25.6	17.9
B	28.9818	94.9186	-6.3	-14.4	12.3	19.2	51.2	98.7	77.3	84.4	106.5	23.0	15.8
C	28.8092	94.7521	-4.3	2.9	10.1	20.8	39.9	64.5	40.9	73.3	83.9	18.6	5.2
D	27.9396	96.8429	2.0	-13.9	6.6	24.9	56.6	70.8	36.7	78.0	78.1	24.1	14.0
E	27.3383	97.1	24.1	-9.4	21.2	18.1	71.5	34.5	30.0	40.1	81.9	33.7	25.9
F	28.8425	94.2416	-8.3	-2.5	12.6	8.6	46.0	33.1	70.1	73.4	87.0	14.2	8.7
G	29.5664	93.4683	-7.6	0.7	9.2	6.6	20.6	25.2	40.0	15.0	40.0	11.9	7.6
J	26.1914	97.0507	0.8	-2.4	22.5	11.9	84.9	60.3	67.2	71.1	85.2	21.2	2.5
K	26.2168	96.4998	-0.9	2.4	20.1	13.4	110.1	55.7	53.3	48.6	111.7	20.0	2.6
L	28.0417	94.1167	-14.3	4.5	13.9	11.0	23.6	29.0	64.2	25.2	64.2	21.0	15.0
M	28.1921	94.1914	-2.4	-3.4	11.5	7.5	29.0	13.2	40.3	32.5	41.6	10.5	4.2
N	27.8903	94.0367	3.0	0.2	13.5	9.5	46.8	35.6	42.5	42.1	49.3	14.2	3.0
P	29.1662	92.1914	4.8	-20.1	23.5	21.6	66.0	38.5	43.7	80.8	91.5	31.4	20.7
R	29.635	93.6417	-9.3	-3.9	13.2	7.3	42.4	19.8	95.4	62.2	106.3	14.2	10.1
S	28.4364	92.8112	-9.3	-3.9	13.2	7.3	42.4	19.8	95.4	62.2	106.3	14.2	10.1
V	27.8966	93.5973	-0.2	0.6	13.4	8.4	50.0	24.1	69.5	31.5	70.0	13.5	0.6
W	28.3507	96.0058	-10.8	-14.6	15.9	20.7	65.6	67.9	61.4	104.8	109.6	25.8	18.2

Table 1 Continued

Nonsummer

Buoy	Latitude	Longitude	U_{mean}	V_{mean}	U_{STD}	V_{STD}	U_{max}	V_{max}	U_{max}	V_{max}	$Speed_{max}$	$Speed_{mean}$	$Velocity_{mean}$
	°N	°W	cm/s	cm/s	cm/s	cm/s	cm/s	cm/s	cm/s	cm/s	cm/s	cm/s	cm/s
							Upcoast		Downcoast				
A	29.5325	93.8122	-14.7	-12.3	21.6	18.9	55.4	54.5	68.9	85.5	102.0	29.0	19.2
B	28.9818	94.9186	-7.6	-13.0	16.3	24.6	78.3	115.8	87.2	139.7	149.4	27.8	15.0
C	28.8092	94.7521	-5.2	-7.8	11.3	12.8	26.3	46.2	42.9	76.6	76.6	16.0	9.4
D	27.9396	96.8429	1.1	-12.6	7.5	26.3	61.7	89.1	55.6	88.3	92.0	24.9	12.6
E	27.3383	97.1	5.2	-0.3	20.0	18.0	38.5	49.8	35.9	52.0	63.1	22.9	5.2
F	28.8425	94.2416	-9.3	-2.5	12.6	10.5	68.1	76.4	77.8	102.2	102.4	15.7	9.6
G	29.5664	93.4683	-8.8	1.2	17.9	13.9	33.9	55.7	68.3	66.3	74.3	20.5	8.8
J	26.1914	97.0507	-2.9	1.5	26.7	21.4	106.0	114.2	94.5	135.9	170.8	27.6	3.3
K	26.2168	96.4998	-1.9	2.9	14.8	16.4	60.2	81.6	55.7	94.5	104.1	18.4	3.5
L	28.0417	94.1167	-1.1	9.6	15.9	20.5	29.5	99.8	40.6	77.0	102.6	24.1	9.6
M	28.1921	94.1914	1.1	2.0	12.5	12.4	30.4	53.6	36.0	61.1	62.3	15.1	2.2
N	27.8903	94.0367	9.4	0.7	14.5	11.6	82.1	59.9	58.5	76.9	86.6	17.6	9.5
P	29.1662	92.1914	-3.5	-2.1	10.7	11.3	37.7	70.5	41.2	56.9	72.5	12.9	4.0
R	29.635	93.6417	-14.0	-4.6	19.3	11.2	56.5	53.7	84.5	68.2	94.3	22.2	14.7
S	28.4364	92.8112	-4.2	-5.9	11.4	24.2	37.6	112.7	52.5	103.5	112.8	21.4	7.3
V	27.8966	93.5973	6.4	2.0	13.0	11.6	78.9	70.5	38.4	65.1	89.3	15.6	6.7
W	28.3507	96.0058	-13.4	-13.1	18.1	22.1	87.2	89.0	66.0	102.8	105.5	29.2	18.7

Table 1 Continued

Summer

Buoy	Latitude	Longitude	U_{mean}	V_{mean}	U_{STD}	V_{STD}	U_{max}	V_{max}	U_{max}	V_{max}	$Speed_{max}$	$Speed_{mean}$	$Velocity_{mean}$
	°N	°W	cm/s	cm/s	cm/s	cm/s	cm/s	cm/s	cm/s	cm/s	cm/s	cm/s	cm/s
							Upcoast		Downcoast				
A	29.5325	93.8122	-0.4	-2.8	15.2	14.9	34.4	29.0	55.4	49.0	72.7	16.9	2.8
B	28.9818	94.9186	1.7	3.4	17.0	22.4	82.8	86.3	124.4	153.0	153.6	20.8	3.8
C	28.8092	94.7521	2.1	4.6	16.1	17.8	54.6	58.5	63.0	72.3	94.3	20.2	5.1
D	27.9396	96.8429	0.0	6.9	7.9	19.9	55.3	72.0	38.6	70.8	73.0	17.8	6.9
E	27.3383	97.1	-17.1	2.5	25.6	17.4	45.5	42.6	65.6	39.7	73.2	29.3	17.2
F	28.8425	94.2416	3.5	2.3	13.9	9.7	72.8	44.3	55.9	74.0	90.5	14.2	4.2
G	29.5664	93.4683	4.2	-3.3	18.8	14.3	50.5	31.7	49.4	40.0	58.8	21.7	5.4
J	26.1914	97.0507	-12.6	-1.0	15.5	5.3	56.9	17.6	68.7	28.9	69.7	17.3	12.6
K	26.2168	96.4998	-18.2	7.7	19.0	12.3	31.8	72.1	88.3	36.0	97.6	24.4	19.8
L	28.0417	94.1167	5.7	11.6	21.4	12.8	55.8	44.6	46.7	21.0	56.4	26.0	13.0
M	28.1921	94.1914	3.1	-1.1	13.6	12.4	43.9	35.2	38.9	26.5	44.0	16.3	3.3
N	27.8903	94.0367	6.8	1.0	13.8	9.8	77.8	48.5	40.7	37.2	78.5	14.9	6.9
P	29.1662	92.1914	1.7	-0.7	13.0	12.3	39.4	39.5	35.6	43.8	53.4	15.1	1.8
R	29.635	93.6417	-1.4	0.5	15.8	8.6	61.9	60.1	71.0	45.5	72.8	14.0	1.5
S	28.4364	92.8112	2.2	6.4	12.3	17.3	36.6	60.5	33.9	56.5	65.9	18.3	6.7
V	27.8966	93.5973	5.7	3.1	12.4	10.2	43.9	43.6	34.7	37.3	48.5	15.0	6.5
W	28.3507	96.0058	-0.9	3.5	14.0	16.1	69.5	76.7	75.6	83.6	105.6	16.8	3.6

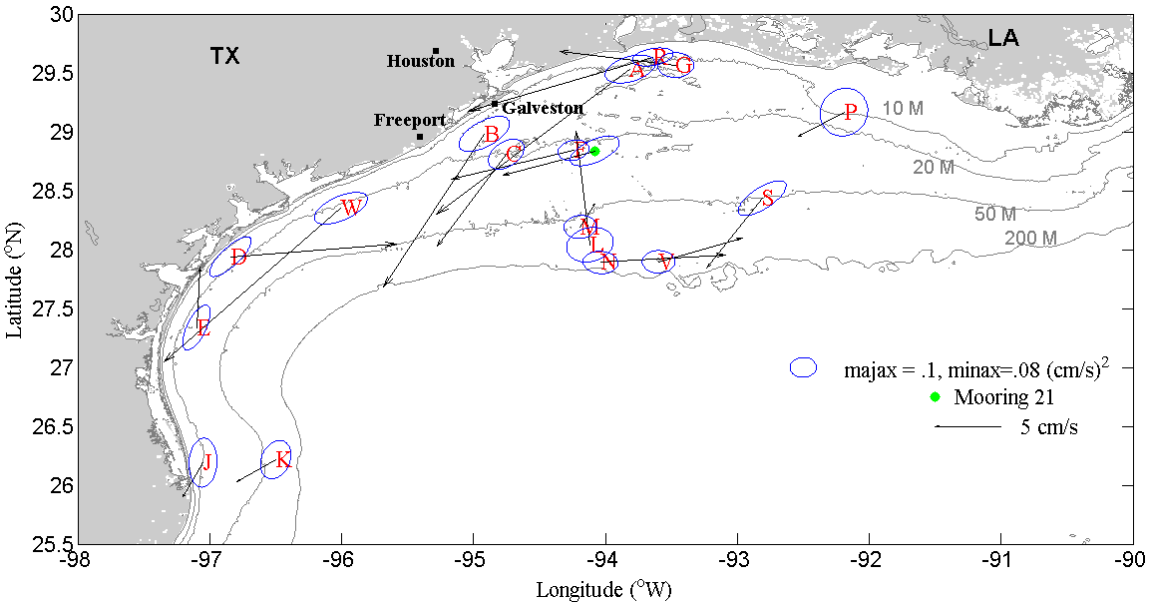

Figure 6. Mean velocity and variance ellipse basemap for non-summer. The black arrows represent the mean u and v-velocities for the non-summer for each TABS buoy and LATEX Mooring 21. Variance ellipses are performed by calculating the semi-major and minor axes of each time series to show the variability in both direction and magnitude at each location. All TABS buoys are marked by red letters and LATEX Mooring 21 is represented by a green marker. Results show coastal locations have downcoast flow present while offshore locations have upcoast flow.

During the summer, positive u-velocity means are observed on areas of the Texas-Louisiana shelf, indicating the presence of upcoast flow (Table 1). Along the Upper Texas Coast, means of 1.7, 2.1, and 3.5 cm s^{-1} are recorded at buoys B, C, and F, respectively. In addition, positive u-velocity means are observed on the outer shelf, with respective values of 5.7, 3.1, 6.8, and 5.7 cm s^{-1} observed at buoys L, M, N, and V. Along the Texas coastal bend, buoy D recorded a neutral u-velocity of 0 cm s^{-1} during the summer. Other locations on the shelf observed negative u-velocity means, signifying

downcoast flow. Near the Texas-Louisiana border, buoys A and R observed u-velocity means of -0.4 and -1.4 cm s^{-1}, respectively. Near the Texas coastal bend, buoys W and E recorded respective u-velocity means of -0.9 and -17.1 cm s^{-1}. Further south, buoys J and K observed mean u-velocities of -12.6 and -18.2 cm s^{-1}, respectively. Figure 7 shows the overall flow trends on the Texas-Louisiana Shelf during the summer, with an upcoast flow present along the upper inner shelf and offshore and other areas displaying downcoast flow.

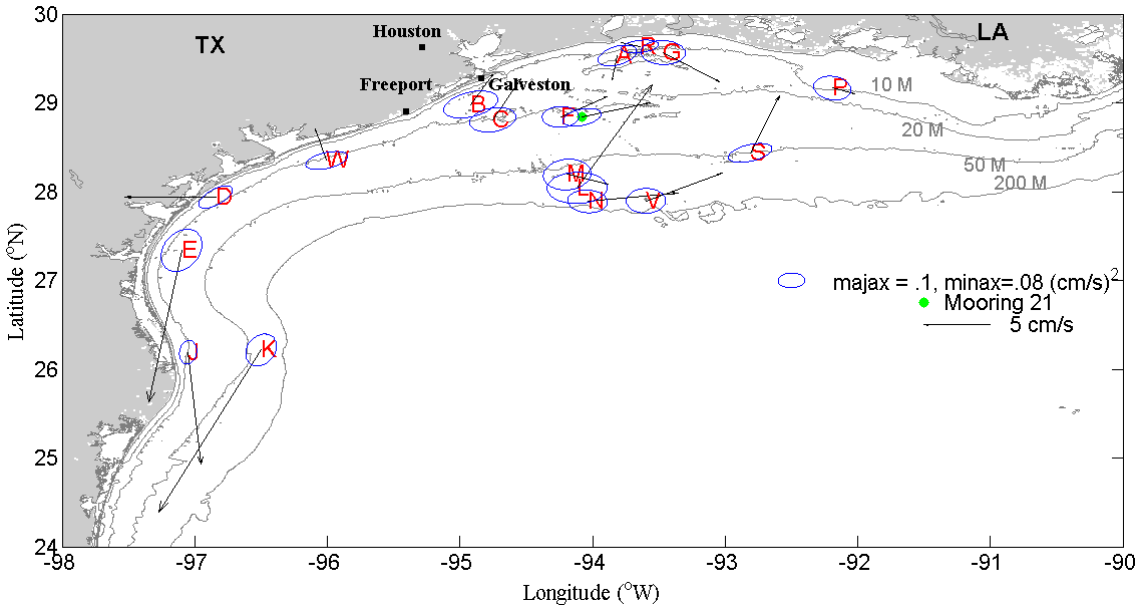

Figure 7. Mean velocity and variance ellipse basemap for summer. The black arrows represent the mean u and v-velocities for the non-summer for each TABS buoy and LATEX Mooring 21. Variance ellipses are performed by calculating the semi-major and minor axes of each time series to show the variability in both direction and magnitude at each location. All TABS buoys are marked by red letters and LATEX Mooring 21 is represented by a green marker. Results show upper coastal locations and offshore locations have upcoast flow present. The flow is more onshore at southern coastal locations.

Mean reversal statistics, as displayed in Table 2, reveal that fewer reversals occur during the summer compared to non-summer at buoys B, D, J, K, N, and V. During the summer, there are an average number of 9, 12, 7, 8, 7, and 9 reversals at buoys B, D, J, K, N, and V, respectively. Buoy B has more reversals during the fall, with a mean reversal number of 12. Buoy D has more reversals occurring in the spring, with an average number of 17 reversals. More reversals occur during the winter for buoys J, K, N, and V, with respective means of 11, 17, 9, and 11. However, the results from Table 2 indicate there are actually only a few seasonal differences in the number of current reversals that occur. Both buoys D and K have a relatively large seasonal reversal spread, ranging from 12-17 reversals at buoy D and 8-17 reversals at buoy K. Other buoys have reversal number spreads that range from 1-4 reversals between different seasons, indicating very little seasonal change in reversal numbers at most locations.

Table 2. Mean reversal numbers by season.

Buoy	Winter	Spring	Summer	Fall
R	7	8	8	7
F	10	8	9	8
B	11	10	9	12
W	8	9	10	10
D	15	17	12	14
J	11	10	7	9
K	17	15	8	12
N	9	8	7	8
V	11	10	9	9

One-way ANOVAs reveal there are significant seasonal differences in the number of normalized reversals at buoys D and K. At buoy D, the ANOVA shows that summer is significantly different than any other season, with a lower number of normalized reversals in the summer compared to other seasons (Figure 8). At buoy K, the ANOVA indicates summer reversal numbers are significantly different compared to the winter and spring seasons, with fewer reversals during the summer (Figure 9). In general, it appears that the likelihood of having a reversal during the summer is the same as any other season at most buoy locations. Therefore, reversal number is likely not a good way to characterize the seasonality of the Texas Coastal Current.

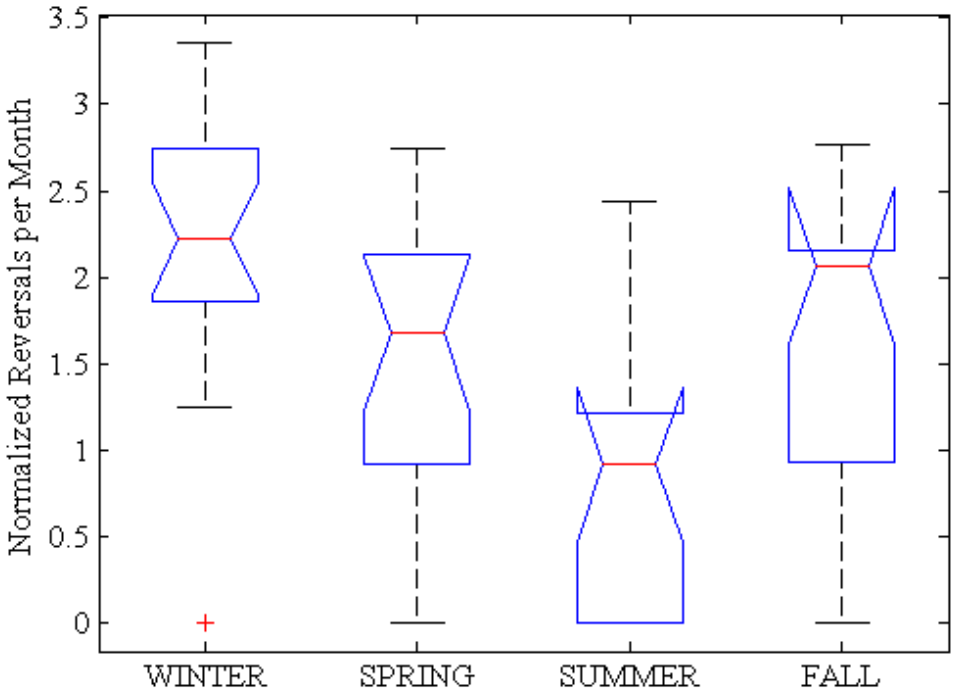

Figure 8. ANOVA of reversal numbers at buoy D. The reversals are normalized by the number of observations recorded each season and are then segmented into reversals per month for better interpretation. Summer is significantly different than all other seasons, with lower reversal numbers compared to winter, spring, and fall. (F=6.38, probability>p=.0007)

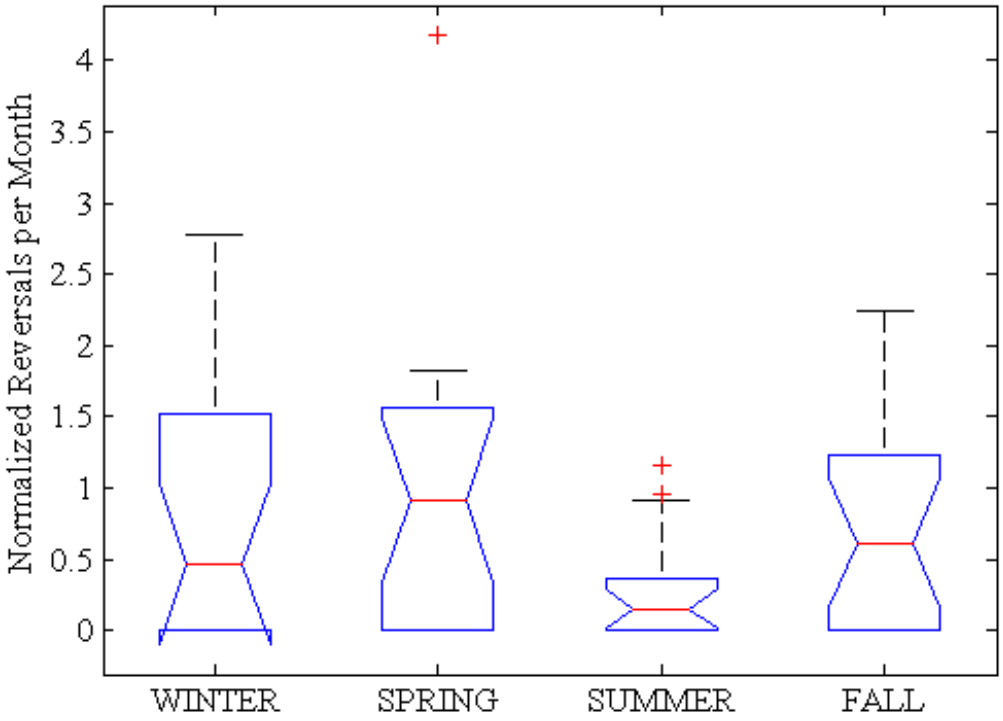

Figure 9. ANOVA of reversal numbers at buoy K. The number of reversals are normalized by the number of observations recorded during each season. The numbers are then segmented into reversals per month for better interpretation. Summer is significantly different than all other seasons, with lower reversal numbers. (F=2.29, probability>p=.0857)

Persistence statistic tables show distinctive seasonal characteristics in both current velocity and duration. Table 3 displays the persistence statistics for each buoy during the summer season. Buoys B, F, N, and V have higher numbers of upcoast currents present, with respective totals of 610, 621, 379, and 305. Table 4 displays the total amount of time current flow is directed upcoast, with buoys B, F, N, and V showing dominant (>50%) upcoast flow during the summer. The currents observed at these

locations are centered at the 0-5 and 5-10 cm s^{-1} velocity classes, with at least 45% of observed currents documented within these ranges. This means most upcoast current reversals are slow (<10 cm s^{-1}) regardless of duration. At each of these locations, maximum upcoast current durations are also observed. Longer current durations are observed at offshore buoys, with currents lasting 1594 and 1306 hours at buoys N and V, respectively. At Buoys B and F, respective maximum current durations of 716 and 1152 hours are observed. At each location, maximum durations occur within the 0-5 cm s^{-1} velocity classes, indicating that longer current durations tend to be slow.

Summer statistics are also evaluated in the downcoast direction at buoys B, F, N, and V. Fewer downcoast currents are observed at each of these locations, with respective totals of 486, 388, 139, and 120. At least 50% of the currents observed at these locations fall into the 0-5 and 5-10 cm s^{-1} velocity classes, meaning downcoast flow also tends to be slow regardless of duration. Maximum current durations are also observed, with durations of 426, 339, 542, and 530 hours recorded at buoys B, F, N, and V. These durations are less compared to when the flow is upcoast at these locations, meaning there is extended current duration upcoast compared to downcoast flow duration during the summer.

Table 3. Summer persistence tables for TABS buoys.

Buoy B; Summers from 1995-2012

UPCOAST

U Velocity (cm/s)	Duration Limits (hours)															Duration Statistics (hours)				
	48	72	96	120	144	168	192	216	240	264	288	312	336	360	>360	Total	Max	Mean	Std Dev	% time
0 - 5	40	30	24	11	7	6	8	7	3	4	6	3	1	0	6	156	716	118	108	25.57
5 - 10	51	26	13	12	6	3	4	4	3	7	4	1	0	0	1	135	381	95	76	22.13
10 - 15	49	28	14	6	6	5	1	4	0	0	1	0	0	0	0	114	287	70	50	18.69
15 - 20	36	15	9	5	1	1	1	2	0	0	1	0	0	0	0	71	280	65	48	11.64
20 - 25	23	13	6	2	1	0	2	1	0	0	0	0	0	0	0	48	200	58	40	7.87
25 - 30	17	10	4	1	1	0	0	0	0	0	0	0	0	0	0	33	139	54	25	5.41
30 - 35	14	6	1	1	0	0	0	0	0	0	0	0	0	0	0	22	102	44	19	3.61
35 - 40	8	2	1	0	0	0	0	0	0	0	0	0	0	0	0	11	91	43	18	1.8
40 - 45	4	2	1	0	0	0	0	0	0	0	0	0	0	0	0	7	84	45	21	1.15
45 - 50	2	1	1	0	0	0	0	0	0	0	0	0	0	0	0	4	78	47	21	0.66
50 - 55	4	1	0	0	0	0	0	0	0	0	0	0	0	0	0	5	53	38	12	0.82
55 - 60	2	0	0	0	0	0	0	0	0	0	0	0	0	0	0	2	41	37	5	0.33
60 - 65	2	0	0	0	0	0	0	0	0	0	0	0	0	0	0	2	35	31	6	0.33
Totals	252	134	74	38	22	15	16	18	6	11	12	4	1	0	7	610				

Table 3 continued

Buoy B; Summers from 1995-2012

DOWNCOAST

U Velocity	Duration Limits (hours)															Duration Statistics (hours)				
(cm/s)	48	72	96	120	144	168	192	216	240	264	288	312	336	360	>360	Total	Max	Mean	Std Dev	% time
0 - 5	49	29	18	8	11	3	4	4	4	4	1	3	3	0	2	143	426	98	84	29.36
5 - 10	37	30	11	12	3	4	3	1	2	1	0	0	1	0	2	107	384	81	68	21.97
10 - 15	48	10	7	2	2	4	1	3	0	0	1	0	0	0	1	79	371	67	63	16.22
15 - 20	27	2	2	3	3	2	0	2	0	1	1	0	0	0	0	43	274	73	64	8.83
20 - 25	15	4	2	3	0	2	0	1	0	1	0	0	0	0	0	28	244	69	57	5.75
25 - 30	8	2	0	3	0	1	0	1	1	0	0	0	0	0	0	16	239	73	65	3.29
30 - 35	6	2	2	1	0	1	0	0	1	0	0	0	0	0	0	13	236	72	58	2.67
35 - 40	8	2	0	0	1	0	0	0	1	0	0	0	0	0	0	12	232	60	60	2.46
40 - 45	4	0	1	0	1	0	0	0	1	0	0	0	0	0	0	7	229	84	77	1.44
45 - 50	4	0	2	0	0	1	0	0	0	0	0	0	0	0	0	7	159	68	46	1.44
50 - 55	3	1	1	0	1	0	0	0	0	0	0	0	0	0	0	6	143	67	44	1.23
55 - 60	3	2	0	0	0	0	0	0	0	0	0	0	0	0	0	5	66	43	17	1.03
60 - 65	2	2	0	0	0	0	0	0	0	0	0	0	0	0	0	4	61	45	16	0.82
65 - 70	2	2	0	0	0	0	0	0	0	0	0	0	0	0	0	4	56	41	16	0.82
70 - 75	1	2	0	0	0	0	0	0	0	0	0	0	0	0	0	3	51	42	15	0.62
75 - 80	2	0	0	0	0	0	0	0	0	0	0	0	0	0	0	2	47	46	2	0.41
80 - 85	2	0	0	0	0	0	0	0	0	0	0	0	0	0	0	2	44	41	4	0.41
85 - 90	2	0	0	0	0	0	0	0	0	0	0	0	0	0	0	2	41	36	8	0.41
90 - 95	1	0	0	0	0	0	0	0	0	0	0	0	0	0	0	1	38	38	0	0.21
95 - 100	1	0	0	0	0	0	0	0	0	0	0	0	0	0	0	1	35	35	0	0.21
100 - 105	1	0	0	0	0	0	0	0	0	0	0	0	0	0	0	1	31	31	0	0.21
Totals	226	90	46	32	22	18	8	12	10	7	3	3	4	0	5	486				

Table 3 continued

Buoy D; Summers from 1996-2012

UPCOAST

U Velocity	Duration Limits (hours)															Duration Statistics (hours)				
(cm/s)	48	72	96	120	144	168	192	216	240	264	288	312	336	360	>360	Total	Max	Mean	Std Dev	% time
0 - 5	79	29	16	8	9	4	0	4	0	0	0	0	1	0	1	151	992	68	87	63.71
5 - 10	24	2	1	1	0	0	0	0	1	0	0	0	1	0	1	31	402	65	90	13.08
10 - 15	3	3	1	0	0	1	0	0	0	0	0	0	1	0	1	10	393	120	131	4.22
15 - 20	2	1	2	0	1	0	0	0	0	0	0	1	1	0	0	8	317	130	114	3.38
20 - 25	1	2	2	0	0	0	0	0	1	0	1	0	0	0	0	7	282	121	94	2.95
25 - 30	2	3	2	0	1	0	0	1	0	0	0	0	0	0	0	9	200	84	51	3.8
30 - 35	1	4	1	1	0	1	0	0	0	0	0	0	0	0	0	8	151	74	36	3.38
35 - 40	4	2	0	0	1	0	0	0	0	0	0	0	0	0	0	7	132	60	33	2.95
40 - 45	3	1	0	0	0	0	0	0	0	0	0	0	0	0	0	4	54	40	11	1.69
45 - 50	2	0	0	0	0	0	0	0	0	0	0	0	0	0	0	2	34	32	4	0.84
Totals	121	47	25	10	12	6	0	5	2	0	1	1	4	0	3	237				

Table 3 continued

Buoy D; Summers from 1996-2012

DOWNCOAST

U Velocity	Duration Limits (hours)															Duration Statistics (hours)				
(cm/s)	48	72	96	120	144	168	192	216	240	264	288	312	336	360	>360	Total	Max	Mean	Std Dev	% time
0 - 5	70	46	15	12	13	8	7	4	2	3	2	2	0	0	3	187	556	88	82	68
5 - 10	29	14	3	4	0	1	0	0	0	0	0	0	0	0	1	52	411	57	56	18.91
10 - 15	14	3	0	1	1	1	0	0	0	0	0	0	0	0	0	20	147	50	34	7.27
15 - 20	8	0	2	0	0	0	0	0	0	0	0	0	0	0	0	10	86	44	23	3.64
20 - 25	5	0	0	0	0	0	0	0	0	0	0	0	0	0	0	5	37	32	5	1.82
25 - 30	1	0	0	0	0	0	0	0	0	0	0	0	0	0	0	1	29	29	0	0.36
Totals	127	63	20	17	14	10	7	4	2	3	2	2	0	0	4	275				

Table 3 continued

Buoy F; Summers from 1996-2012

UPCOAST

U Velocity (cm/s)	Duration Limits (hours)															Duration Statistics (hours)				
	48	72	96	120	144	168	192	216	240	264	288	312	336	360	>360	Total	Max	Mean	Std Dev	% time
0 - 5	39	21	24	17	10	11	5	4	0	4	1	0	1	1	11	149	1152	129	154	23.99
5 - 10	53	23	17	18	9	4	2	0	4	2	1	2	0	2	3	140	663	95	96	22.54
10 - 15	45	23	14	11	12	1	1	4	4	0	0	0	0	0	0	115	233	75	51	18.52
15 - 20	47	17	6	10	3	1	2	2	0	0	0	0	0	0	0	88	206	61	42	14.17
20 - 25	26	11	7	1	2	0	2	0	0	0	0	0	0	0	0	49	188	57	35	7.89
25 - 30	19	10	2	3	0	0	0	0	0	0	0	0	0	0	0	34	119	49	25	5.48
30 - 35	15	3	2	1	0	0	0	0	0	0	0	0	0	0	0	21	113	45	22	3.38
35 - 40	11	1	0	1	0	0	0	0	0	0	0	0	0	0	0	13	108	39	22	2.09
40 - 45	6	1	0	0	0	0	0	0	0	0	0	0	0	0	0	7	65	34	14	1.13
45 - 50	2	0	0	0	0	0	0	0	0	0	0	0	0	0	0	2	39	35	5	0.32
50 - 55	2	0	0	0	0	0	0	0	0	0	0	0	0	0	0	2	32	29	4	0.32
55 - 60	1	0	0	0	0	0	0	0	0	0	0	0	0	0	0	1	28	28	0	0.16
Totals	266	110	72	62	36	17	12	10	8	6	2	2	1	3	14	621				

Table 3 continued

Buoy F; Summers from 1996-2012

DOWNCOAST

U Velocity	Duration Limits (hours)															Duration Statistics (hours)				
(cm/s)	48	72	96	120	144	168	192	216	240	264	288	312	336	360	>360	Total	Max	Mean	Std Dev	% time
0 - 5	43	27	16	15	8	6	3	4	1	2	3	1	1	1	0	131	339	91	70	33.76
5 - 10	43	25	16	9	3	1	2	2	2	1	0	0	1	0	0	105	330	73	54	27.06
10 - 15	29	17	10	7	2	0	1	0	1	0	0	0	0	0	0	67	230	62	38	17.27
15 - 20	25	9	6	3	0	0	0	0	0	0	0	0	0	0	0	43	120	51	24	11.08
20 - 25	21	4	2	0	0	0	0	0	0	0	0	0	0	0	0	27	89	38	17	6.96
25 - 30	6	1	1	0	0	0	0	0	0	0	0	0	0	0	0	8	78	40	18	2.06
30 - 35	0	2	0	0	0	0	0	0	0	0	0	0	0	0	0	2	64	59	7	0.52
35 - 40	1	1	0	0	0	0	0	0	0	0	0	0	0	0	0	2	52	48	5	0.52
40 - 45	2	0	0	0	0	0	0	0	0	0	0	0	0	0	0	2	42	37	7	0.52
45 - 50	1	0	0	0	0	0	0	0	0	0	0	0	0	0	0	1	32	32	0	0.26
Totals	171	86	51	34	13	7	6	6	4	3	3	1	2	1	0	388				

Table 3 continued

Buoy J; Summers from 1998-2012

UPCOAST

U Velocity	Duration Limits (hours)															Duration Statistics (hours)				
(cm/s)	48	72	96	120	144	168	192	216	240	264	288	312	336	360	>360	Total	Max	Mean	Std Dev	% time
0 - 5	24	15	7	4	5	2	3	1	0	0	0	0	0	0	0	61	209	71	46	37.2
5 - 10	26	7	4	4	1	1	0	0	0	0	0	0	0	0	0	43	145	55	32	26.22
10 - 15	21	4	1	0	1	0	0	0	0	0	0	0	0	0	0	27	131	45	22	16.46
15 - 20	13	3	0	1	0	0	0	0	0	0	0	0	0	0	0	17	118	41	23	10.37
20 - 25	5	2	0	0	0	0	0	0	0	0	0	0	0	0	0	7	56	35	12	4.27
25 - 30	2	1	0	0	0	0	0	0	0	0	0	0	0	0	0	3	49	38	9	1.83
30 - 35	3	0	0	0	0	0	0	0	0	0	0	0	0	0	0	3	43	32	10	1.83
35 - 40	1	0	0	0	0	0	0	0	0	0	0	0	0	0	0	1	36	36	0	0.61
40 - 45	1	0	0	0	0	0	0	0	0	0	0	0	0	0	0	1	31	31	0	0.61
45 - 50	1	0	0	0	0	0	0	0	0	0	0	0	0	0	0	1	25	25	0	0.61
Totals	97	32	12	9	7	3	3	1	0	0	0	0	0	0	0	164				

Table 3 continued

Buoy J; Summers from 1998-2012

DOWNCOAST

U Velocity	Duration Limits (hours)															Duration Statistics (hours)				
(cm/s)	48	72	96	120	144	168	192	216	240	264	288	312	336	360	>360	Total	Max	Mean	Std Dev	% time
0 - 5	10	5	1	5	3	2	9	4	1	2	1	1	5	5	15	69	1764	276	277	11.66
5 - 10	14	6	7	4	8	7	5	2	2	2	1	4	5	3	10	80	1579	210	230	13.51
10 - 15	26	17	12	9	6	7	4	3	7	2	1	3	3	0	3	103	812	127	120	17.4
15 - 20	31	16	14	11	5	8	2	3	3	1	3	1	0	0	1	99	684	100	89	16.72
20 - 25	39	14	5	8	4	6	2	3	1	0	1	0	0	0	1	84	442	80	69	14.19
25 - 30	25	7	7	3	8	2	0	1	1	0	0	0	0	0	0	54	237	73	49	9.12
30 - 35	17	8	5	3	1	1	1	0	0	0	0	0	0	0	0	36	187	63	37	6.08
35 - 40	19	6	3	2	0	0	1	0	0	0	0	0	0	0	0	31	181	53	33	5.24
40 - 45	13	6	0	0	1	0	0	0	0	0	0	0	0	0	0	20	123	42	22	3.38
45 - 50	8	1	0	1	0	0	0	0	0	0	0	0	0	0	0	10	111	39	25	1.69
50 - 55	3	0	1	0	0	0	0	0	0	0	0	0	0	0	0	4	75	43	23	0.68
55 - 60	1	1	0	0	0	0	0	0	0	0	0	0	0	0	0	2	53	43	14	0.34
Totals	206	87	55	46	36	33	24	16	15	7	7	9	13	8	30	592				

Table 3 continued

Buoy K; Summers from 1998-2012

UPCOAST

U Velocity	Duration Limits (hours)															Duration Statistics (hours)				
(cm/s)	48	72	96	120	144	168	192	216	240	264	288	312	336	360	>360	Total	Max	Mean	Std Dev	% time
0 - 5	19	7	2	4	3	2	1	0	0	0	0	0	0	0	0	38	189	65	44	48.72
5 - 10	11	3	3	3	0	0	0	0	0	0	0	0	0	0	0	20	102	56	26	25.64
10 - 15	8	3	2	0	0	0	0	0	0	0	0	0	0	0	0	13	88	46	23	16.67
15 - 20	1	3	0	0	0	0	0	0	0	0	0	0	0	0	0	4	71	58	15	5.13
20 - 25	1	1	0	0	0	0	0	0	0	0	0	0	0	0	0	2	55	42	18	2.56
25 - 30	1	0	0	0	0	0	0	0	0	0	0	0	0	0	0	1	38	38	0	1.28
Totals	41	17	7	7	3	2	1	0	0	0	0	0	0	0	0	78				

Table 3 continued

Buoy K; Summers from 1998-2012

DOWNCOAST

U Velocity	Duration Limits (hours)															Duration Statistics (hours)				
(cm/s)	48	72	96	120	144	168	192	216	240	264	288	312	336	360	>360	Total	Max	Mean	Std Dev	% time
0 - 5	8	4	2	3	4	1	2	0	2	2	2	0	1	1	17	49	1878	340	368	9.88
5 - 10	12	5	5	6	5	2	3	0	3	2	3	1	1	2	10	60	1878	237	311	12.1
10 - 15	12	9	5	7	8	3	2	0	4	1	4	0	1	1	7	64	1878	186	259	12.9
15 - 20	15	6	9	6	8	0	1	2	3	2	2	1	1	0	4	60	1878	165	263	12.1
20 - 25	15	8	7	5	5	0	4	2	0	1	0	0	0	1	3	51	1817	142	257	10.28
25 - 30	13	9	11	5	2	2	2	0	0	1	0	0	1	0	3	49	655	115	142	9.88
30 - 35	25	9	4	2	0	0	1	1	0	0	0	1	0	0	3	46	642	93	130	9.27
35 - 40	21	6	0	1	1	0	1	0	0	0	0	0	0	1	2	33	627	90	145	6.65
40 - 45	10	3	1	1	1	0	0	0	0	1	0	0	0	0	2	19	606	119	175	3.83
45 - 50	7	3	1	0	1	0	1	1	0	0	0	0	0	1	1	16	474	114	128	3.23
50 - 55	9	0	0	1	1	0	0	2	0	0	0	0	0	0	1	14	433	96	111	2.82
55 - 60	5	2	1	0	0	1	1	0	0	0	0	0	0	1	0	11	350	95	98	2.22
60 65	0	3	2	1	1	0	0	0	0	0	0	0	0	0	0	7	142	81	32	1.41
65 70	5	4	0	0	0	0	0	0	0	0	0	0	0	0	0	9	51	40	11	1.81
70 75	6	0	0	0	0	0	0	0	0	0	0	0	0	0	0	6	39	34	6	1.21
75 80	2	0	0	0	0	0	0	0	0	0	0	0	0	0	0	2	31	30	1	0.4
Totals	165	71	48	38	37	9	18	8	12	10	11	3	5	8	53	496				

Table 3 continued

Buoy N; Summers from 1998-2012

UPCOAST

U Velocity (cm/s)	Duration Limits (hours)															Duration Statistics (hours)				
	48	72	96	120	144	168	192	216	240	264	288	312	336	360	>360	Total	Max	Mean	Std Dev	% time
0 - 5	22	15	6	2	8	4	2	1	1	3	4	2	0	0	12	82	1594	194	271	21.64
5 - 10	33	22	8	2	4	2	1	3	3	2	1	1	0	0	7	89	1067	128	178	23.48
10 - 15	26	13	10	8	1	1	0	4	0	2	2	0	0	0	3	70	891	106	126	18.47
15 - 20	18	5	6	5	1	2	0	0	0	2	0	1	0	1	1	42	802	100	133	11.08
20 - 25	17	6	3	1	2	0	0	0	0	0	0	1	0	1	1	32	720	88	135	8.44
25 - 30	17	3	0	2	0	0	0	0	1	0	1	0	1	0	0	25	315	71	78	6.6
30 - 35	10	2	0	0	0	0	1	1	0	0	0	1	0	0	0	15	301	71	82	3.96
35 - 40	3	1	0	1	0	1	0	0	1	0	0	0	0	0	0	7	223	84	75	1.85
40 - 45	1	1	1	1	0	0	0	1	0	0	0	0	0	0	0	5	209	100	65	1.32
45 - 50	1	3	0	0	1	0	0	0	0	0	0	0	0	0	0	5	121	62	35	1.32
50 - 55	1	1	0	1	0	0	0	0	0	0	0	0	0	0	0	3	102	66	31	0.79
55 - 60	1	1	0	0	0	0	0	0	0	0	0	0	0	0	0	2	49	45	6	0.53
60 - 65	1	0	0	0	0	0	0	0	0	0	0	0	0	0	0	1	35	35	0	0.26
65 - 70	1	0	0	0	0	0	0	0	0	0	0	0	0	0	0	1	29	29	0	0.26
Totals	152	73	34	23	17	10	4	10	6	9	8	6	1	2	24	379				

Table 3 continued

Buoy N; Summers from 1998-2012

DOWNCOAST

U Velocity	Duration Limits (hours)															Duration Statistics (hours)				
(cm/s)	48	72	96	120	144	168	192	216	240	264	288	312	336	360	>360	Total	Max	Mean	Std Dev	% time
0 - 5	23	13	1	3	1	4	1	2	2	0	0	1	0	0	4	55	542	106	120	39.57
5 - 10	13	3	4	2	3	3	1	0	0	1	1	0	1	0	1	33	404	102	92	23.74
10 - 15	13	7	2	1	0	0	0	1	1	1	1	0	0	0	0	27	283	73	72	19.42
15 - 20	5	3	4	1	0	0	0	0	0	0	0	0	0	0	0	13	100	56	27	9.35
20 - 25	5	2	0	0	0	0	0	0	0	0	0	0	0	0	0	7	65	41	14	5.04
25 - 30	3	0	0	0	0	0	0	0	0	0	0	0	0	0	0	3	40	33	6	2.16
30 - 35	1	0	0	0	0	0	0	0	0	0	0	0	0	0	0	1	30	30	0	0.72
Totals	63	28	11	7	4	7	2	3	3	2	2	1	1	0	5	139				

Table 3 continued

Buoy R; Summers from 1998-2012

UPCOAST

U Velocity	Duration Limits (hours)															Duration Statistics (hours)				
(cm/s)	48	72	96	120	144	168	192	216	240	264	288	312	336	360	>360	Total	Max	Mean	Std Dev	% time
0 - 5	29	29	14	7	13	7	4	5	0	3	5	2	1	0	4	123	539	114	99	27.83
5 - 10	37	15	10	12	10	9	1	4	2	1	1	1	1	0	1	105	414	95	72	23.76
10 - 15	50	19	14	5	6	3	1	0	0	0	0	0	0	0	0	98	188	61	37	22.17
15 - 20	32	15	5	2	0	1	0	0	0	0	0	0	0	0	0	55	148	49	25	12.44
20 - 25	27	5	1	0	0	0	0	0	0	0	0	0	0	0	0	33	88	38	14	7.47
25 - 30	13	1	0	0	0	0	0	0	0	0	0	0	0	0	0	14	62	36	10	3.17
30 - 35	5	1	0	0	0	0	0	0	0	0	0	0	0	0	0	6	54	35	10	1.36
35 - 40	4	0	0	0	0	0	0	0	0	0	0	0	0	0	0	4	47	32	10	0.9
40 - 45	2	0	0	0	0	0	0	0	0	0	0	0	0	0	0	2	41	33	10	0.45
45 - 50	1	0	0	0	0	0	0	0	0	0	0	0	0	0	0	1	35	35	0	0.23
50 - 55	1	0	0	0	0	0	0	0	0	0	0	0	0	0	0	1	28	28	0	0.23
Totals	201	85	44	26	29	20	6	9	2	4	6	3	2	0	5	442				

Table 3 continued

Buoy R; Summers from 1998-2012

DOWNCOAST

U Velocity	Duration Limits (hours)															Duration Statistics (hours)				
(cm/s)	48	72	96	120	144	168	192	216	240	264	288	312	336	360	>360	Total	Max	Mean	Std Dev	% time
0 - 5	29	17	17	11	4	6	3	3	4	4	2	3	3	2	5	113	476	128	110	22.83
5 - 10	36	16	18	6	6	2	7	1	3	2	2	1	3	1	0	104	357	98	81	21.01
10 - 15	42	18	9	7	3	3	1	0	2	0	0	2	1	1	0	89	338	75	68	17.98
15 - 20	34	9	5	5	3	1	1	0	1	0	0	1	1	0	0	61	320	70	61	12.32
20 - 25	16	8	7	2	1	1	0	1	0	0	0	1	0	0	0	37	298	71	56	7.47
25 - 30	10	7	4	1	0	0	1	0	0	0	1	0	0	0	0	24	278	73	55	4.85
30 - 35	9	6	2	1	2	1	0	0	0	0	0	0	0	0	0	21	147	62	37	4.24
35 - 40	13	3	2	0	1	0	0	0	0	0	0	0	0	0	0	19	122	48	26	3.84
40 - 45	8	1	1	1	0	0	0	0	0	0	0	0	0	0	0	11	101	47	23	2.22
45 - 50	6	1	1	0	0	0	0	0	0	0	0	0	0	0	0	8	93	44	24	1.62
50 - 55	3	2	0	0	0	0	0	0	0	0	0	0	0	0	0	5	63	41	17	1.01
55 - 60	1	1	0	0	0	0	0	0	0	0	0	0	0	0	0	2	53	40	18	0.4
60 - 65	1	0	0	0	0	0	0	0	0	0	0	0	0	0	0	1	26	26	0	0.2
Totals	208	89	66	34	20	14	13	5	10	6	5	8	8	4	5	495				

Table 3 continued

Buoy V; Summers from 2002-2012

UPCOAST

U Velocity	Duration Limits (hours)															Duration Statistics (hours)				
(cm/s)	48	72	96	120	144	168	192	216	240	264	288	312	336	360	>360	Total	Max	Mean	Std Dev	% time
0 - 5	17	9	13	3	5	0	2	3	3	5	0	1	0	1	5	67	1306	154	205	21.97
5 - 10	27	10	14	6	1	4	1	4	0	2	1	1	0	1	1	73	1206	103	148	23.93
10 - 15	17	19	8	2	1	2	0	2	1	1	1	0	1	0	1	56	621	92	98	18.36
15 - 20	18	11	5	4	0	2	1	2	0	0	0	0	0	0	0	43	210	72	50	14.1
20 - 25	18	8	4	1	1	1	1	0	0	0	0	0	0	0	0	34	181	59	38	11.15
25 - 30	13	5	3	0	0	0	0	0	0	0	0	0	0	0	0	21	91	44	20	6.89
30 - 35	8	2	0	0	0	0	0	0	0	0	0	0	0	0	0	10	67	38	14	3.28
35 - 40	1	0	0	0	0	0	0	0	0	0	0	0	0	0	0	1	32	32	0	0.33
Totals	119	64	47	16	8	9	5	11	4	8	2	2	1	2	7	305				

Table 3 continued

Buoy V; Summers from 2002-2012

DOWNCOAST

U Velocity	Duration Limits (hours)															Duration Statistics (hours)				
(cm/s)	48	72	96	120	144	168	192	216	240	264	288	312	336	360	>360	Total	Max	Mean	Std Dev	% time
0 - 5	22	7	6	3	2	2	0	1	0	2	0	0	2	0	1	48	530	93	97	40
5 - 10	14	7	4	0	2	1	0	1	2	1	0	0	0	0	0	32	250	75	63	26.67
10 - 15	13	3	1	2	0	0	0	2	0	0	0	0	0	0	0	21	200	62	52	17.5
15 - 20	5	3	1	1	0	0	0	0	0	0	0	0	0	0	0	10	100	59	26	8.33
20 - 25	2	2	1	0	0	0	0	0	0	0	0	0	0	0	0	5	82	51	20	4.17
25 - 30	3	1	0	0	0	0	0	0	0	0	0	0	0	0	0	4	61	42	14	3.33
Totals	59	23	13	6	4	3	0	4	2	3	0	0	2	0	1	120				

Table 3 continued

Buoy W; Summers from 2002-2012

UPCOAST

U Velocity	Duration Limits (hours)															Duration Statistics (hours)				
(cm/s)	48	72	96	120	144	168	192	216	240	264	288	312	336	360	>360	Total	Max	Mean	Std Dev	% time
0 - 5	31	17	14	7	3	11	7	0	3	3	1	1	1	0	0	99	329	99	69	32.04
5 - 10	33	23	7	6	5	4	0	2	1	0	0	0	0	0	0	81	231	71	46	26.21
10 - 15	27	15	2	6	2	1	0	0	0	0	0	0	0	0	0	53	165	57	33	17.15
15 - 20	23	7	3	1	1	0	0	0	0	0	0	0	0	0	0	35	137	48	26	11.33
20 - 25	16	2	0	1	1	0	0	0	0	0	0	0	0	0	0	20	129	44	27	6.47
25 - 30	8	1	0	2	0	0	0	0	0	0	0	0	0	0	0	11	116	45	32	3.56
30 - 35	1	0	0	1	0	0	0	0	0	0	0	0	0	0	0	2	103	67	39	0.65
35 - 40	0	2	0	0	0	0	0	0	0	0	0	0	0	0	0	2	56	55	2	0.65
40 - 45	2	0	0	0	0	0	0	0	0	0	0	0	0	0	0	2	46	45	1	0.65
45 - 50	2	0	0	0	0	0	0	0	0	0	0	0	0	0	0	2	38	36	3	0.65
50 - 55	1	0	0	0	0	0	0	0	0	0	0	0	0	0	0	1	33	33	0	0.32
55 - 60	1	0	0	0	0	0	0	0	0	0	0	0	0	0	0	1	27	27	0	0.32
Totals	145	67	26	24	12	16	7	2	4	3	1	1	1	0	0	309				

Table 3 continued

Buoy W; Summers from 2002-2012

DOWNCOAST

U Velocity	Duration Limits (hours)															Duration Statistics (hours)				
(cm/s)	48	72	96	120	144	168	192	216	240	264	288	312	336	360	>360	Total	Max	Mean	Std Dev	% time
0 - 5	31	16	13	11	8	3	1	6	1	1	0	0	2	2	1	96	500	101	83	27.35
5 - 10	28	24	14	7	3	3	2	2	0	0	0	1	1	0	0	85	322	76	54	24.22
10 - 15	40	15	6	7	1	0	1	0	0	0	0	0	1	0	0	71	316	57	42	20.23
15 - 20	29	4	2	2	0	0	0	0	0	0	0	1	0	0	0	38	310	48	44	10.83
20 - 25	15	4	3	1	0	1	0	0	0	0	0	0	0	0	0	24	152	51	32	6.84
25 - 30	11	3	0	0	1	0	0	0	0	0	0	0	0	0	0	15	139	44	29	4.27
30 - 35	5	1	0	0	1	0	0	0	0	0	0	0	0	0	0	7	131	50	37	1.99
35 - 40	3	1	0	0	1	0	0	0	0	0	0	0	0	0	0	5	123	53	40	1.42
40 - 45	3	0	0	1	0	0	0	0	0	0	0	0	0	0	0	4	114	53	42	1.14
45 - 50	2	1	0	0	0	0	0	0	0	0	0	0	0	0	0	3	60	41	17	0.85
50 - 55	1	0	0	0	0	0	0	0	0	0	0	0	0	0	0	1	48	41	11	0.28
55 - 60	2	0	0	0	0	0	0	0	0	0	0	0	0	0	0	2	35	31	6	0.57
Totals	170	69	38	29	15	7	4	8	1	1	0	2	4	2	1	351				

Table 4. Comparison of current flow upcoast vs. downcoast.

	Summer		Non-Summer	
Buoys	Upcoast	Downcoast	Upcoast	Downcoast
R	47.17%	52.83%	21.37%	78.63%
F	61.55%	38.45%	22.30%	77.70%
B	55.66%	44.34%	29.16%	70.84%
W	46.82%	53.18%	21.06%	76.79%
D	46.29%	53.71%	58.54%	41.46%
J	21.69%	78.31%	50.68%	49.32%
K	13.59%	86.41%	48.31%	51.69%
N	73.17%	26.83%	70.93%	29.07%
V	71.76%	28.24%	63.30%	36.70%

However, not all buoy locations show the same upcoast trend during the summer. Buoys D, J, K, R, and W have higher numbers of downcoast currents present, with respective totals of 275, 592, 496, 495, and 351. Table 4 displays the total amount of time current flow is directed downcoast, with buoys D, J, K, R, and W showing dominant downcoast flow during the summer. The currents observed at buoys D, R, and W are centered at the 0-5 and 5-10 cm s^{-1} velocity classes, with at least 43% of observed currents documented within these ranges. Buoys J and K display more currents centered at the 5-10, 10-15, and 15-20 cm s^{-1} velocity classes, with 38-43% of currents observed in these velocity ranges. This means most downcoast currents are slow (velocity<10 cm s^{-1}) regardless of duration, with slightly faster currents observed along the southwestern shelf. Longer current durations are observed at the southern buoys, with currents lasting 1764 and 1878 hours at buoys J and K, respectively. At Buoys D, R, and W, respective

maximum current durations of 556, 476, and 500 hours are observed. At each location, maximum durations occur within the 0-5 cm s^{-1} velocity classes, indicating longer current durations tend to be slow.

Summer statistics are also evaluated in the upcoast direction at buoys D, J, K, R, and W. Fewer upcoast currents are observed at each of these locations, with respective totals of 237, 164, 78, 442, and 309. Fifty one-76% of the currents observed at these locations fall into the 0-5 and 5-10 cm s^{-1} velocity classes, meaning upcoast flow also tends to be slow regardless of duration. Maximum current durations are also observed, with durations of 992, 209, 189, 539 and 329 hours recorded at buoys D, J, K, R, and W. For buoys J, K, and W, these durations are less compared to when the flow is downcoast, while the upcoast durations are higher for buoys R and D.

Persistence statistics for the non-summer months are displayed in Table 5. Buoys R, B, F, W, and K have higher numbers of downcoast currents present, with respective totals of 2138, 2617, 2174, 1925, and 1224. Table 4 displays the total amount of time current flow is directed downcoast, with buoys R, B, F, W, and K showing dominant downcoast flow during the non-summer. The currents observed at these locations are centered at the 0-5, 5-10, and 10-15 cm s^{-1} velocity classes, with at least 45% of observed currents documented within these ranges. At each of these locations, maximum downcoast current durations are also observed. Longer current durations are observed at upper coastal buoys, with currents lasting 1067, 1303, 1229, and 1631 hours at buoys R, B, F, and W, respectively. At buoy K, the maximum current duration observed was 595

hours are observed. This maximum duration occurred within the 0-5 cm s^{-1} velocity classes, indicating longer current durations tend to be slow.

Non-summer statistics are also evaluated in the upcoast direction at buoys R, B, F, W, and K. Fewer upcoast currents are observed at each of these locations, with respective totals of 581, 1077, 624, 528, and 1144. At least 53% of the currents observed at these locations fall into the 0-5 and 5-10 cm s^{-1} velocity classes, meaning upcoast flow tends to be slow regardless of duration. Maximum current durations are also observed, with durations of 471, 410, 329, 247, and 990 hours recorded at buoys R, B, F, W, J, and K. Besides the maximum duration at buoy K, the upcoast current durations are shorter compared to when the flow is downcoast at upper coastal locations, meaning there are longer current durations downcoast compared to when the flow is upcoast during the non-summer.

Table 5. Non-summer persistence tables for TABS buoys.

Buoy B; Non-summers from 1995-2012

UPCOAST

U Velocity	Duration Limits (hours)															Duration Statistics (hours)				
(cm/s)	48	72	96	120	144	168	192	216	240	264	288	312	336	360	>360	Total	Max	Mean	Std Dev	% time
0 - 5	190	70	48	32	11	6	9	6	3	2	0	1	1	1	2	382	410	67	55	35.47
5 - 10	124	53	30	20	8	5	3	2	1	1	0	0	1	0	0	248	334	62	43	23.03
10 - 15	103	26	16	11	1	3	1	3	1	0	0	0	0	0	0	165	237	55	39	15.32
15 - 20	72	23	8	7	3	1	0	0	0	0	0	0	0	0	0	114	150	49	28	10.58
20 - 25	56	13	6	1	0	0	0	0	0	0	0	0	0	0	0	76	116	42	18	7.06
25 - 30	39	8	1	0	0	0	0	0	0	0	0	0	0	0	0	48	74	37	12	4.46
30 - 35	27	3	0	0	0	0	0	0	0	0	0	0	0	0	0	30	65	32	10	2.79
35 - 40	7	1	0	0	0	0	0	0	0	0	0	0	0	0	0	8	54	34	11	0.74
40 - 45	3	0	0	0	0	0	0	0	0	0	0	0	0	0	0	3	36	34	2	0.28
45 - 50	1	0	0	0	0	0	0	0	0	0	0	0	0	0	0	1	33	33	0	0.09
50 - 55	1	0	0	0	0	0	0	0	0	0	0	0	0	0	0	1	29	29	0	0.09
55 - 60	1	0	0	0	0	0	0	0	0	0	0	0	0	0	0	1	26	26	0	0.09
Totals	624	197	109	71	23	15	13	11	5	3	0	1	2	1	2	1077				

Table 5 continued

Buoy B; Non-summers from 1995-2012

DOWNCOAST

U Velocity	Duration Limits (hours)															Duration Statistics (hours)				
(cm/s)	48	72	96	120	144	168	192	216	240	264	288	312	336	360	>360	Total	Max	Mean	Std Dev	% time
0 - 5	135	79	52	24	37	27	26	11	15	16	8	11	4	2	43	490	1303	143	156	18.72
5 - 10	203	91	61	43	35	26	25	11	15	6	5	7	2	3	17	550	628	101	94	21.02
10 - 15	251	108	67	40	28	15	12	12	8	2	3	3	0	1	1	551	361	73	55	21.05
15 - 20	280	89	44	17	13	7	4	4	2	1	0	0	0	0	0	461	263	54	37	17.62
20 - 25	177	63	15	9	6	3	1	0	0	0	0	0	0	0	0	274	182	48	27	10.47
25 - 30	138	20	5	3	0	2	0	0	0	0	0	0	0	0	0	168	161	39	20	6.42
30 - 35	53	6	2	0	0	1	0	0	0	0	0	0	0	0	0	62	147	37	19	2.37
35 - 40	25	3	1	0	0	0	0	0	0	0	0	0	0	0	0	29	76	35	12	1.11
40 - 45	9	2	0	0	0	0	0	0	0	0	0	0	0	0	0	11	66	38	13	0.42
45 - 50	5	1	0	0	0	0	0	0	0	0	0	0	0	0	0	6	59	37	12	0.23
50 - 55	4	1	0	0	0	0	0	0	0	0	0	0	0	0	0	5	52	37	10	0.19
55 - 60	4	0	0	0	0	0	0	0	0	0	0	0	0	0	0	4	45	35	9	0.15
60 - 65	3	0	0	0	0	0	0	0	0	0	0	0	0	0	0	3	39	33	6	0.11
65 - 70	2	0	0	0	0	0	0	0	0	0	0	0	0	0	0	2	32	30	2	0.08
70 - 75	1	0	0	0	0	0	0	0	0	0	0	0	0	0	0	1	25	25	0	0.04
Totals	1290	463	247	136	119	81	68	38	40	25	16	21	6	6	61	2617				

Table 5 continued

Buoy D; Non-summers from 1996-2012

UPCOAST

U Velocity	Duration Limits (hours)															Duration Statistics (hours)				
(cm/s)	48	72	96	120	144	168	192	216	240	264	288	312	336	360	>360	Total	Max	Mean	Std Dev	% time
0 - 5	327	139	86	47	41	18	17	9	5	5	3	4	2	0	5	708	490	74	61	57.56
5 - 10	241	56	25	10	4	5	2	1	1	1	0	0	0	0	0	346	242	48	32	28.13
10 - 15	77	19	4	3	1	1	1	0	0	0	0	0	0	0	0	106	192	43	27	8.62
15 - 20	33	6	1	0	1	0	0	0	0	0	0	0	0	0	0	41	124	38	18	3.33
20 - 25	16	2	0	0	0	0	0	0	0	0	0	0	0	0	0	18	66	34	10	1.46
25 - 30	6	0	0	0	0	0	0	0	0	0	0	0	0	0	0	6	32	29	3	0.49
30 - 35	4	0	0	0	0	0	0	0	0	0	0	0	0	0	0	4	28	26	2	0.33
35 - 40	1	0	0	0	0	0	0	0	0	0	0	0	0	0	0	1	26	26	0	0.08
Totals	705	222	116	60	47	24	20	10	6	6	3	4	2	0	5	1230				

Table 5 continued

Buoy D; Non-summers from 1996-2012

DOWNCOAST

U Velocity	Duration Limits (hours)															Duration Statistics (hours)				
(cm/s)	48	72	96	120	144	168	192	216	240	264	288	312	336	360	>360	Total	Max	Mean	Std Dev	% time
0 - 5	364	108	57	32	8	9	4	3	1	1	0	0	0	0	0	587	256	53	33	67.39
5 - 10	146	34	11	3	0	0	0	0	0	0	0	0	0	0	0	194	116	41	18	22.27
10 - 15	48	7	2	0	0	0	0	0	0	0	0	0	0	0	0	57	74	37	12	6.54
15 - 20	17	3	0	0	0	0	0	0	0	0	0	0	0	0	0	20	65	36	12	2.3
20 - 25	7	1	0	0	0	0	0	0	0	0	0	0	0	0	0	8	57	36	10	0.92
25 - 30	3	0	0	0	0	0	0	0	0	0	0	0	0	0	0	3	33	29	4	0.34
30 - 35	1	0	0	0	0	0	0	0	0	0	0	0	0	0	0	1	29	29	0	0.11
35 - 40	1	0	0	0	0	0	0	0	0	0	0	0	0	0	0	1	26	26	0	0.11
Totals	587	153	70	35	8	9	4	3	1	1	0	0	0	0	0	871				

Table 5 continued

Buoy F; Non-summers from 1996-2012

UPCOAST

U Velocity	Duration Limits (hours)															Duration Statistics (hours)				
(cm/s)	48	72	96	120	144	168	192	216	240	264	288	312	336	360	>360	Total	Max	Mean	Std Dev	% time
0 - 5	157	59	36	21	7	4	1	1	2	2	0	0	1	0	0	291	329	59	41	46.41
5 - 10	103	26	16	6	2	2	2	1	0	0	0	1	0	0	0	159	310	52	38	25.36
10 - 15	58	17	7	1	1	1	0	0	0	0	0	0	0	0	0	85	165	45	24	13.56
15 - 20	31	14	0	0	0	0	0	0	0	0	0	0	0	0	0	45	72	40	14	7.18
20 - 25	20	2	0	0	0	0	0	0	0	0	0	0	0	0	0	22	64	35	10	3.51
25 - 30	10	1	0	0	0	0	0	0	0	0	0	0	0	0	0	11	53	35	7	1.75
30 - 35	9	0	0	0	0	0	0	0	0	0	0	0	0	0	0	9	42	29	5	1.44
35 - 40	2	0	0	0	0	0	0	0	0	0	0	0	0	0	0	2	36	31	7	0.32
40 - 45	1	0	0	0	0	0	0	0	0	0	0	0	0	0	0	1	32	32	0	0.16
45 - 50	1	0	0	0	0	0	0	0	0	0	0	0	0	0	0	1	28	28	0	0.16
50 - 55	1	0	0	0	0	0	0	0	0	0	0	0	0	0	0	1	25	25	0	0.16
Totals	390	119	59	28	10	7	3	2	2	2	0	1	1	0	0	624				

Table 5 continued

Buoy F; Non-summers from 1996-2012

DOWNCOAST

U Velocity	Duration Limits (hours)															Duration Statistics (hours)				
(cm/s)	48	72	96	120	144	168	192	216	240	264	288	312	336	360	>360	Total	Max	Mean	Std Dev	% time
0 - 5	78	59	47	31	22	35	18	13	17	9	8	7	12	7	45	408	1229	169	174	18.36
5 - 10	179	82	66	42	32	21	18	16	14	4	6	11	5	3	13	512	889	103	96	23.04
10 - 15	207	84	49	29	31	17	13	4	9	2	6	2	0	2	2	457	508	78	66	20.57
15 - 20	181	72	28	27	14	9	4	0	4	3	0	0	0	0	1	343	362	63	46	15.44
20 - 25	138	33	21	17	5	3	2	0	0	0	0	0	0	0	0	219	185	53	32	9.86
25 - 30	92	22	15	6	0	0	0	0	0	0	0	0	0	0	0	135	119	45	23	6.08
30 - 35	43	16	6	1	0	0	0	0	0	0	0	0	0	0	0	66	101	43	18	2.97
35 - 40	22	9	3	0	0	0	0	0	0	0	0	0	0	0	0	34	89	44	17	1.53
40 - 45	16	7	0	0	0	0	0	0	0	0	0	0	0	0	0	23	68	40	14	1.04
45 - 50	10	1	0	0	0	0	0	0	0	0	0	0	0	0	0	11	49	37	9	0.5
50 - 55	8	0	0	0	0	0	0	0	0	0	0	0	0	0	0	8	43	33	6	0.36
55 - 60	4	0	0	0	0	0	0	0	0	0	0	0	0	0	0	4	35	29	4	0.18
60 - 65	2	0	0	0	0	0	0	0	0	0	0	0	0	0	0	2	27	26	1	0.09
Totals	940	377	235	153	104	85	55	33	44	18	20	20	17	12	61	2174				

Table 5 continued

Buoy J; Non-summers from 1998-2012

UPCOAST

U Velocity (cm/s)	Duration Limits (hours)															Duration Statistics (hours)				
	48	72	96	120	144	168	192	216	240	264	288	312	336	360	>360	Total	Max	Mean	Std Dev	% time
0 - 5	116	53	38	27	17	9	10	5	8	3	4	3	0	1	7	301	844	92	90	17.47
5 - 10	121	43	36	20	13	9	7	8	4	3	2	1	0	2	3	272	836	84	84	15.79
10 - 15	121	51	27	22	7	7	5	5	2	0	0	0	0	2	2	251	831	73	73	14.57
15 - 20	111	41	24	15	8	4	2	2	2	0	1	0	0	2	1	213	696	66	66	12.36
20 - 25	94	28	23	10	6	2	2	3	0	1	1	0	1	1	0	172	352	64	52	9.98
25 - 30	76	28	13	8	5	3	2	1	1	1	0	0	0	1	0	139	346	62	49	8.07
30 - 35	57	24	11	4	4	1	2	1	1	0	0	0	0	1	0	106	342	59	47	6.15
35 - 40	49	16	6	3	2	1	1	1	0	0	0	0	0	1	0	80	338	57	48	4.64
40 - 45	47	5	4	2	1	1	1	1	0	0	0	0	1	0	0	63	334	53	51	3.66
45 - 50	25	9	3	1	0	2	0	0	0	1	0	0	0	0	0	41	247	56	44	2.38
50 - 55	14	9	1	1	1	1	0	0	0	0	0	0	0	0	0	27	145	51	31	1.57
55 - 60	14	6	1	0	1	0	0	0	0	0	0	0	0	0	0	22	140	46	26	1.28
60 - 65	8	3	0	0	1	0	0	0	0	0	0	0	0	0	0	12	135	45	29	0.7
65 - 70	7	1	0	0	0	0	0	0	0	0	0	0	0	0	0	8	72	41	17	0.46
70 - 75	4	1	0	0	0	0	0	0	0	0	0	0	0	0	0	5	57	40	12	0.29
75 - 80	3	1	0	0	0	0	0	0	0	0	0	0	0	0	0	4	51	39	8	0.23
80 - 85	4	0	0	0	0	0	0	0	0	0	0	0	0	0	0	4	43	34	6	0.23
85 - 90	2	0	0	0	0	0	0	0	0	0	0	0	0	0	0	2	30	29	1	0.12
90 - 95	1	0	0	0	0	0	0	0	0	0	0	0	0	0	0	1	25	25	0	0.06
Totals	874	319	187	113	66	40	32	27	18	9	8	4	2	11	13	1723				

Table 5 continued

Buoy J; Non-summers from 1998-2012

DOWNCOAST

U Velocity	Duration Limits (hours)															Duration Statistics (hours)				
(cm/s)	48	72	96	120	144	168	192	216	240	264	288	312	336	360	>360	Total	Max	Mean	Std Dev	% time
0 - 5	105	38	37	24	18	14	7	8	6	6	4	8	2	5	12	294	664	113	105	17.53
5 - 10	108	43	32	24	21	7	8	11	8	4	3	3	3	2	3	280	612	96	86	16.7
10 - 15	97	42	34	23	10	6	14	8	4	2	3	2	2	1	2	250	573	88	75	14.91
15 - 20	95	46	28	13	6	5	12	8	3	1	2	2	0	1	0	222	344	78	62	13.24
20 - 25	77	43	20	11	4	5	5	6	1	2	0	1	0	0	0	175	295	70	53	10.44
25 - 30	70	36	11	7	4	6	4	1	1	0	0	0	0	0	0	140	288	64	48	8.35
30 - 35	67	27	11	4	5	2	0	0	0	0	0	0	0	0	0	116	166	52	30	6.92
35 - 40	57	12	5	4	1	0	0	0	0	0	0	0	0	0	0	79	127	46	23	4.71
40 - 45	36	10	3	2	0	0	0	0	0	0	0	0	0	0	0	51	115	44	21	3.04
45 - 50	19	7	2	0	0	0	0	0	0	0	0	0	0	0	0	28	91	42	17	1.67
50 - 55	14	3	0	0	0	0	0	0	0	0	0	0	0	0	0	17	56	36	11	1.01
55 - 60	10	0	0	0	0	0	0	0	0	0	0	0	0	0	0	10	47	36	7	0.6
60 - 65	7	0	0	0	0	0	0	0	0	0	0	0	0	0	0	7	42	34	5	0.42
65 - 70	7	0	0	0	0	0	0	0	0	0	0	0	0	0	0	7	36	29	4	0.42
70 - 75	1	0	0	0	0	0	0	0	0	0	0	0	0	0	0	1	28	26	2	0.06
Totals	770	307	183	112	69	45	50	42	23	15	12	16	7	9	17	1677				

Table 5 continued

Buoy K; Non-summers from 1998-2012

UPCOAST

U Velocity (cm/s)	Duration Limits (hours)															Duration Statistics (hours)				
	48	72	96	120	144	168	192	216	240	264	288	312	336	360	>360	Total	Max	Mean	Std Dev	% time
0 - 5	167	51	33	19	17	9	12	2	3	2	1	2	0	1	5	324	990	76	83	28.32
5 - 10	166	52	22	16	11	2	3	3	4	1	1	1	0	1	1	284	605	63	59	24.83
10 - 15	126	39	14	9	5	2	0	3	1	1	1	0	0	0	0	201	288	55	43	17.57
15 - 20	85	21	9	3	2	2	0	0	1	2	0	0	0	0	0	125	264	52	41	10.93
20 - 25	71	8	7	1	2	1	0	1	0	0	0	0	0	0	0	91	210	44	30	7.95
25 - 30	39	4	4	2	1	0	0	1	0	0	0	0	0	0	0	51	198	44	33	4.46
30 - 35	17	5	1	0	1	1	0	0	0	0	0	0	0	0	0	25	165	47	34	2.19
35 - 40	11	2	0	1	0	1	0	0	0	0	0	0	0	0	0	15	152	50	36	1.31
40 - 45	6	2	0	2	0	0	0	0	0	0	0	0	0	0	0	10	102	48	27	0.87
45 - 50	3	1	1	0	0	0	0	0	0	0	0	0	0	0	0	5	96	47	29	0.44
50 - 55	2	0	1	0	0	0	0	0	0	0	0	0	0	0	0	3	90	47	37	0.26
55 - 60	0	0	1	0	0	0	0	0	0	0	0	0	0	0	0	1	85	85	0	0.09
60 - 65	0	0	1	0	0	0	0	0	0	0	0	0	0	0	0	1	81	81	0	0.09
65 - 70	0	0	1	0	0	0	0	0	0	0	0	0	0	0	0	1	76	76	0	0.09
70 - 75	0	1	0	0	0	0	0	0	0	0	0	0	0	0	0	1	71	71	0	0.09
75 - 80	0	1	0	0	0	0	0	0	0	0	0	0	0	0	0	1	66	66	0	0.09
80 - 85	0	1	0	0	0	0	0	0	0	0	0	0	0	0	0	1	60	60	0	0.09
85 - 90	0	1	0	0	0	0	0	0	0	0	0	0	0	0	0	1	55	55	0	0.09
90 - 95	0	1	0	0	0	0	0	0	0	0	0	0	0	0	0	1	49	49	0	0.09
95 - 100	1	0	0	0	0	0	0	0	0	0	0	0	0	0	0	1	41	41	0	0.09
100 - 105	1	0	0	0	0	0	0	0	0	0	0	0	0	0	0	1	33	33	0	0.09
Totals	695	190	95	53	39	18	15	10	9	6	3	3	0	2	6	1144				

Table 5 continued

Buoy K; Non-summers from 1998-2012

DOWNCOAST

U Velocity	Duration Limits (hours)															Duration Statistics (hours)				
(cm/s)	48	72	96	120	144	168	192	216	240	264	288	312	336	360	>360	Total	Max	Mean	Std Dev	% time
0 - 5	115	70	34	31	21	15	9	6	3	6	2	3	1	3	10	329	595	97	94	26.88
5 - 10	136	52	40	23	10	5	3	1	2	3	3	1	1	1	7	288	588	79	81	23.53
10 - 15	121	47	18	19	6	4	2	3	0	0	3	0	1	1	5	230	578	71	74	18.79
15 - 20	82	26	15	7	4	4	2	1	1	2	0	1	0	0	2	147	557	67	70	12.01
20 - 25	51	15	9	8	4	2	0	0	2	0	0	1	0	0	1	93	412	66	59	7.6
25 - 30	43	16	3	4	1	1	0	1	0	1	0	0	0	0	0	70	250	54	41	5.72
30 - 35	26	8	1	1	0	1	0	0	0	0	0	0	0	0	0	37	148	45	23	3.02
35 - 40	15	2	0	1	0	0	0	0	0	0	0	0	0	0	0	18	114	39	21	1.47
40 - 45	7	1	0	0	0	0	0	0	0	0	0	0	0	0	0	8	50	34	10	0.65
45 - 50	3	0	0	0	0	0	0	0	0	0	0	0	0	0	0	3	40	35	4	0.25
50 - 55	1	0	0	0	0	0	0	0	0	0	0	0	0	0	0	1	34	34	0	0.08
Totals	600	237	120	94	46	32	16	12	8	12	8	6	3	5	25	1224				

Table 5 continued

Buoy N; Non-summers from 1998-2012

UPCOAST

U Velocity	Duration Limits (hours)															Duration Statistics (hours)				
(cm/s)	48	72	96	120	144	168	192	216	240	264	288	312	336	360	>360	Total	Max	Mean	Std Dev	% time
0 - 5	53	30	25	16	6	7	7	8	4	6	2	1	1	0	35	201	2279	191	282	18.68
5 - 10	65	36	20	18	8	3	8	8	7	3	5	2	2	2	20	207	1772	144	200	19.24
10 - 15	79	33	26	6	9	13	10	3	4	4	1	2	2	2	6	200	1254	108	148	18.59
15 - 20	69	34	13	16	8	4	4	0	0	2	2	2	2	0	5	161	637	88	101	14.96
20 - 25	55	18	12	10	6	4	1	1	2	2	0	0	1	0	2	114	502	79	79	10.59
25 - 30	39	15	11	4	1	0	4	2	0	0	0	1	0	0	1	78	460	71	67	7.25
30 - 35	25	13	4	2	1	1	1	0	0	1	0	0	0	0	1	49	373	65	62	4.55
35 - 40	14	5	2	0	0	3	0	0	0	0	0	0	0	0	1	25	363	68	71	2.32
40 - 45	13	2	3	1	0	0	0	0	1	0	0	0	0	0	0	20	223	54	45	1.86
45 - 50	8	1	1	0	0	0	0	0	0	0	0	0	0	0	0	10	92	45	19	0.93
50 - 55	2	1	1	0	0	0	0	0	0	0	0	0	0	0	0	4	84	50	25	0.37
55 - 60	0	1	1	0	0	0	0	0	0	0	0	0	0	0	0	2	75	62	18	0.19
60 - 65	1	1	0	0	0	0	0	0	0	0	0	0	0	0	0	2	64	54	14	0.19
65 - 70	2	0	0	0	0	0	0	0	0	0	0	0	0	0	0	2	45	38	10	0.19
70 - 75	1	0	0	0	0	0	0	0	0	0	0	0	0	0	0	1	32	32	0	0.09
Totals	426	190	119	73	39	35	35	22	18	18	10	8	8	4	71	1076				

Table 5 continued

Buoy N; Non-summers from 1998-2012

DOWNCOAST

U Velocity	Duration Limits (hours)															Duration Statistics (hours)				
(cm/s)	48	72	96	120	144	168	192	216	240	264	288	312	336	360	>360	Total	Max	Mean	Std Dev	% time
0 - 5	52	33	21	14	10	4	4	5	3	2	3	1	2	1	5	160	507	99	93	36.28
5 - 10	45	25	16	11	4	6	2	2	1	2	0	0	0	2	1	117	402	80	67	26.53
10 - 15	39	16	8	5	4	1	0	1	2	0	0	0	0	0	0	76	230	62	44	17.23
15 - 20	14	15	7	0	2	1	0	0	0	0	0	0	0	0	0	39	148	60	29	8.84
20 - 25	16	9	1	1	0	0	0	0	0	0	0	0	0	0	0	27	99	47	17	6.12
25 - 30	7	3	1	0	0	0	0	0	0	0	0	0	0	0	0	11	74	42	19	2.49
30 - 35	1	3	0	0	0	0	0	0	0	0	0	0	0	0	0	4	55	43	13	0.91
35 - 40	3	1	0	0	0	0	0	0	0	0	0	0	0	0	0	4	49	37	9	0.91
40 - 45	1	0	0	0	0	0	0	0	0	0	0	0	0	0	0	1	42	42	0	0.23
45 - 50	1	0	0	0	0	0	0	0	0	0	0	0	0	0	0	1	36	36	0	0.23
50 - 55	1	0	0	0	0	0	0	0	0	0	0	0	0	0	0	1	28	28	0	0.23
Totals	180	105	54	31	20	12	6	8	6	4	3	1	2	3	6	441				

Table 5 continued

Buoy R; Non-summers from 1998-2012

UPCOAST

U Velocity	Duration Limits (hours)															Duration Statistics (hours)				
(cm/s)	48	72	96	120	144	168	192	216	240	264	288	312	336	360	>360	Total	Max	Mean	Std Dev	% time
0 - 5	106	45	27	13	9	3	3	0	0	1	1	0	0	0	2	210	471	65	54	36.14
5 - 10	74	32	14	12	5	2	0	0	0	0	0	0	0	0	0	139	167	56	31	23.92
10 - 15	66	25	8	2	0	1	0	0	0	0	0	0	0	0	0	102	149	46	22	17.56
15 - 20	43	16	3	0	0	0	0	0	0	0	0	0	0	0	0	62	82	42	15	10.67
20 - 25	29	5	2	0	0	0	0	0	0	0	0	0	0	0	0	36	74	39	13	6.2
25 - 30	16	3	0	0	0	0	0	0	0	0	0	0	0	0	0	19	66	37	11	3.27
30 - 35	8	1	0	0	0	0	0	0	0	0	0	0	0	0	0	9	60	33	11	1.55
35 - 40	2	1	0	0	0	0	0	0	0	0	0	0	0	0	0	3	53	35	15	0.52
40 - 45	1	0	0	0	0	0	0	0	0	0	0	0	0	0	0	1	43	43	0	0.17
Totals	345	128	54	27	14	6	3	0	0	1	1	0	0	0	2	581				

Table 5 continued

Buoy R; Non-summers from 1998-2012

DOWNCOAST

U Velocity	Duration Limits (hours)															Duration Statistics (hours)				
(cm/s)	48	72	96	120	144	168	192	216	240	264	288	312	336	360	>360	Total	Max	Mean	Std Dev	% time
0 - 5	55	50	31	13	19	21	14	18	13	12	8	7	6	1	34	302	1067	174	174	14.07
5 - 10	95	57	31	23	19	19	17	13	14	7	4	4	2	2	24	331	931	134	140	15.42
10 - 15	112	75	48	23	25	11	8	7	4	3	7	3	3	2	12	343	879	101	102	15.98
15 - 20	139	57	41	18	12	8	6	6	4	3	7	4	0	2	2	309	689	82	77	14.39
20 - 25	130	42	26	12	10	8	3	8	2	4	2	2	0	1	1	251	388	72	63	11.69
25 - 30	102	44	12	9	7	6	6	2	0	2	1	0	0	0	1	192	380	64	53	8.94
30 - 35	84	28	10	11	7	2	1	0	1	1	0	0	0	0	0	145	251	58	40	6.75
35 - 40	59	27	7	4	3	1	2	0	0	0	0	0	0	0	0	103	175	53	33	4.8
40 - 45	41	13	4	5	2	1	0	0	0	0	0	0	0	0	0	66	163	51	30	3.07
45 - 50	32	9	5	1	1	0	0	0	0	0	0	0	0	0	0	48	138	47	23	2.24
50 - 55	22	5	2	1	1	0	0	0	0	0	0	0	0	0	0	31	124	43	24	1.44
55 - 60	13	3	1	0	0	0	0	0	0	0	0	0	0	0	0	17	76	38	15	0.79
Totals	884	410	218	120	106	77	57	54	38	32	29	20	11	8	74	2138				

Table 5 continued

Buoy V; Non-summers from 2002-2012

UPCOAST

U Velocity	Duration Limits (hours)															Duration Statistics (hours)				
(cm/s)	48	72	96	120	144	168	192	216	240	264	288	312	336	360	>360	Total	Max	Mean	Std Dev	% time
0 - 5	75	31	22	10	17	9	11	4	2	3	6	3	2	0	14	209	1090	125	155	25.24
5 - 10	85	31	16	11	10	10	9	5	4	2	3	0	1	2	7	196	543	97	97	23.67
10 - 15	70	27	20	10	11	5	1	2	1	0	1	1	0	0	5	154	493	80	83	18.6
15 - 20	47	27	11	5	4	2	1	1	0	0	0	0	0	0	4	102	479	73	78	12.32
20 - 25	48	9	5	5	1	0	3	1	0	0	0	1	0	0	0	73	291	57	49	8.82
25 - 30	25	4	3	2	0	1	2	0	0	0	1	0	0	0	0	38	278	60	53	4.59
30 - 35	13	0	3	2	0	0	2	0	0	0	0	0	0	0	0	20	169	62	46	2.42
35 - 40	6	2	2	2	1	0	0	0	0	0	0	0	0	0	0	13	124	63	38	1.57
40 - 45	5	0	3	0	0	0	0	0	0	0	0	0	0	0	0	8	86	54	22	0.97
45 - 50	6	0	2	0	0	0	0	0	0	0	0	0	0	0	0	8	79	40	22	0.97
50 - 55	0	2	0	0	0	0	0	0	0	0	0	0	0	0	0	2	65	59	7	0.24
55 - 60	2	0	0	0	0	0	0	0	0	0	0	0	0	0	0	2	43	39	6	0.24
60 - 65	2	0	0	0	0	0	0	0	0	0	0	0	0	0	0	2	36	30	8	0.24
65 - 70	1	0	0	0	0	0	0	0	0	0	0	0	0	0	0	1	30	30	0	0.12
Totals	385	133	87	47	44	27	29	13	7	5	11	5	3	2	30	828				

Table 5 continued

Buoy V; Non-summers from 2002-2012

DOWNCOAST

U Velocity	Duration Limits (hours)															Duration Statistics (hours)				
(cm/s)	48	72	96	120	144	168	192	216	240	264	288	312	336	360	>360	Total	Max	Mean	Std Dev	% time
0 - 5	68	40	23	7	11	9	2	6	6	3	0	0	2	0	6	183	584	93	95	38.13
5 - 10	64	25	7	15	4	1	3	6	3	0	0	0	0	0	1	129	533	75	69	26.88
10 - 15	39	20	11	5	0	3	1	1	0	0	1	0	0	0	0	81	278	62	44	16.88
15 - 20	24	8	5	1	4	1	0	0	0	0	0	0	0	0	0	43	162	56	36	8.96
20 - 25	13	4	3	1	0	0	0	0	0	0	0	0	0	0	0	21	116	50	26	4.38
25 - 30	8	2	2	0	0	0	0	0	0	0	0	0	0	0	0	12	91	47	21	2.5
30 - 35	7	0	0	0	0	0	0	0	0	0	0	0	0	0	0	7	46	36	7	1.46
35 - 40	3	0	0	0	0	0	0	0	0	0	0	0	0	0	0	3	37	31	6	0.63
40 - 45	1	0	0	0	0	0	0	0	0	0	0	0	0	0	0	1	30	30	0	0.21
Totals	227	99	51	29	19	14	6	13	9	3	1	0	2	0	7	480				

Table 5 continued

Buoy W; Non-summers from 2002-2012

UPCOAST

U Velocity	Duration Limits (hours)															Duration Statistics (hours)				
(cm/s)	48	72	96	120	144	168	192	216	240	264	288	312	336	360	>360	Total	Max	Mean	Std Dev	% time
0 - 5	84	37	17	15	5	8	4	1	2	1	0	0	0	0	0	174	247	66	46	32.95
5 - 10	66	19	10	8	5	4	2	1	0	0	0	0	0	0	0	115	207	60	40	21.78
10 - 15	43	9	15	4	5	0	1	0	0	0	0	0	0	0	0	77	191	58	35	14.58
15 - 20	28	16	6	1	3	0	0	0	0	0	0	0	0	0	0	54	131	51	26	10.23
20 - 25	27	11	2	0	0	0	0	0	0	0	0	0	0	0	0	40	76	43	14	7.58
25 - 30	24	5	0	0	0	0	0	0	0	0	0	0	0	0	0	29	64	38	10	5.49
30 - 35	16	2	0	0	0	0	0	0	0	0	0	0	0	0	0	18	55	35	9	3.41
35 - 40	9	0	0	0	0	0	0	0	0	0	0	0	0	0	0	9	48	33	7	1.7
40 - 45	6	0	0	0	0	0	0	0	0	0	0	0	0	0	0	6	41	31	6	1.14
45 - 50	3	0	0	0	0	0	0	0	0	0	0	0	0	0	0	3	32	28	4	0.57
50 - 55	1	0	0	0	0	0	0	0	0	0	0	0	0	0	0	1	30	30	0	0.19
55 - 60	1	0	0	0	0	0	0	0	0	0	0	0	0	0	0	1	27	27	0	0.19
60 - 65	1	0	0	0	0	0	0	0	0	0	0	0	0	0	0	1	25	25	0	0.19
Totals	309	99	50	28	18	12	7	2	2	1	0	0	0	0	0	528				

Table 5 continued

Buoy W; Non-summers from 2002-2012

DOWNCOAST

U Velocity	Duration Limits (hours)															Duration Statistics (hours)				
(cm/s)	48	72	96	120	144	168	192	216	240	264	288	312	336	360	>360	Total	Max	Mean	Std Dev	% time
0 - 5	55	35	24	24	14	11	14	14	8	11	7	8	3	3	29	260	1631	176	193	13.51
5 - 10	77	49	43	28	16	18	14	8	12	6	11	8	4	0	14	308	780	127	121	16
10 - 15	104	63	34	23	17	18	14	7	8	2	6	7	1	1	8	313	771	103	96	16.26
15 - 20	133	57	39	27	12	10	7	3	5	1	3	1	1	0	5	304	543	80	72	15.79
20 - 25	134	50	25	19	12	4	4	2	1	4	0	1	0	0	2	258	382	67	56	13.4
25 - 30	118	37	22	7	8	3	2	1	0	0	1	1	0	0	0	200	303	56	41	10.39
30 - 35	80	18	18	5	0	1	1	1	0	1	1	0	0	0	0	126	267	53	40	6.55
35 - 40	64	14	6	3	0	0	1	1	0	0	0	0	0	0	0	89	214	46	31	4.62
40 - 45	28	10	3	0	0	0	0	1	0	0	0	0	0	0	0	42	200	43	29	2.18
45 - 50	16	2	1	0	0	0	0	0	0	0	0	0	0	0	0	19	78	34	14	0.99
50 - 55	5	0	0	0	0	0	0	0	0	0	0	0	0	0	0	5	42	33	7	0.26
55 - 60	1	0	0	0	0	0	0	0	0	0	0	0	0	0	0	1	29	29	0	0.05
Totals	815	335	215	136	79	65	57	38	34	25	29	26	9	4	58	1925				

Different seasonal persistence trends are observed during the non-summer at buoys D, J, N, and V. More upcoast currents are present at these locations, with totals of 1230, 1723, 1076, and 828, respectively. Table 4 shows the amount of time current flow is flowing upcoast, with buoys D, J, N, and V showing dominant upcoast flow in the non-summer. Currents observed are centered at the 0-5 and 5-10 cm s^{-1} velocity classes, with at least 33% of observed currents documented within these ranges. This means most upcoast currents are slow (<10 cm s^{-1}) regardless of duration. Longer current durations are observed at offshore buoys, with currents lasting 2279 and 1090 hours at buoys N and V, respectively. At buoys D and J, respective maximum current durations of 490 and 844 hours are observed. At each location, maximum durations occur within the 0-5 cm s^{-1} velocity classes, indicating longer current durations tend to be slow.

Non-summer statistics are also evaluated in the downcoast direction at buoys D, J, N and V. Fewer downcoast currents are observed at each of these locations, with respective totals of 871, 1677, 441, and 480. At least 43% of the currents observed at these locations fall into the 0-5 and 5-10 cm s^{-1} velocity classes, meaning downcoast flow also tends to be slow regardless of duration. Maximum current durations are also observed, with durations of 256, 664, 507, and 584 hours recorded at buoys D, J, N and V. These durations are less compared to when the flow is upcoast, indicating there is longer current durations upcoast compared to when the flow is downcoast.

Persistence statistics are input into a one-way ANOVA to determine if seasonal differences are statistically significant. At coastal buoys B, F, R, and W, current persistence during the summer is significantly different than non-summer, as displayed

in Figure 10. At each of these locations, current duration is longer during the summer, with means of 104.16, 105.05, 110.38, and 85.09 hours, respectively. Durations during the non-summer months at these locations tend to fall between 35-60 hours. Other locations experience significant differences in persistence, but between non-summer months. Buoy D and V have significant differences in current duration between winter and spring (Figure 11). At buoy V, spring has longer current persistence, with a mean duration of 150.55 hours, compared to a mean duration of 85.39 hours in the winter. Longer current durations occur during the winter at buoy D, with an average persistence of 79.16 hours, compared to 53.79 hours in the spring. There is also a significant difference between fall and spring at buoy D, with fall having a longer duration, an average of 75.55 hours compared to spring. In addition, there is a significant difference in persistence between fall and winter at buoy K (Figure 12). Fall has longer mean current persistence, at 82.42 hours, compared to winter with 52.50 hours. No significant seasonal differences in persistence are found at buoys J and N (Figure 13).

In addition to quantifying reversals and persistence in current flow, the length of transport is calculated. Transport is calculated by multiplying the current velocity and reversal duration, taking into account the area under the reversal curve, and is given in terms of distance. Figure 14 displays the seasonal upcoast transport present at each buoy location. Buoys R, F, B, and W show longer upcoast transport during the summer, with respective distances of 338.61, 460.97, 428.27, and 287.45 km. Transport during the non-summer typically falls well below 280 km at these locations, meaning less upcoast transport occurs in the non-summer months.

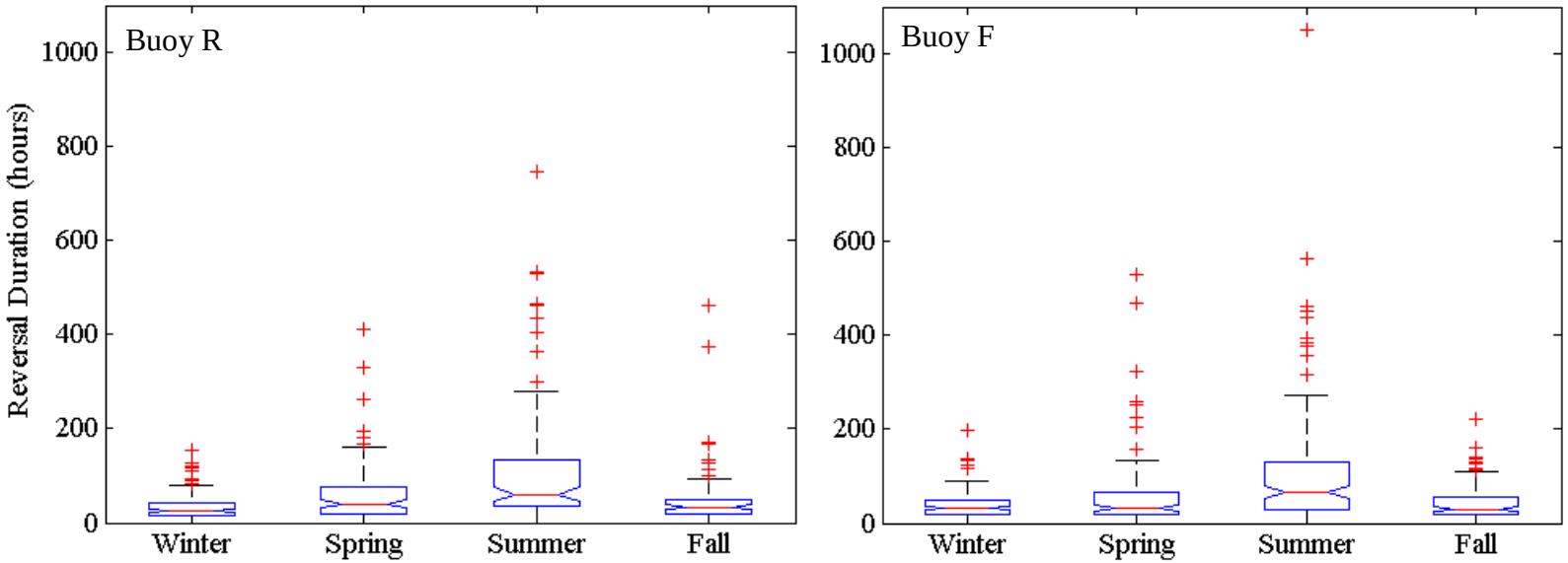

Figure 10. ANOVA for seasonal current persistence at buoys R, F, B, and W. Seasonal current persistence is displayed at buoys R, F, B, and W. Each location shows current persistence is significantly different during the summer compared to the non-summer months. (Buoy R – F=17.16, probability>p=1.60569e^{-10}; Buoy F – F=18.44, probability>p=2.15945e^{-11}; Buoy B – F=21.36, probability>p=3.05034e^{-13}; Buoy W – F=9.68, probability>p=3.64633e^{-06})

Figure 10 continued

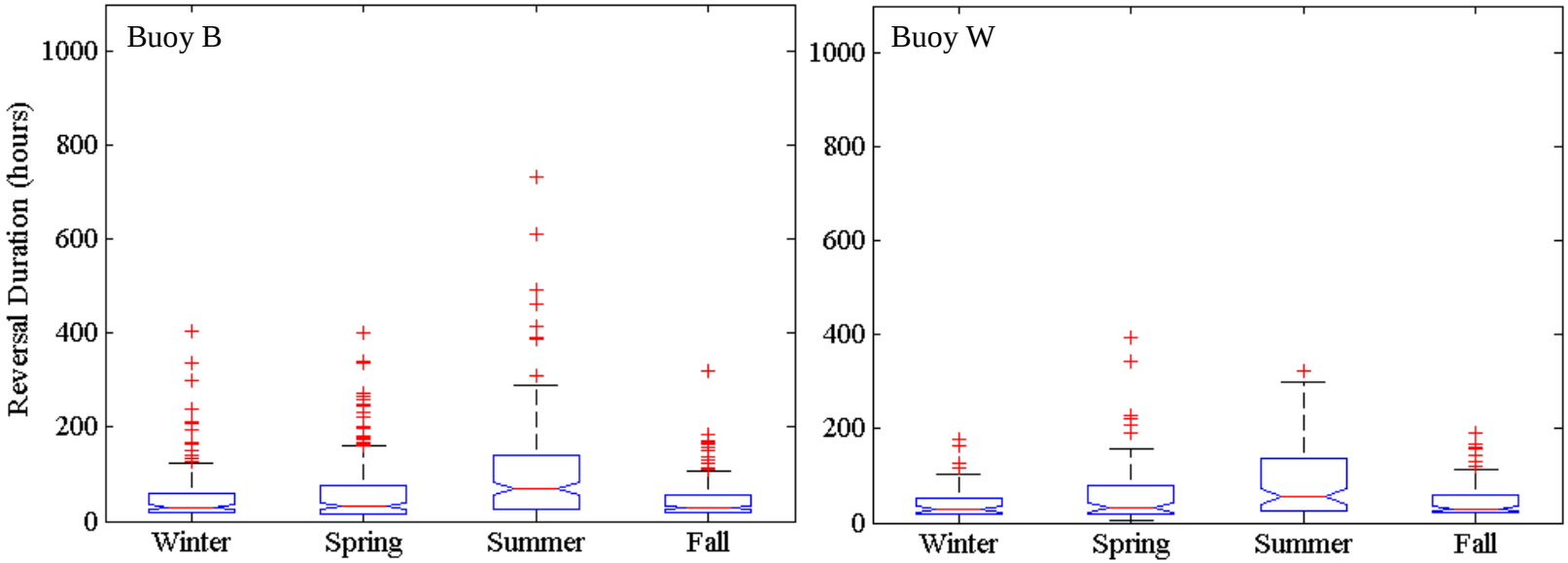

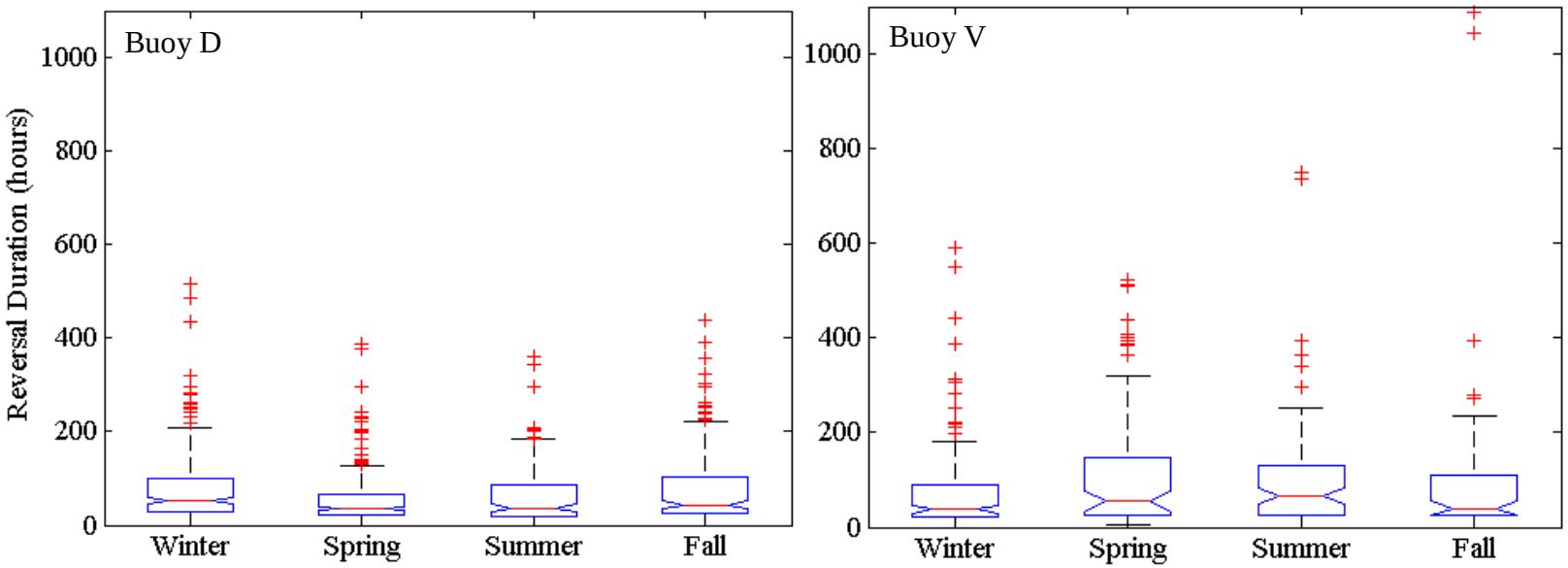

Figure 11. ANOVA for seasonal current persistence at buoys D and V. Buoy D has a significant difference in current persistence between winter and spring and fall and spring. Longer current durations occur during the winter and fall compared to spring at this location. Buoy V has a significant difference in persistence between winter and spring as well, but with longer current durations during the spring. (Buoy D – F=7.27, probability>p=8.02665e^{-05}; Buoy V – F=2.51, probability>p=.0589)

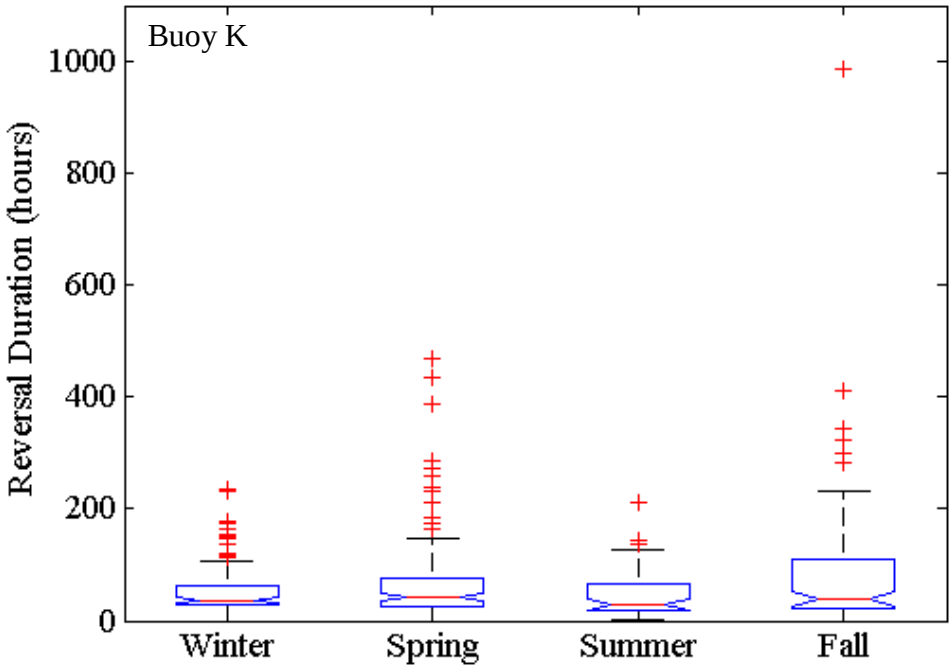

Figure 12. ANOVA for seasonal current persistence at buoy K. There is a significant difference in current persistence present between winter and fall, with fall having longer current durations compared to winter. (F=3.54, probability>p=.0147)

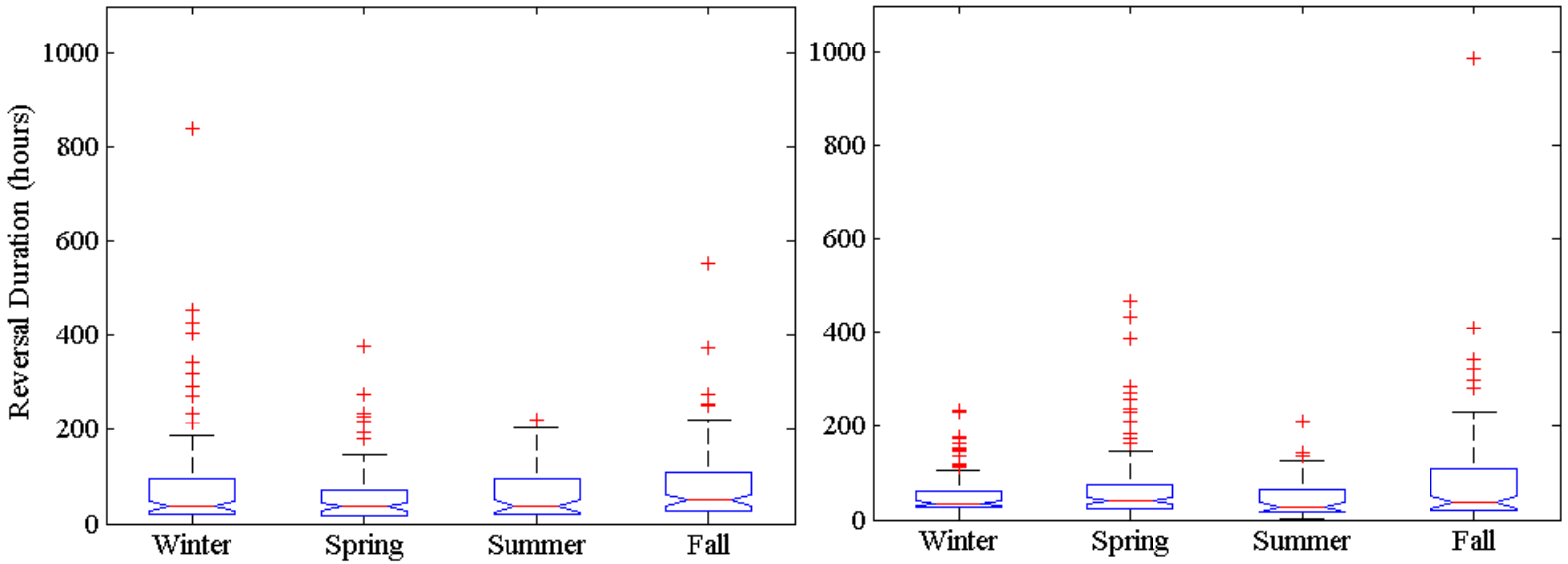

Figure 13. ANOVA for seasonal current persistence at buoys J and N. No significant differences in current persistence are found between seasons at both locations. (Buoy J – F=2.59, probability>p=.0524; Buoy N – F=1.37, probability>p=.2516)

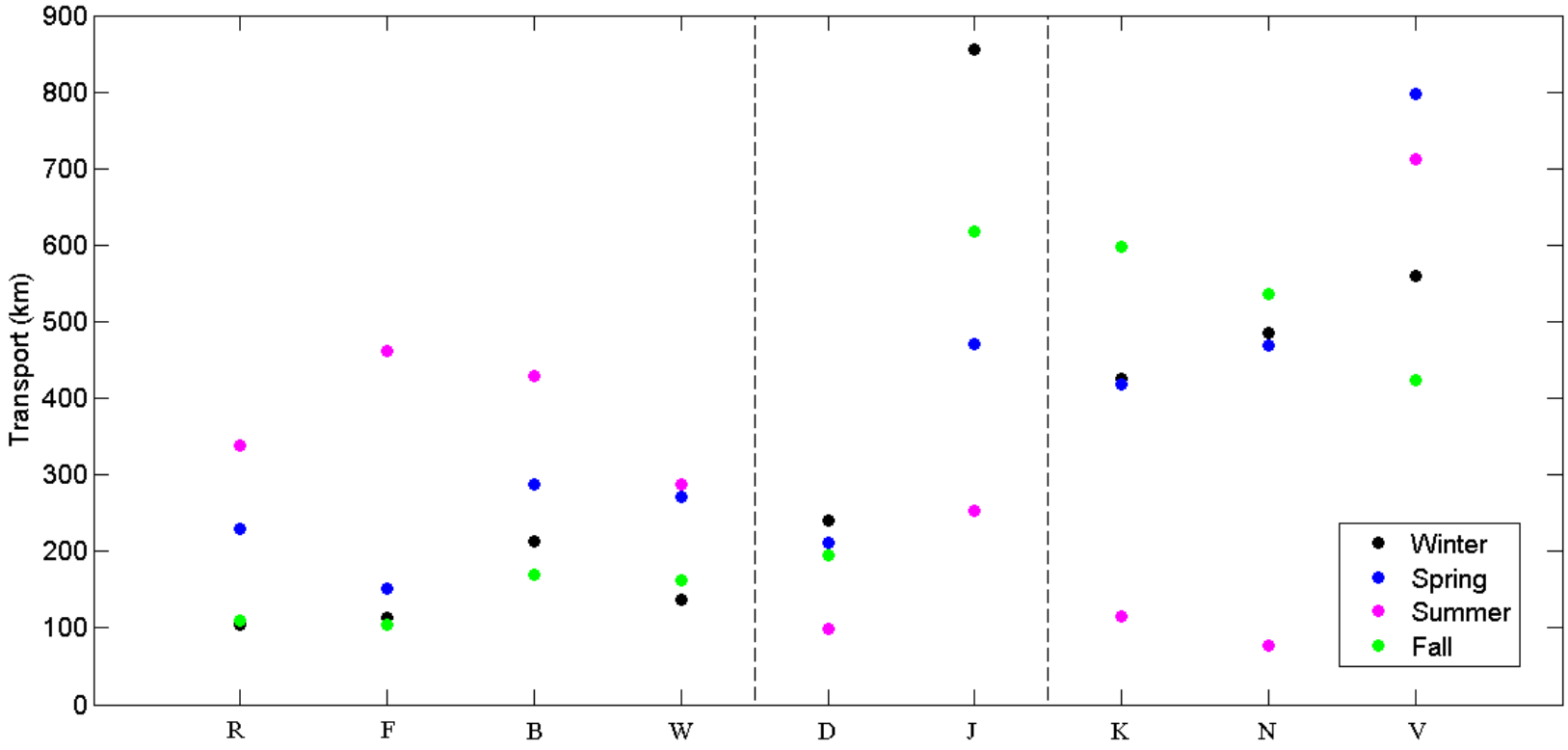

Figure 14. Seasonal upcoast transport comparison. The length of the upcoast transport by season is shown. More upcoast transport occurs during the summer for buoys R, F, B, and W than any other season. Buoys D and J have higher upcoast transport during the winter. Offshore buoys K and N have higher upcoast transport during the spring while buoy V has higher upcoast transport during the spring.

Buoys D and J have longer upcoast transport during the winter months, with distances of 241.10 and 855.72 km, respectively. Transport is still relatively long during the spring and fall months for both buoys D and J. The distance of transport at buoy D is 210.83 km during the spring and 195.35 km during the fall. Buoy J has transport distances of 470.04 km in the spring and 618.13 km during the fall. Both buoys D and J have lower transport distances during the summer months, with respective distances of 98.23 km and 252.24 km.

Upcoast transport is longer during the fall months at buoys K and N, with distances of 598.27 and 537.0 km respectively. Transport remains long during the other non-summer months, with winter distances of 425.57 km at buoy K and 469.16 km at buoy N. Fall distances at buoys K and N are 598.27 km and 537.0 km, respectively. Upcoast transport is shortest during the summer months at both locations, with respective distances of 115.07 km and 77.27 km observed.

Buoy V has higher transport during the spring and summer, with respective distances of 796.86 and 712.69 km. Upcoast transport is lower during the winter at this location, with a distance of 560.64 observed. Fall tends to have the lowest transport distance at this location, with 423.61 km.

ANOVAs are used to evaluate the seasonal differences in spectral energy of current velocity within the weather band frequencies. Results show significant seasonal differences only occur at buoys J and R (Figure 15). All other buoys have no significant differences in the spectral variance between the seasons, meaning there is little variance in the spectral energy within the weather band frequencies throughout the year at these

locations. However, in general, summer has the least variance in the weather band at all buoy locations.

At buoy J, spring has more spectral variance compared to summer. This means that there is more variance in the current velocity during the spring at buoy J in the weather band frequencies. This is likely due to the frequent passages of fronts and air masses during the spring months. Significantly less variance is present in weather band spectral energy during the summer. Some variance is present within the winter and spring spectral energy at buoy J.

Buoy R has significantly higher spectral variance present during the spring. This means that more variance is present in the current energy during the spring in the 2-15 day timescale. Again, this is likely due to the most frequent passages of fronts and air masses. Winter, summer, and fall all have significantly less variance present at this location.

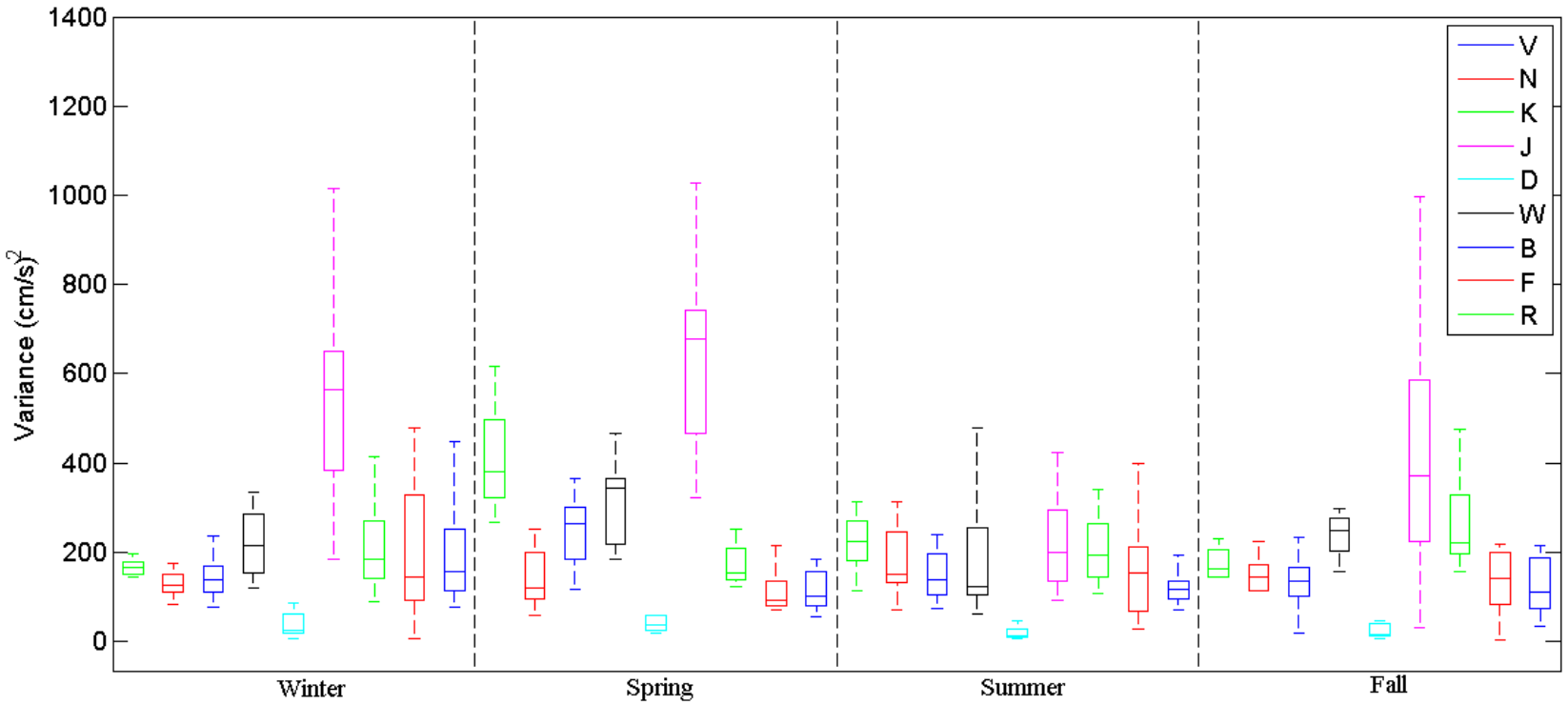

Figure 15. Seasonal spectral variance comparison. Spectral energy from current velocities within the weather band frequencies are compared. Winter and spring tend to have more variance, while summer has the least variance present. Buoy J has the greatest variance throughout the year, while buoy D has the least variance.

Wavelet analysis shows some consistency regarding frequency variance at buoy locations. Within the 2-15 day scale-average time series, spring has the most variance at buoys R, F, B, N, and V (Figures 16-20), likely due to increased frontal activity in the spring months. Some variability is present in the other non-summer months at these locations, but summer consistently has the least variance within the weather band. Buoys W, D, J, and K have most variability in non-summer months (Figures 21-24), while summer has the least variance at these locations within the weather band frequencies.

Wavelet transforms also display patterns of variance within the weather band frequencies. Figures 25-33 show wavelet spectrums for each buoy location. All buoy locations show the greatest energy variability is present during the 1-4 day time periods. Greatest relative power, shown in red, is present consistently around the 4-day time period. Relative power decreases as the time period decreases, with the least relative power, shown in blue, present consistently around the 1-day time period. Peaks in relative current power are also present in the 8-16 day time period, consistent with the weather band.

At certain locations on the Texas-Louisiana shelf, seasonal variability exists in the wind stress. Figure 34 shows the 15-day averaged time series of the along-shore and cross-shelf wind stress along with the along-shore current at buoy B. A relationship can be seen between the along-shore wind stress and the along-shore. Upcoast wind stress is present during the summer months, resulting in an upcoast flow in the along-shore current. When downcoast wind stress dominates during the non-summer months, the along-shore current also switches to a mostly downcoast flow.

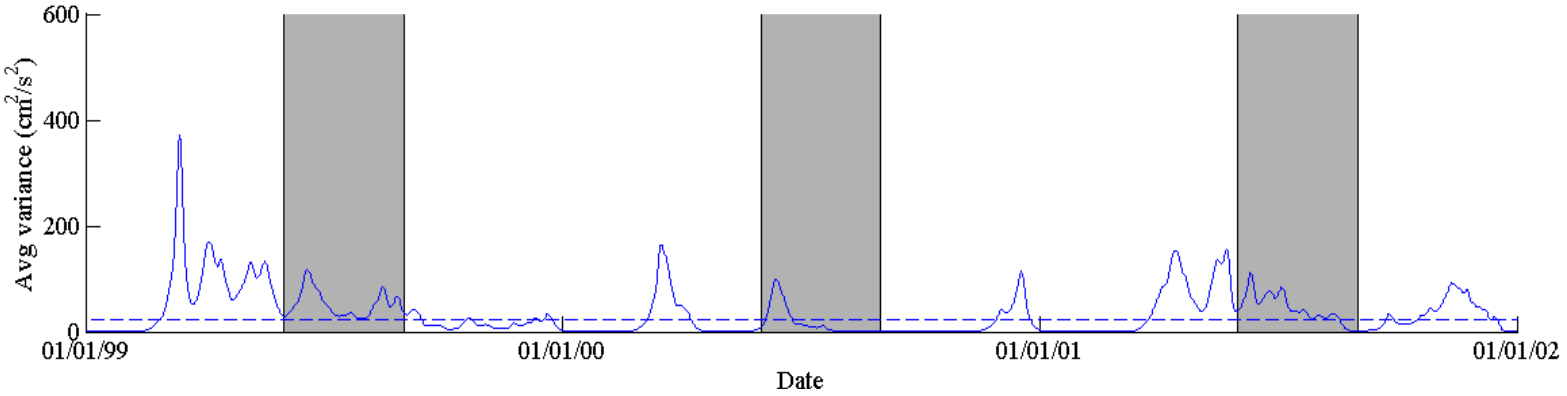

Figure 16. Weather band scale-averaged time series for buoy R. Scale-averaged time series is used to identify peaks of variance throughout the record. The gray boxes highlight the summer, June 1 through August 30. Buoy R shows most variance occurring during the spring, with occasional peaks in variance during other seasons.

Figure 16 continued

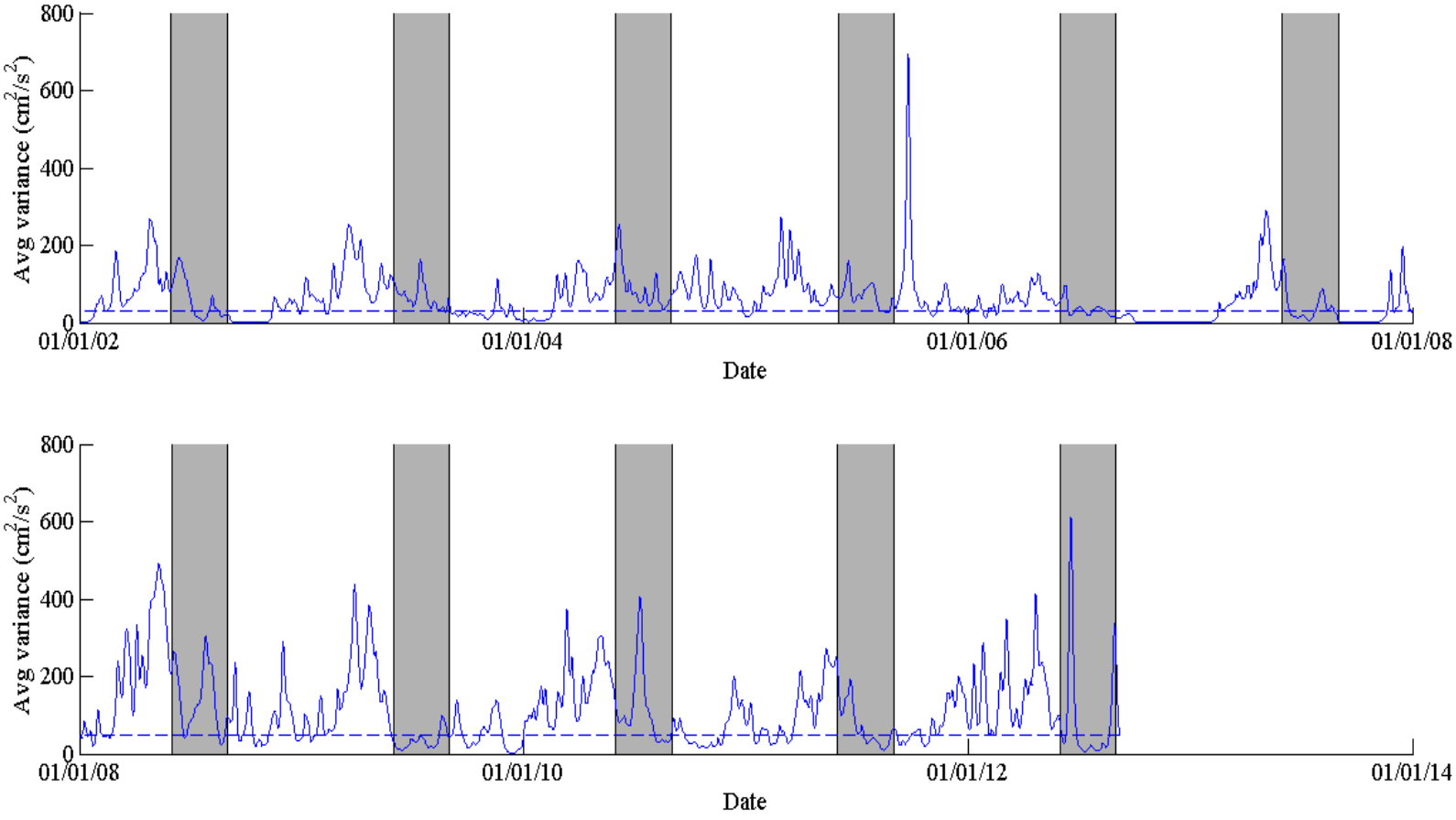

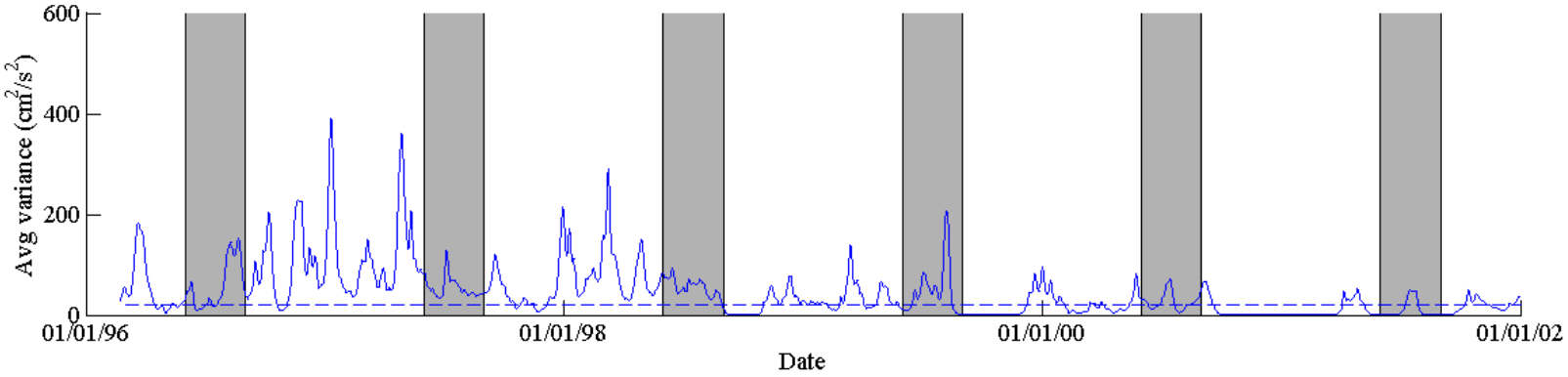

Figure 17. Weather band scale-averaged time series for buoy F. Scale-averaged time series is used to identify peaks of variance throughout the record. The gray boxes highlight the summer, June 1 through August 30. Buoy F shows most variance occurring during the spring, with occasional peaks in variance during other seasons.

Figure 17 continued

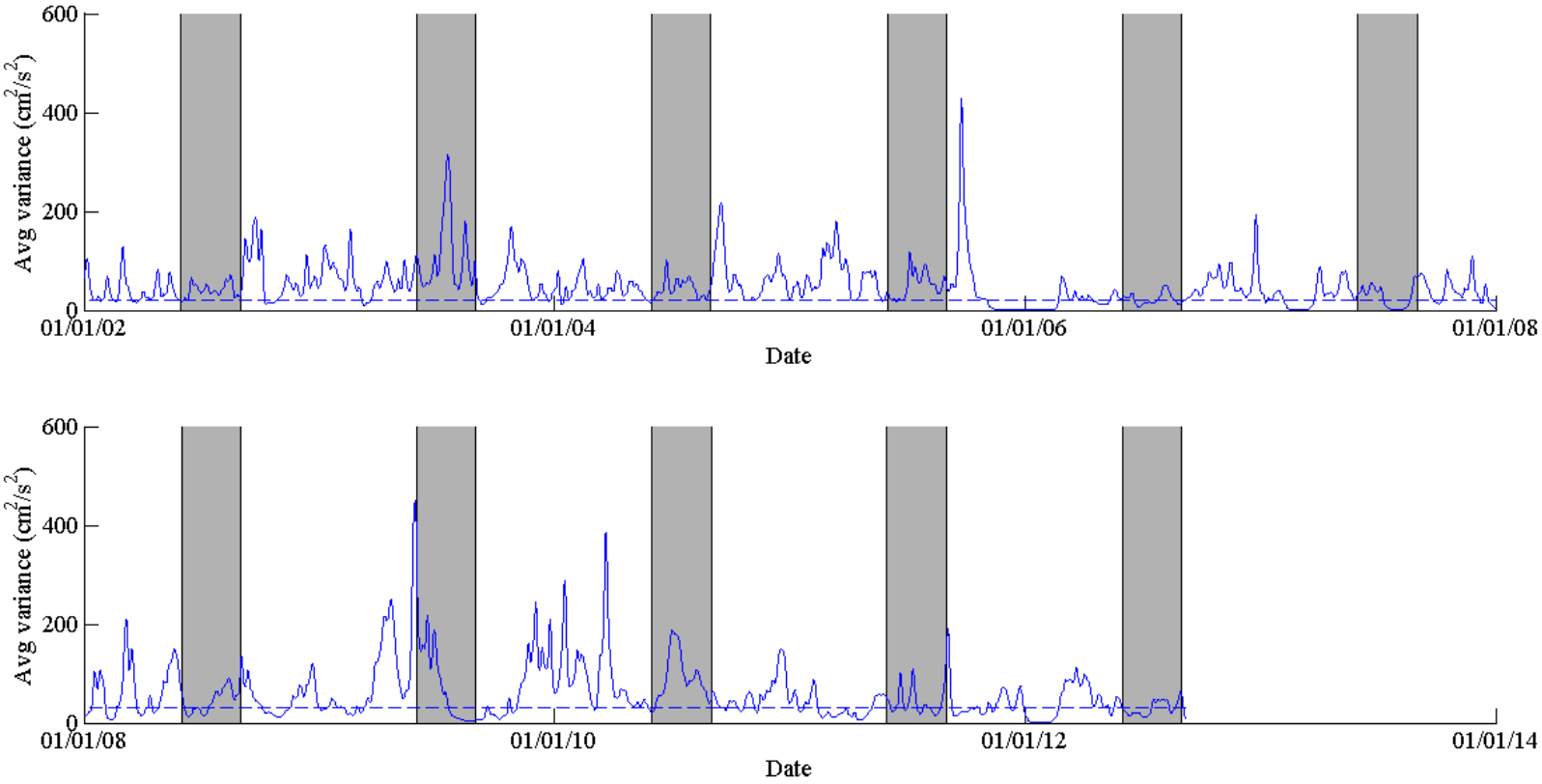

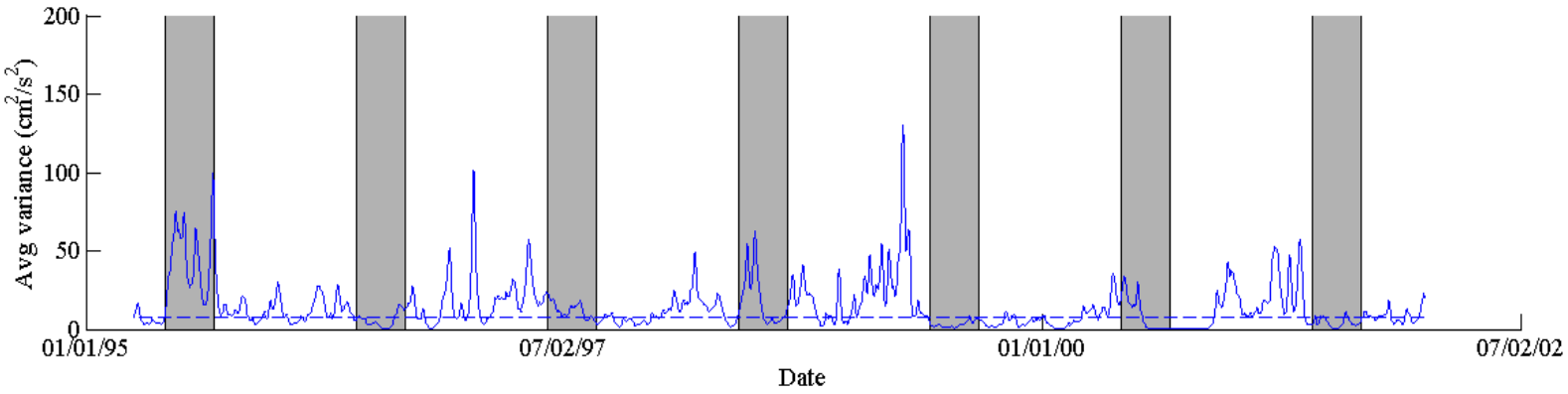

Figure 18. Weather band scale-averaged time series for buoy B. Scale-averaged time series is used to identify peaks of variance throughout the record. The gray boxes highlight the summer, June 1 through August 30. Buoy B shows most variance occurring during the spring, with occasional peaks in variance during other seasons.

Figure 18 continued

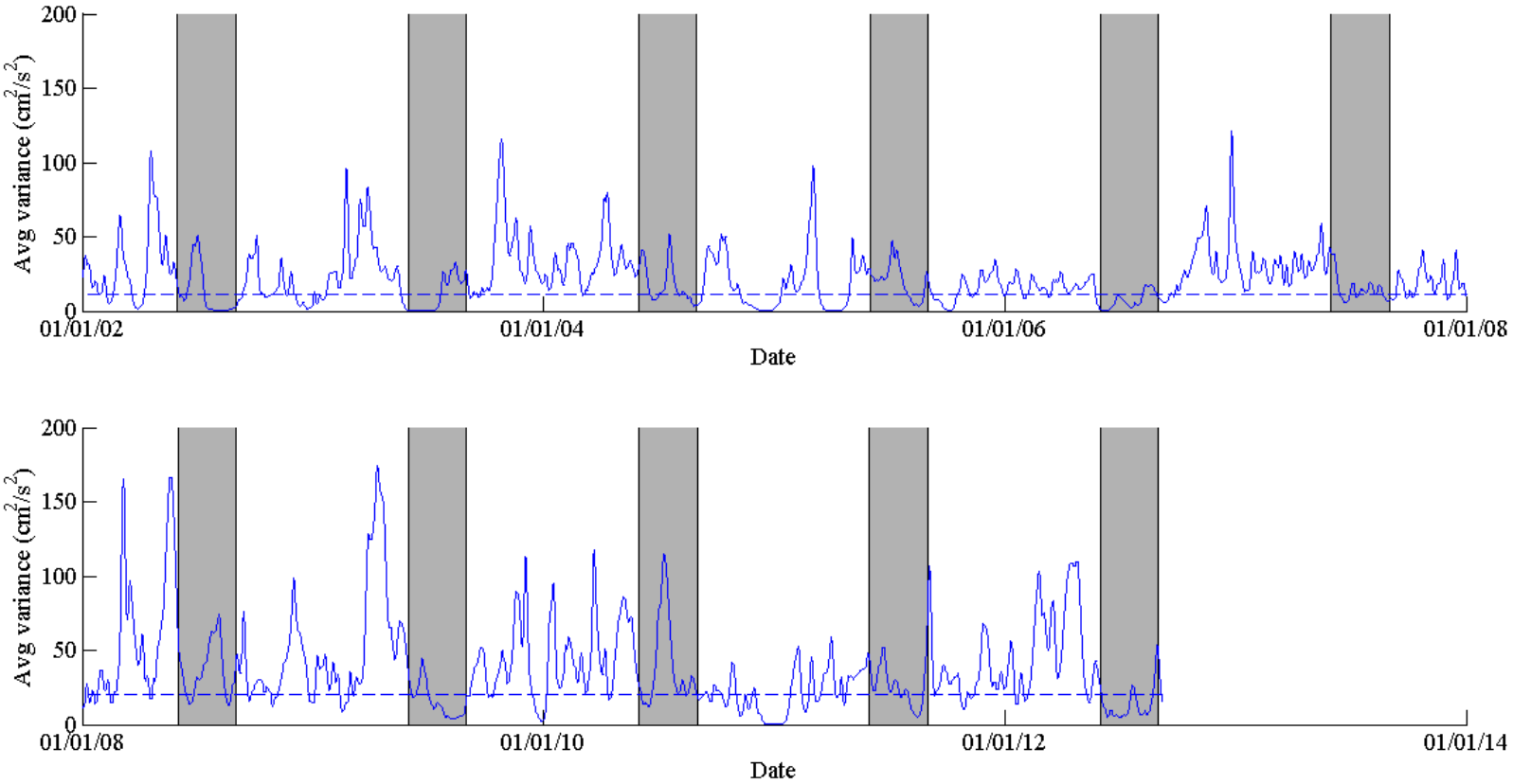

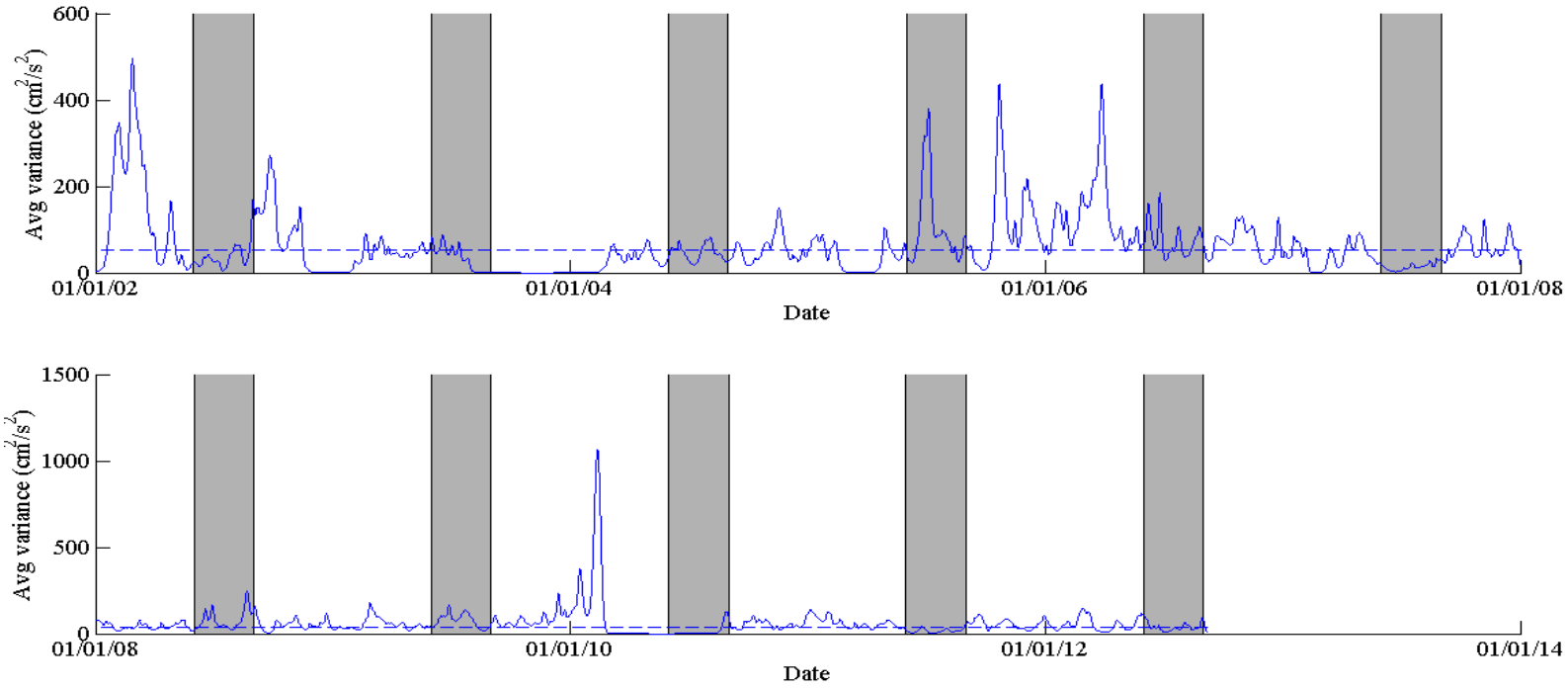

Figure 19. Weather band scale-averaged time series for buoy N. Scale-averaged time series is used to identify peaks of variance throughout the record. The gray boxes highlight the summer, June 1 through August 30. Buoy N shows most variance occurring during the spring. Some variance is found during the fall and winter while vary little variance is present during the summer.

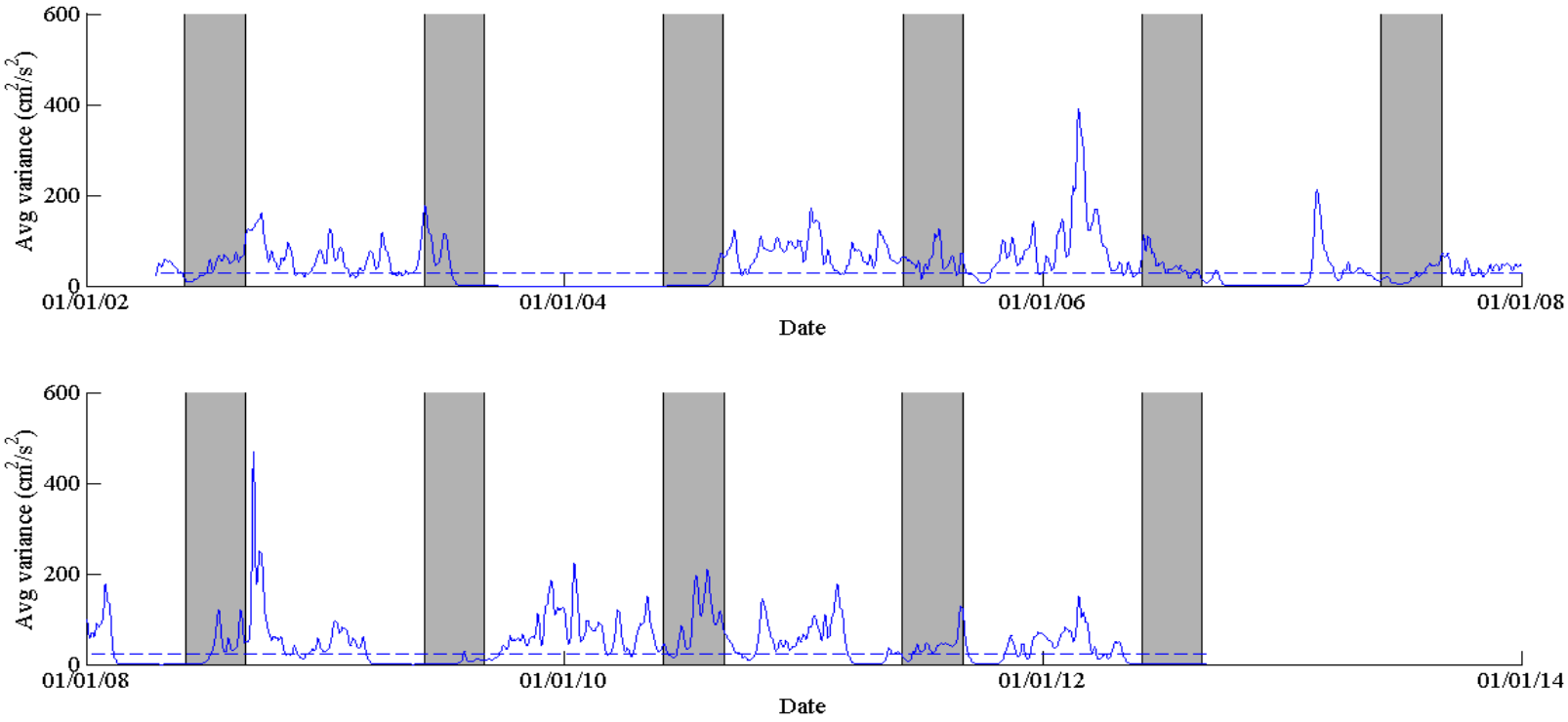

Figure 20. Weather band scale-averaged time series for buoy V. Scale-averaged time series is used to identify peaks of variance throughout the record. The gray boxes highlight the summer, June 1 through August 30. Buoy V shows most variance occurring during the spring. Some variance is found during the fall and winter while vary little variance is present during the summer.

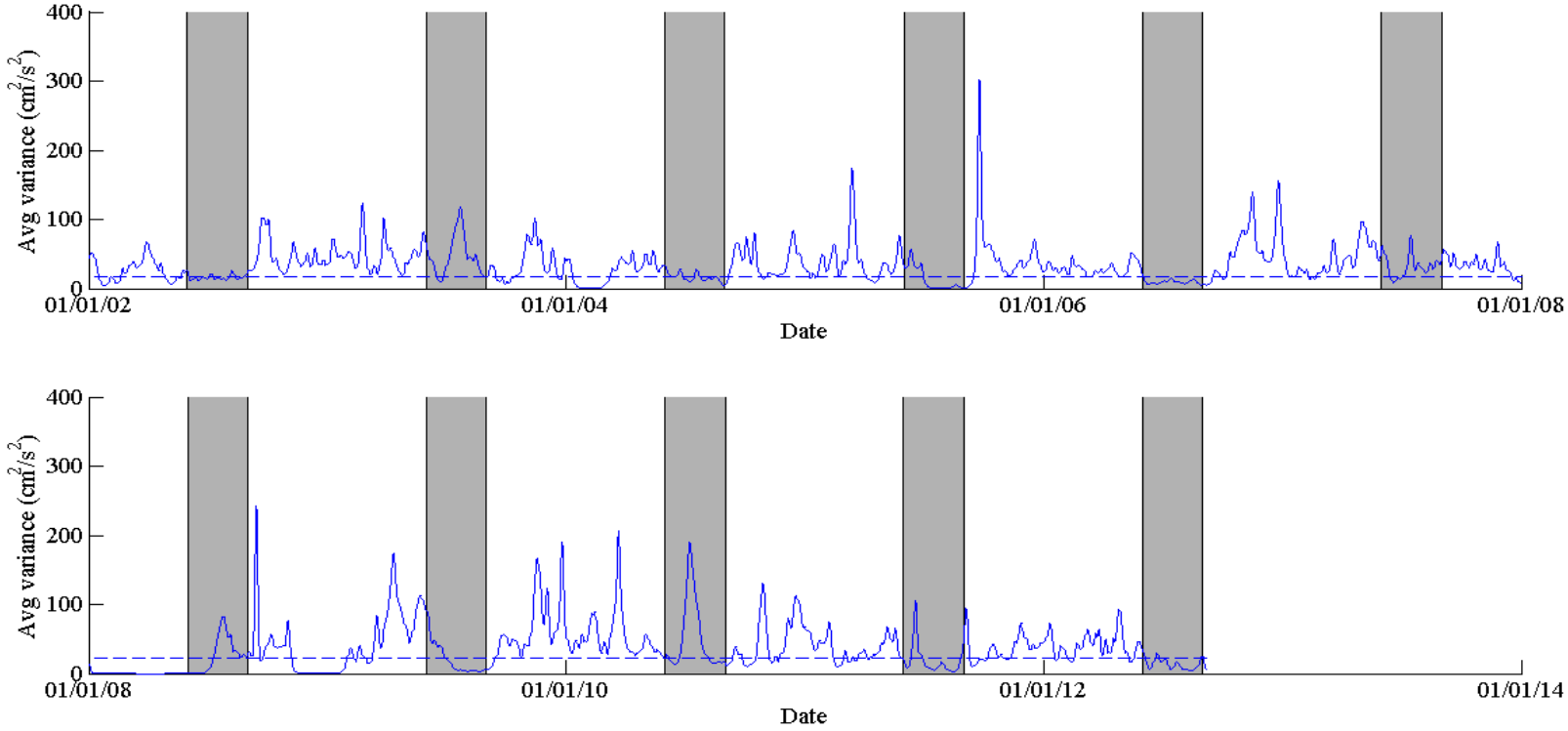

Figure 21. Weather band scale-averaged time series for buoy W. Scale-averaged time series is used to identify peaks of variance throughout the record. The gray boxes highlight the summer, June 1 through August 30. Buoy W shows variance is present during most of the non-summer periods, while little variance is present within the summers.

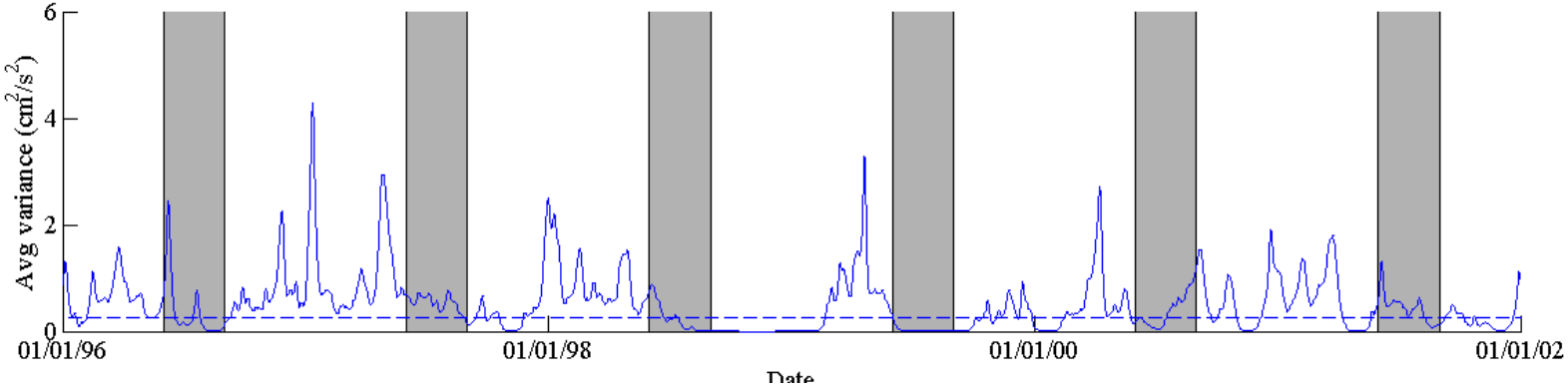

Figure 22. Weather band scale-averaged time series for buoy D. Scale-averaged time series is used to identify peaks of variance throughout the record. The gray boxes highlight the summer, June 1 through August 30. Buoy D displays variability in the non-summer months, while little variance is present during the summer periods.

Figure 22 continued

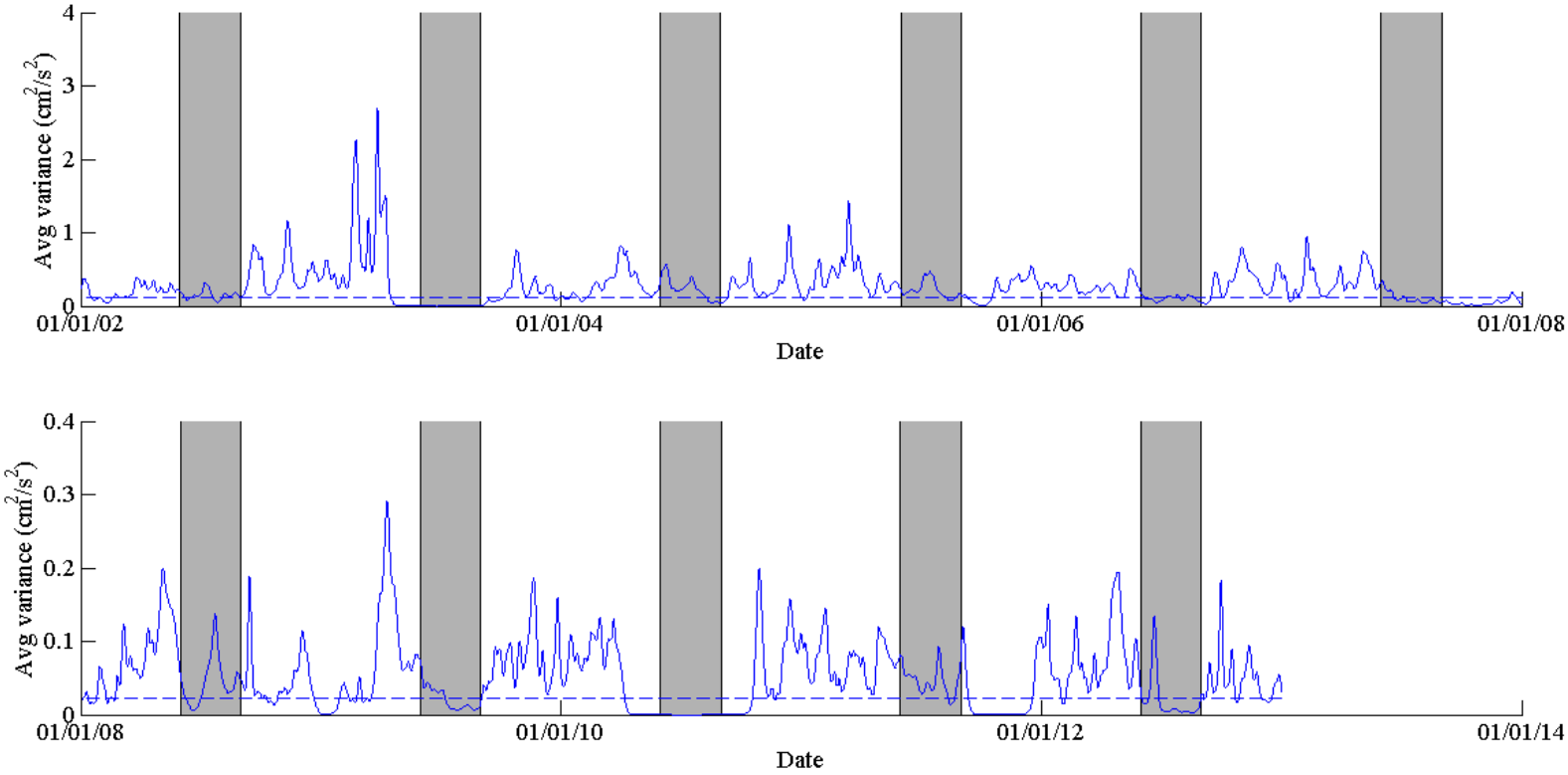

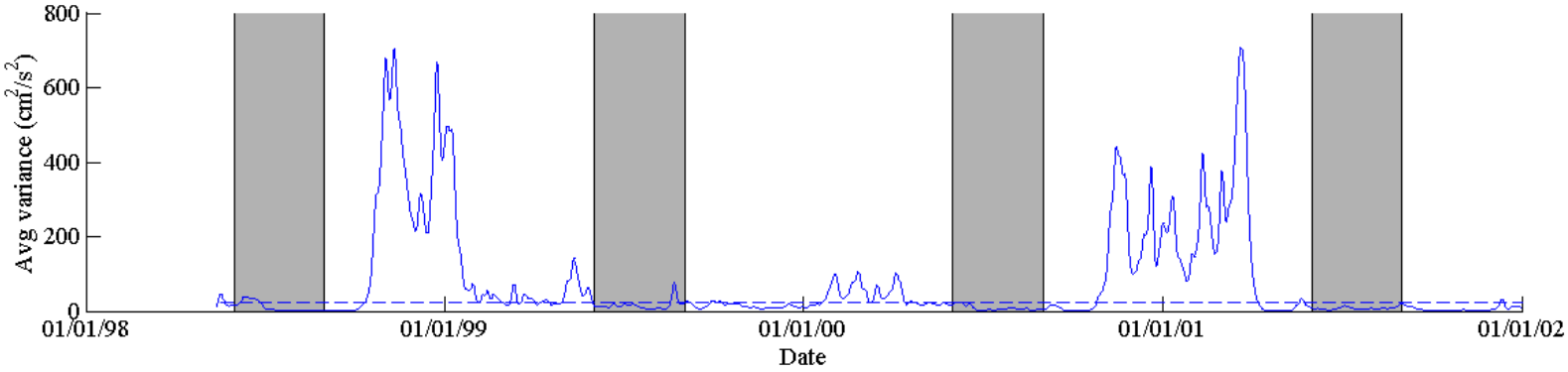

Figure 23. Weather band scale-averaged time series for buoy J. Scale-averaged time series is used to identify peaks of variance throughout the record. The gray boxes highlight the summer, June 1 through August 30. Buoy J has variance peaks present during the non-summer months, with little variance present during the summer months.

Figure 23 continued

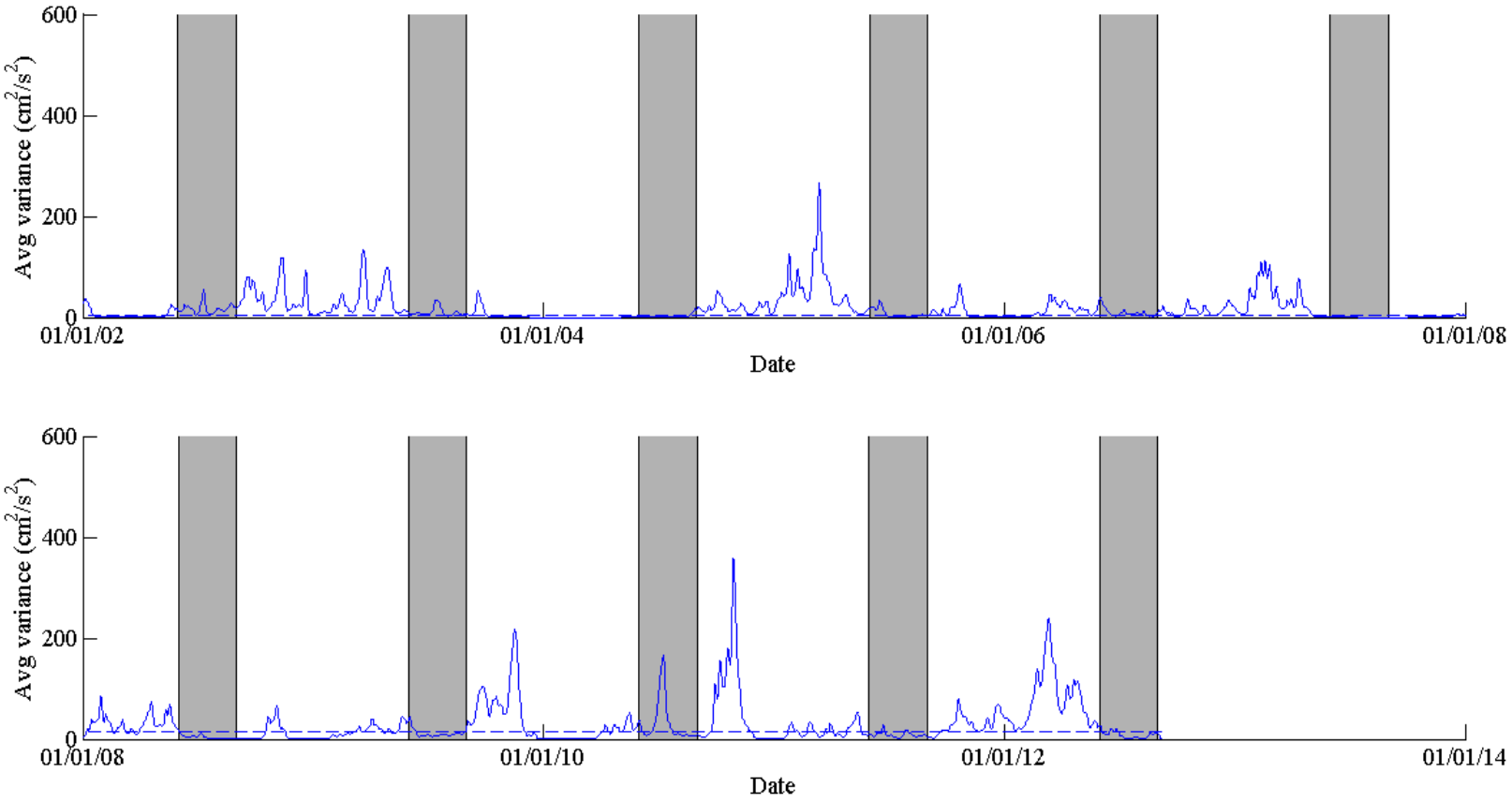

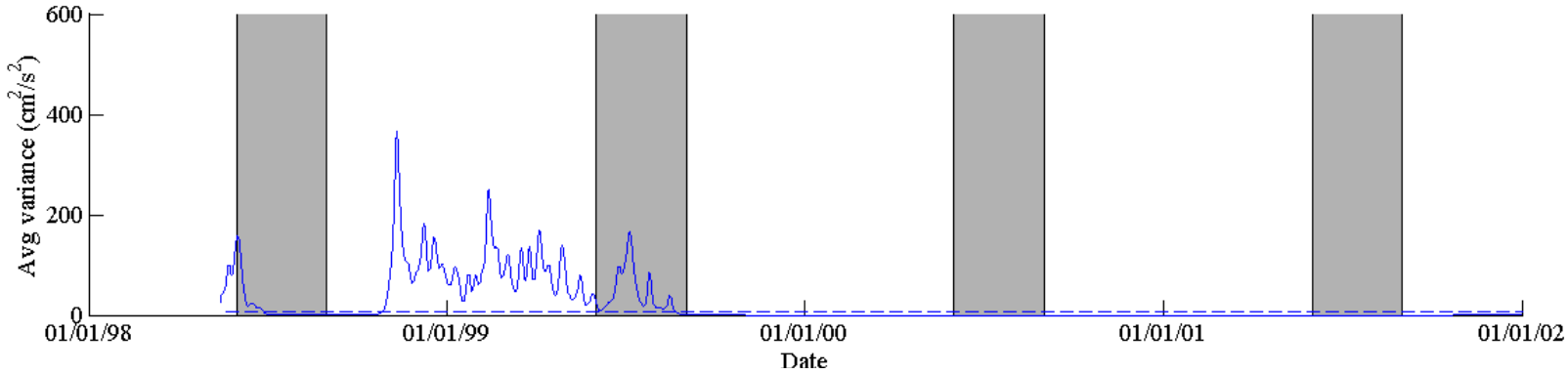

Figure 24. Weather band scale-averaged time series for buoy K. Scale-averaged time series is used to identify peaks of variance throughout the record. The gray boxes highlight the summer, June 1 through August 30. Buoy K has variance peaks present during the non-summer months, with occasional variance present during the summers.

Figure 24 continued

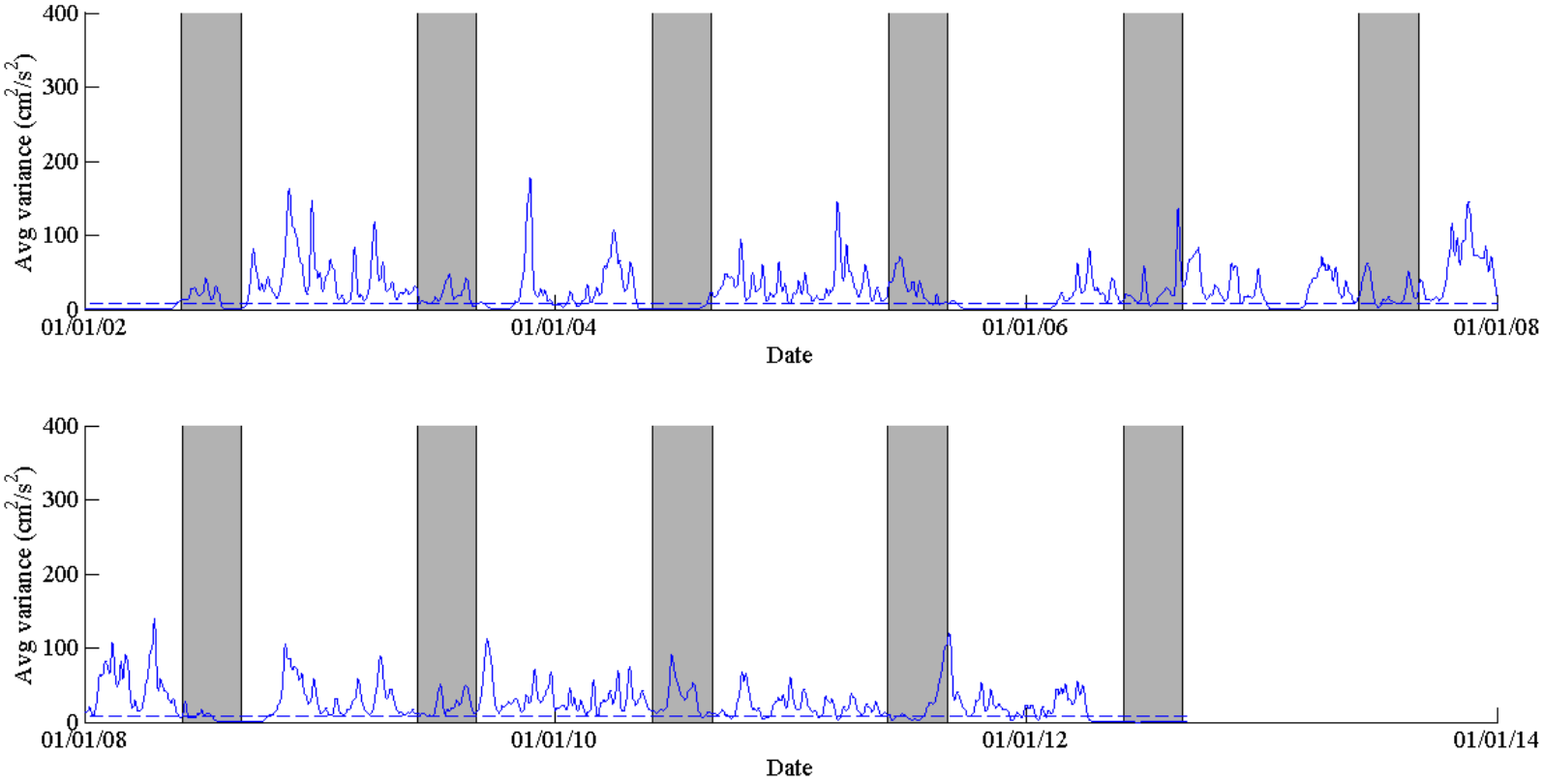

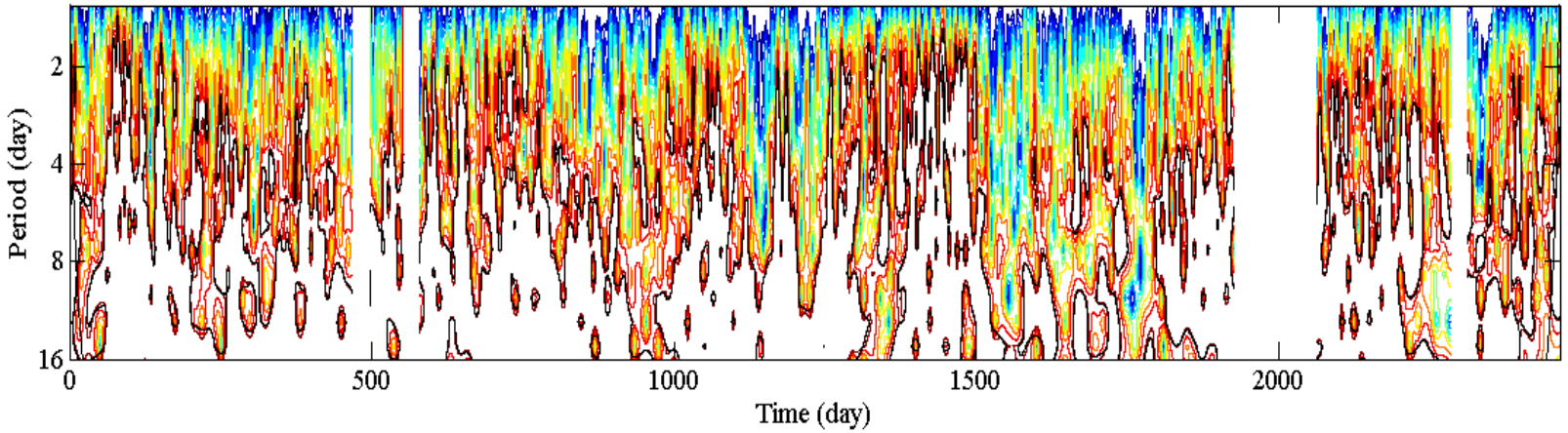

Figure 25. Wavelet spectrum transform for buoy B. Top image displays years 1995-2001, the middle image shows years 2002-2007, and 2008-2012 are shown in the last figure. Wavelet spectrum is useful for finding frequency peaks present on certain time scales. Periods where gaps are present in the current data have been masked out. Red indicates greatest relative power, while blue indicates least relative power present. Variance is present within the 4-16 day time period, consistent with the weather band frequencies.

Figure 25 continued

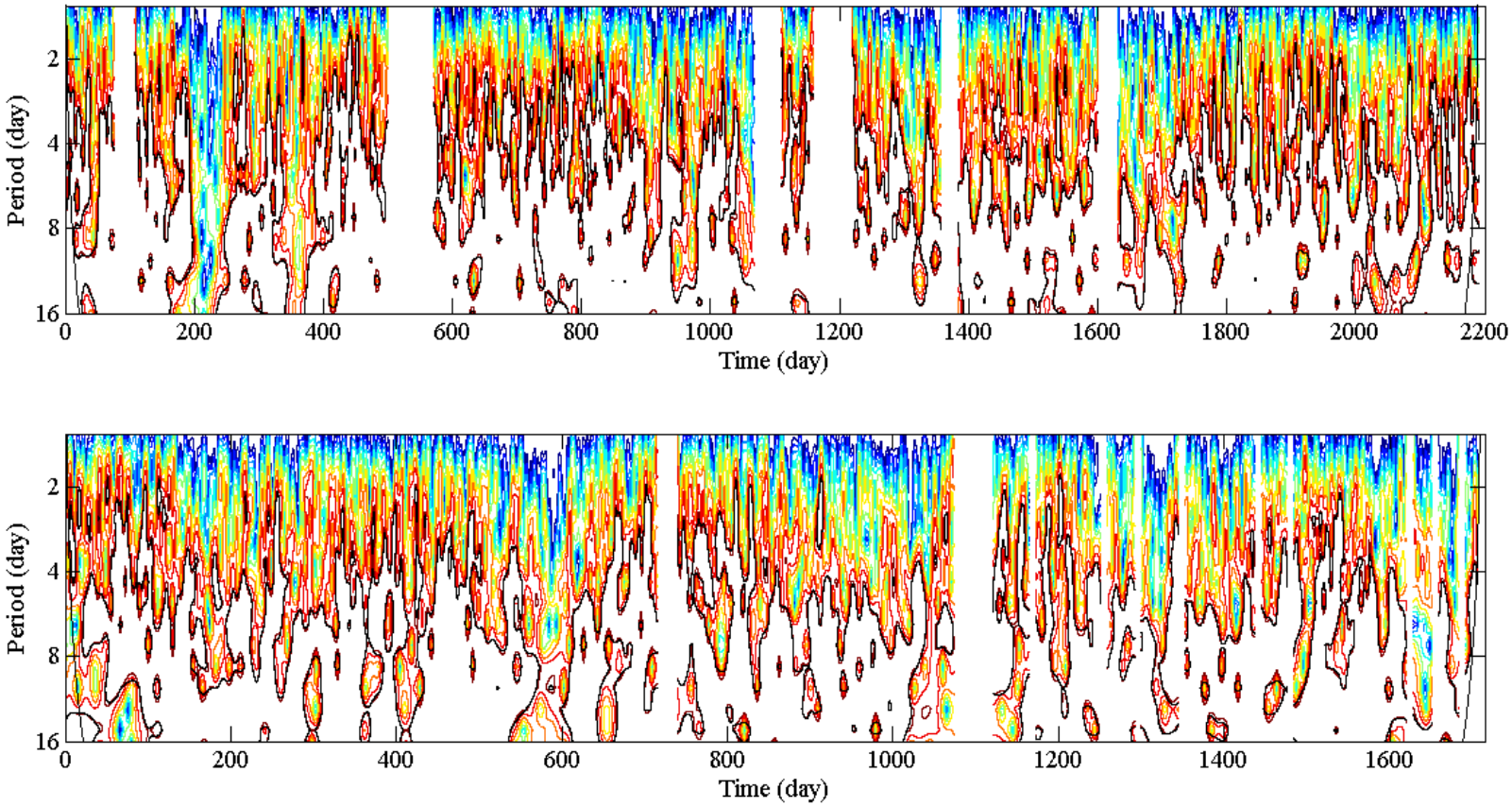

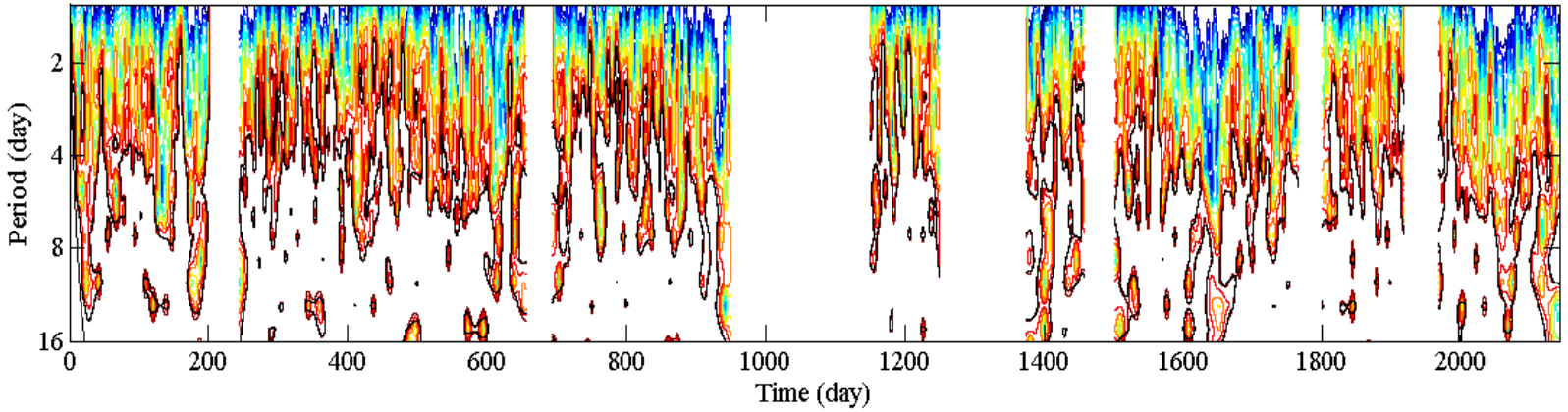

Figure 26. Wavelet spectrum transform for buoy D. Top image displays years 1996-2001, the middle image shows years 2002-2007, and 2008-2012 are shown in the last figure. Areas where data gaps are present have been masked out. Wavelet spectrum is useful for finding frequency peaks present on certain time scales. Red indicates greatest relative power while blue represents least relative power. Buoy D has most variance present in the 4-8 day time period, with periods of variance present in the 8-16 day time period. This is consistent with the weather band frequencies.

Figure 26 continued

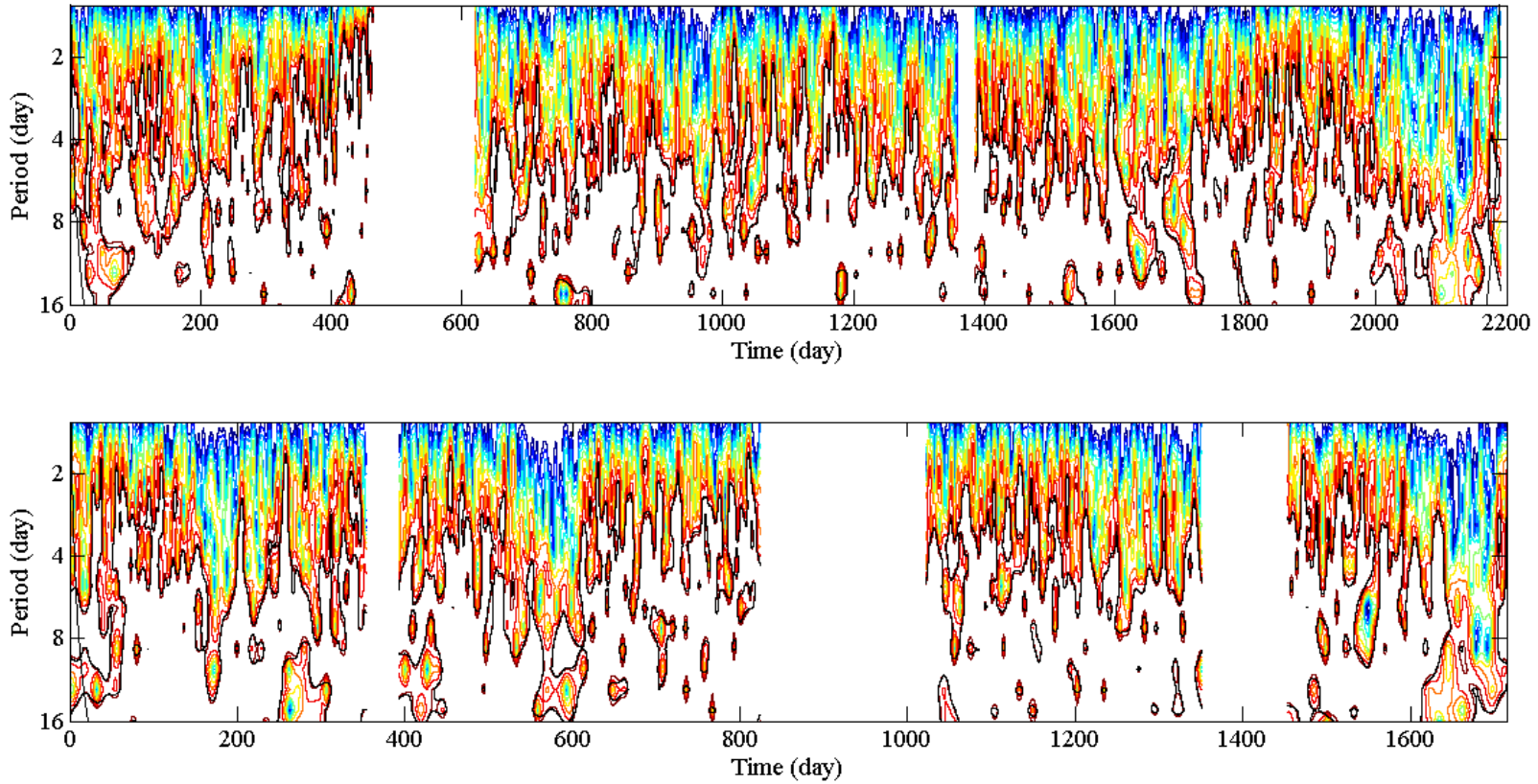

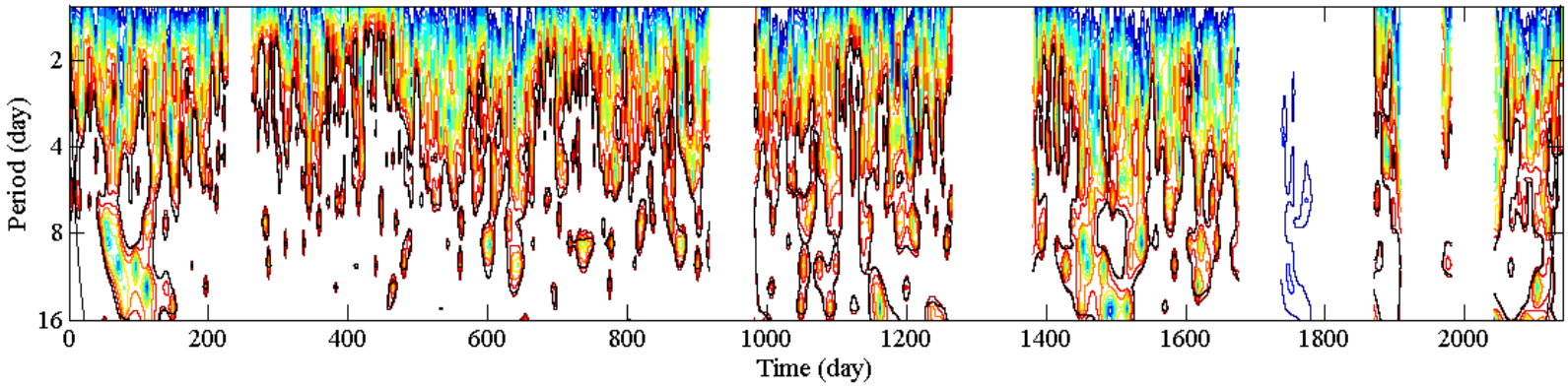

Figure 27. Wavelet spectrum transform for buoy F. Top image displays years 1996-2001, the middle image shows years 2002-2007, and 2008-2012 are shown in the last figure. Areas where data gaps are present have been masked out. Wavelet spectrum is useful for finding frequency peaks present on certain time scales. Red indicates greatest relative power while blue represents least relative power. Buoy F has most variance present in the 4-8 day time period, with periods of variance present in the 8-16 day time period. This is consistent with the weather band frequencies.

Figure 27 continued

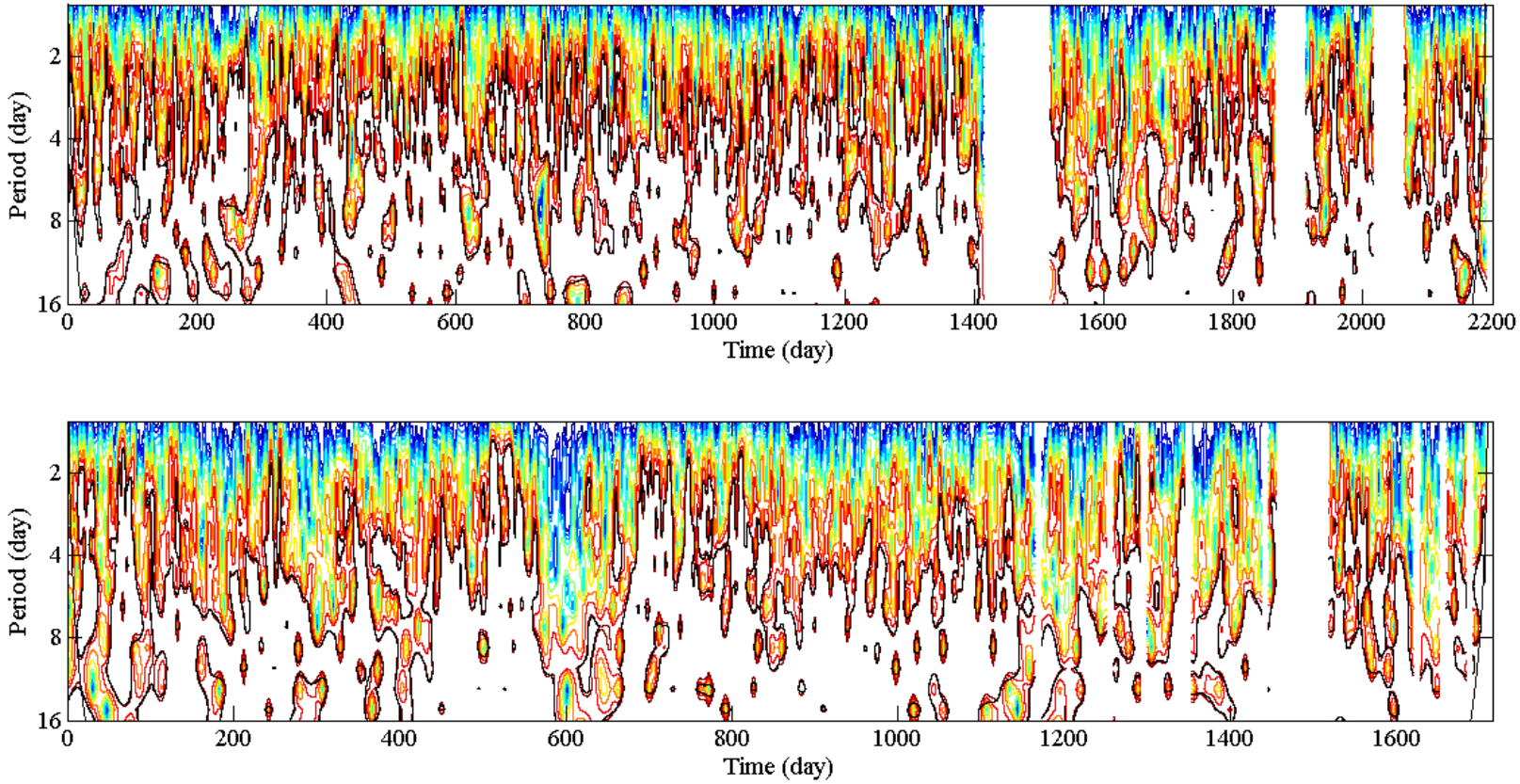

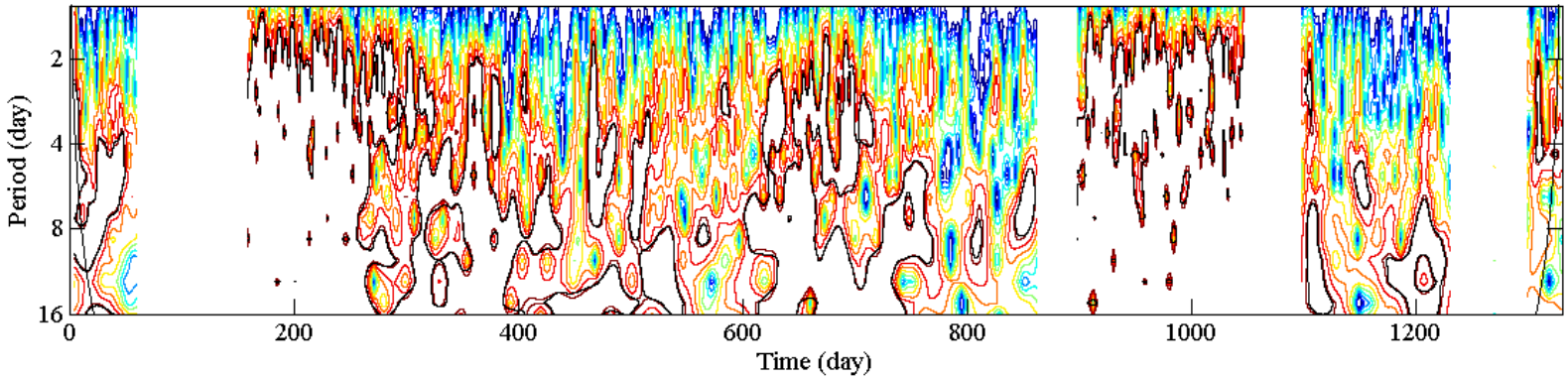

Figure 28. Wavelet spectrum transform for buoy J. Top image displays years 1998-2001, the middle image shows years 2002-2007, and 2008-2012 are shown in the last figure. Areas where data gaps are present have been masked out. Wavelet spectrum is useful for finding frequency peaks present on certain time scales. Red indicates greatest relative power while blue represents least relative power. Buoy J has most variance present in the 4-16 day time period, consistent with the weather band frequencies.

Figure 28 continued

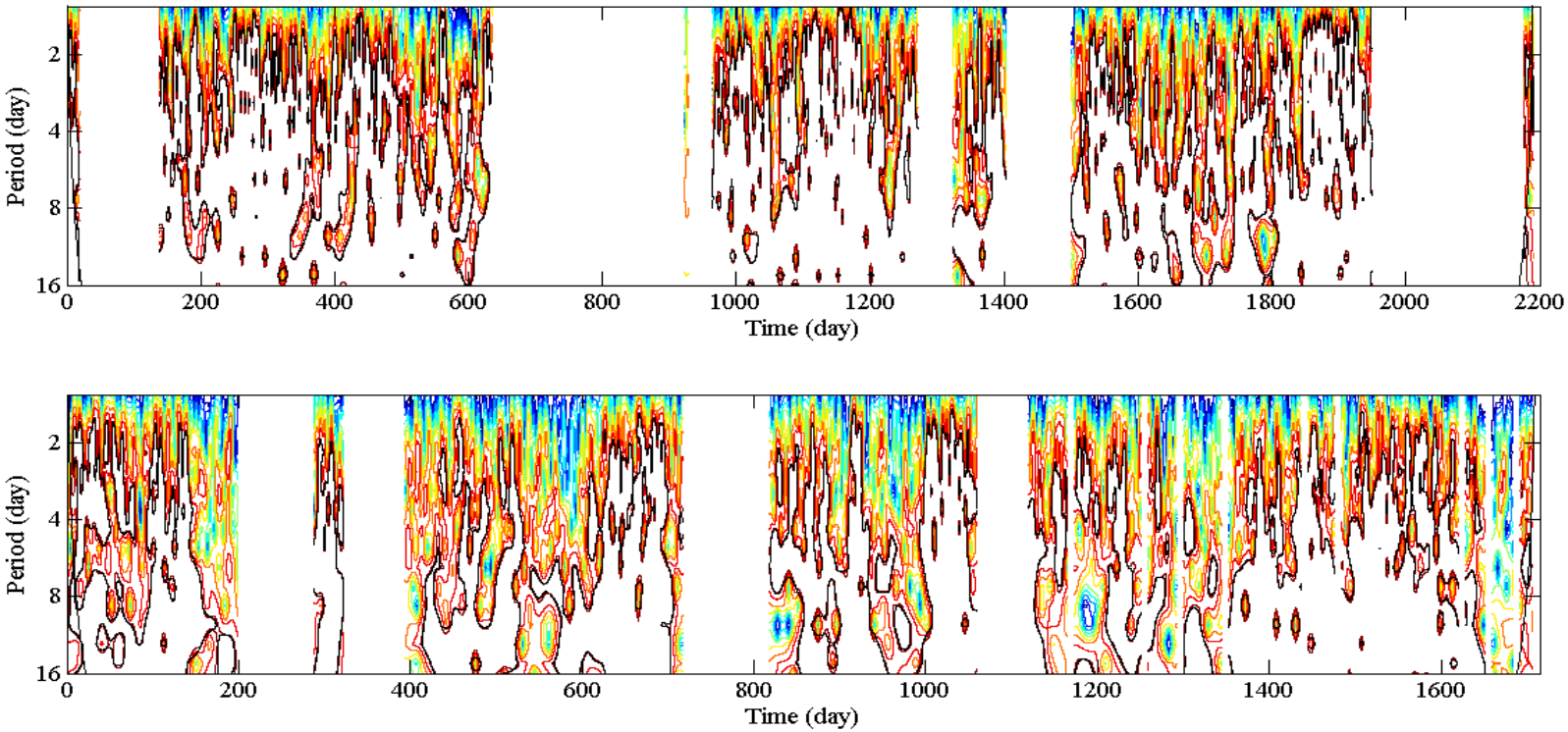

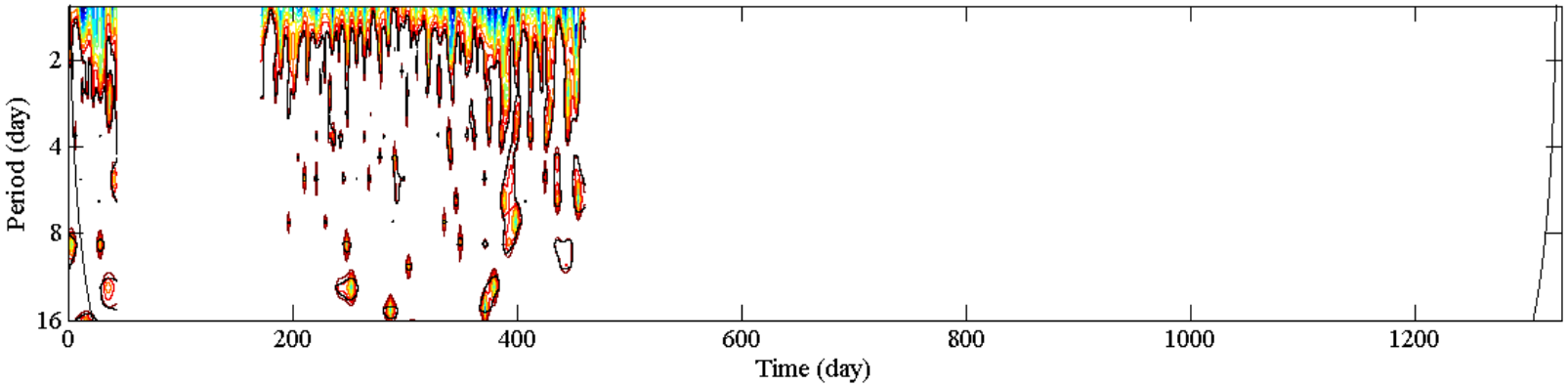

Figure 29. Wavelet spectrum transform for buoy K. Top image displays years 1998-2001, the middle image shows years 2002-2007, and 2008-2012 are shown in the last figure. Areas where data gaps are present have been masked out. Wavelet spectrum is useful for finding frequency peaks present on certain time scales. Red indicates greatest relative power while blue represents least relative power. Buoy K has most variance present in the 2-4 day time period, with periods of variance present in the 4-16 day time period. This is consistent with the weather band frequencies.

Figure 29 continued

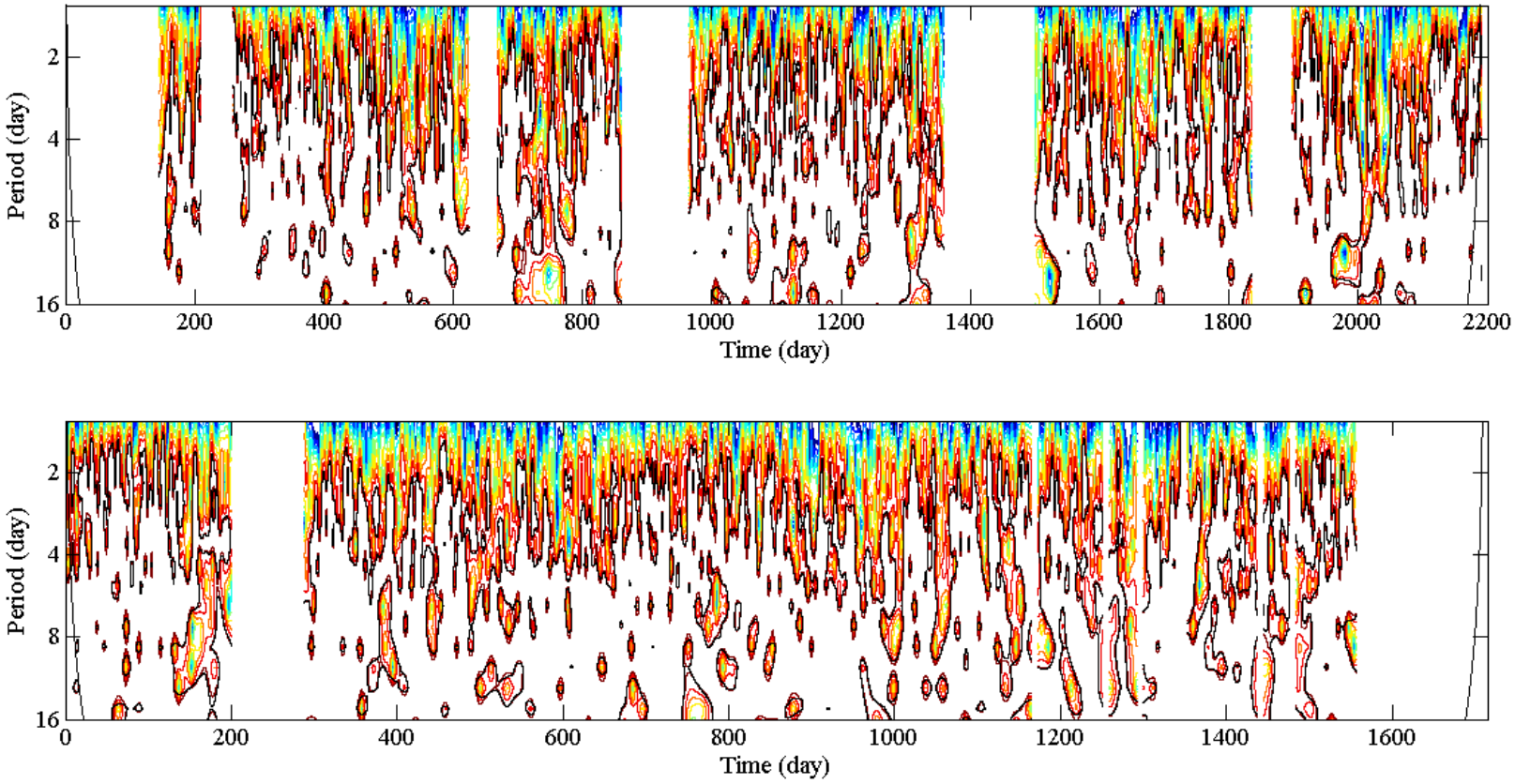

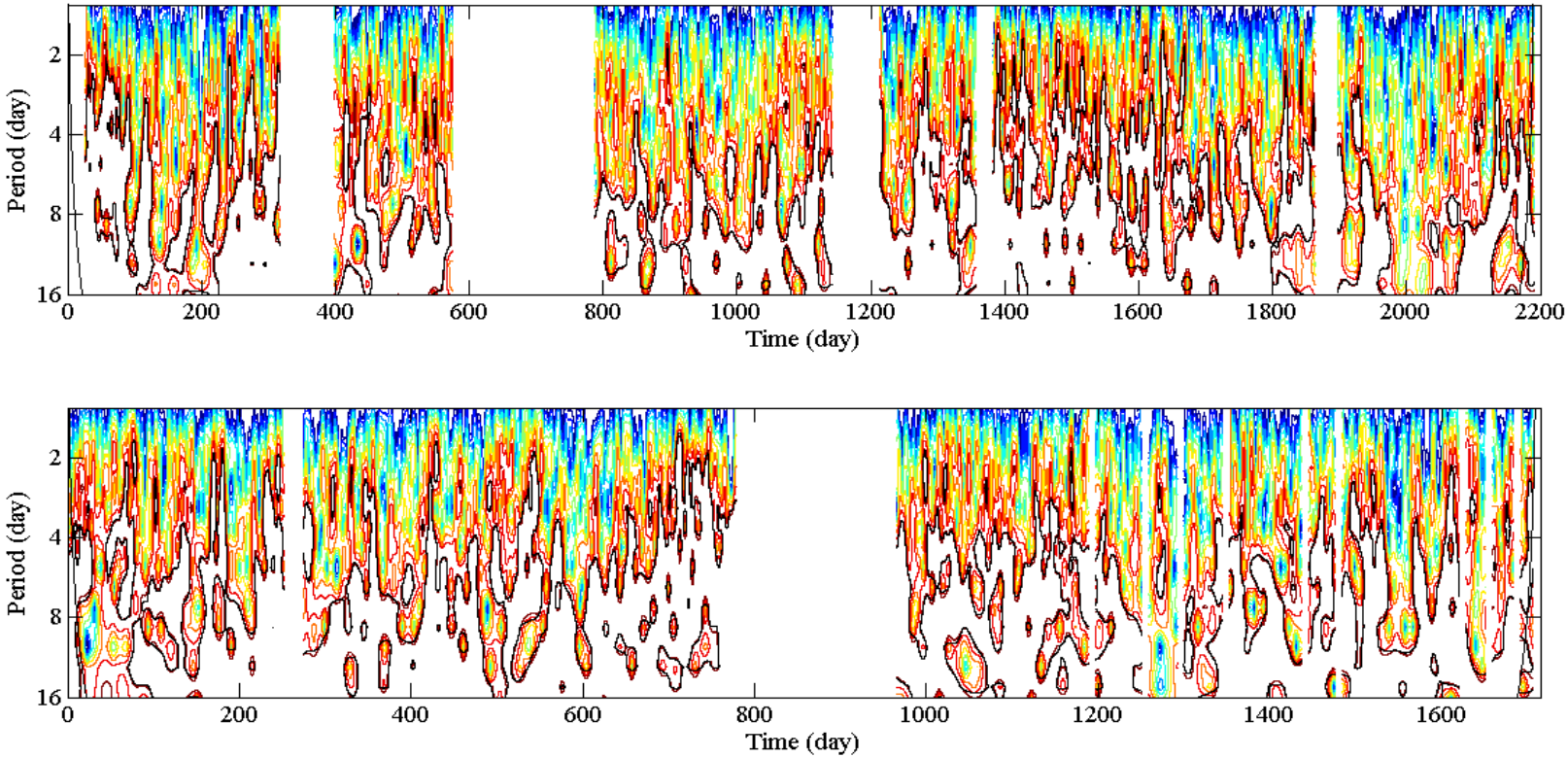

Figure 30. Wavelet spectrum transform for buoy N. Top image displays years 2002-2007 and 2008-2012 are shown in the last figure. Areas where data gaps are present have been masked out. Wavelet spectrum is useful for finding frequency peaks present on certain time scales. Red indicates greatest relative power while blue represents least relative power. Buoy N has most variance present in the 2-8 day time period, with periods of variance present in the 8-16 day time period. This is consistent with the weather band frequencies.

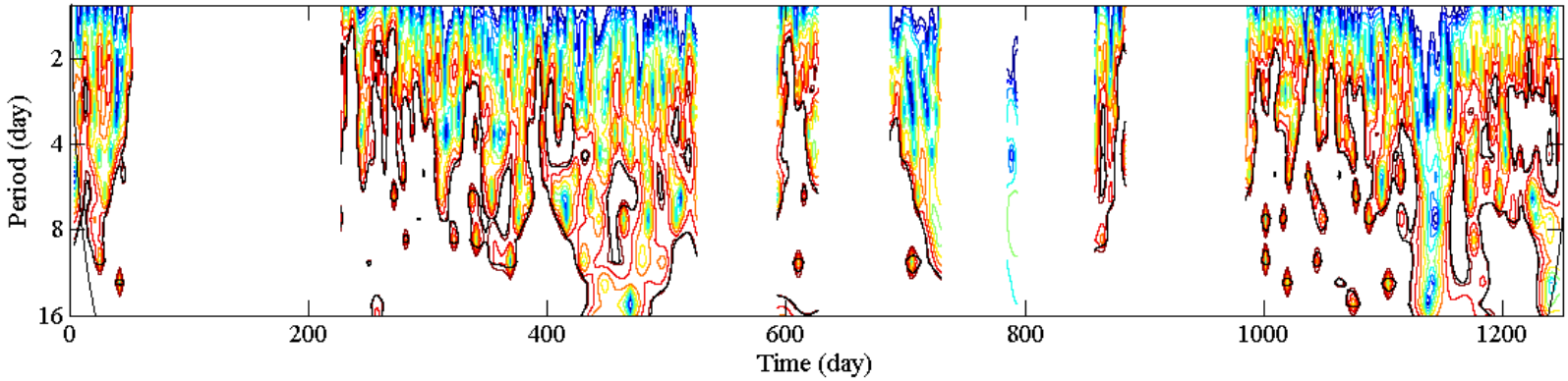

Figure 31. Wavelet spectrum transform for buoy R. Top image displays years 1998-2001, the middle image shows years 2002-2007, and 2008-2012 are shown in the last figure. Areas where data gaps are present have been masked out. Wavelet spectrum is useful for finding frequency peaks present on certain time scales. Red indicates greatest relative power while blue represents least relative power. Buoy R has most variance present in the 2-8 day time period, with periods of variance present in the 8-16 day time period. This is consistent with the weather band frequencies.

Figure 31 continued

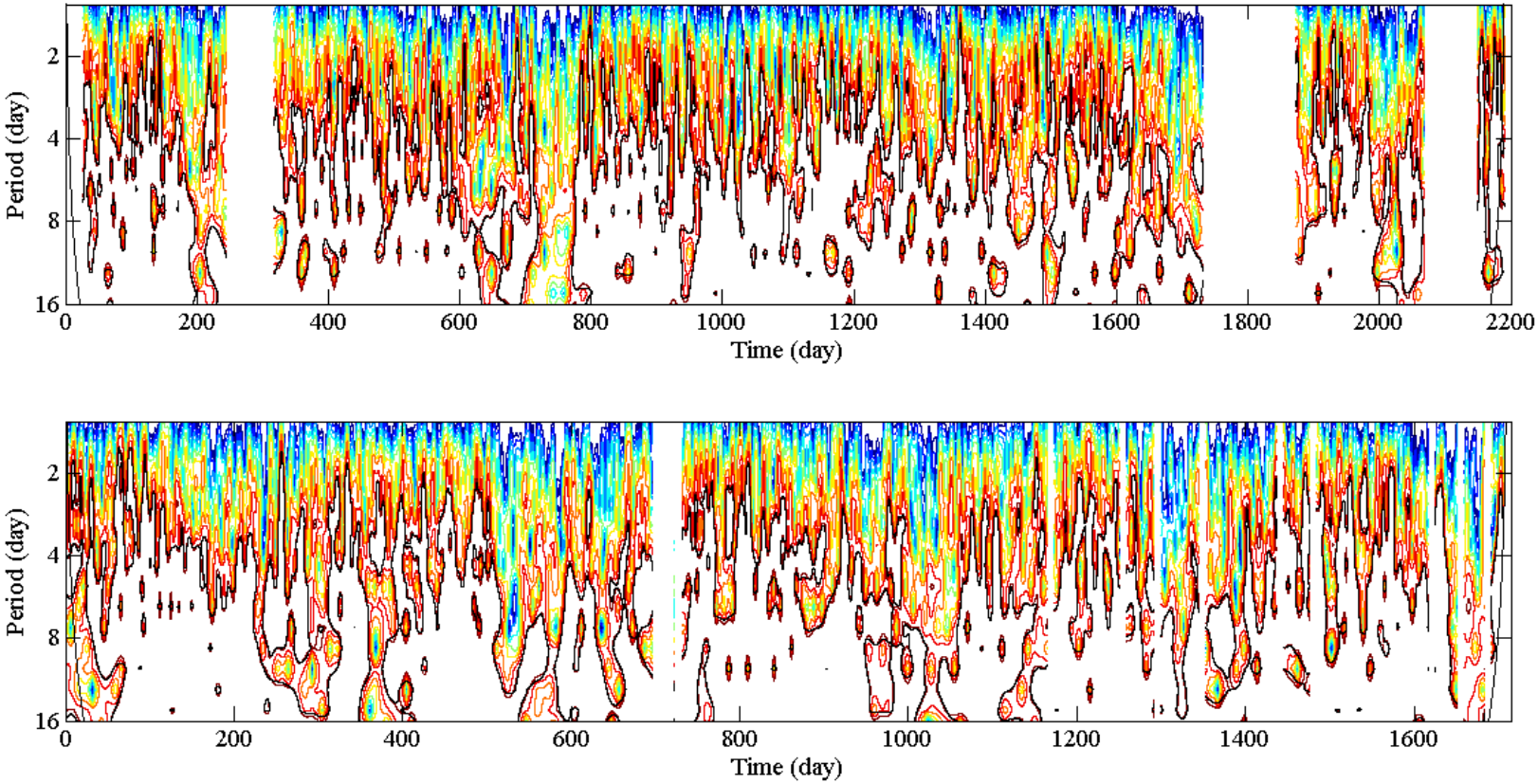

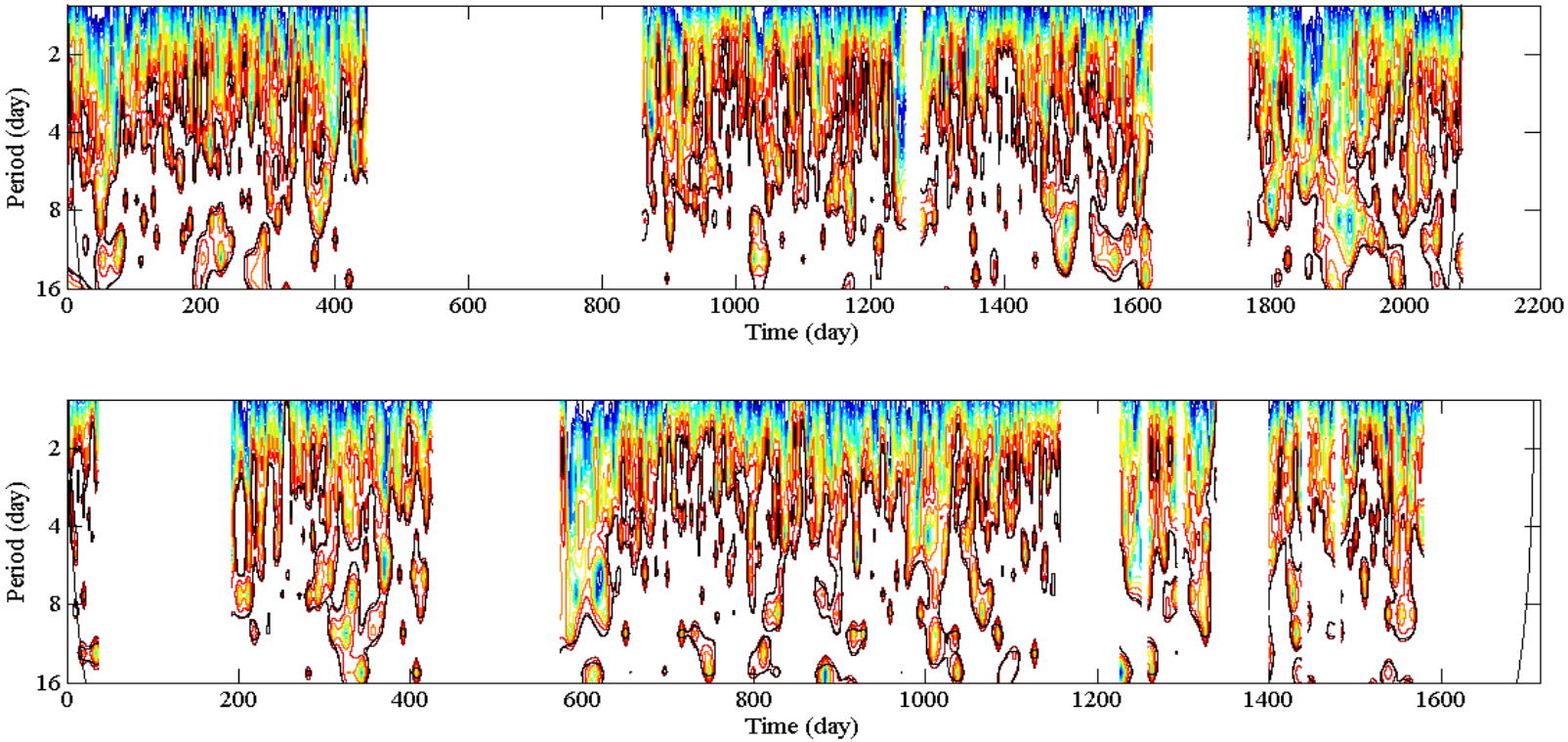

Figure 32. Wavelet spectrum transform for buoy V. Top image displays years 2002-2007 and 2008-2012 are shown in the last figure. Areas where data gaps are present have been masked out. Wavelet spectrum is useful for finding frequency peaks present on certain time scales. Red indicates greatest relative power while blue represents least relative power. Buoy V has most variance present in the 4-8 day time period, with periods of variance present in the 8-16 day time period. This is consistent with the weather band frequencies.

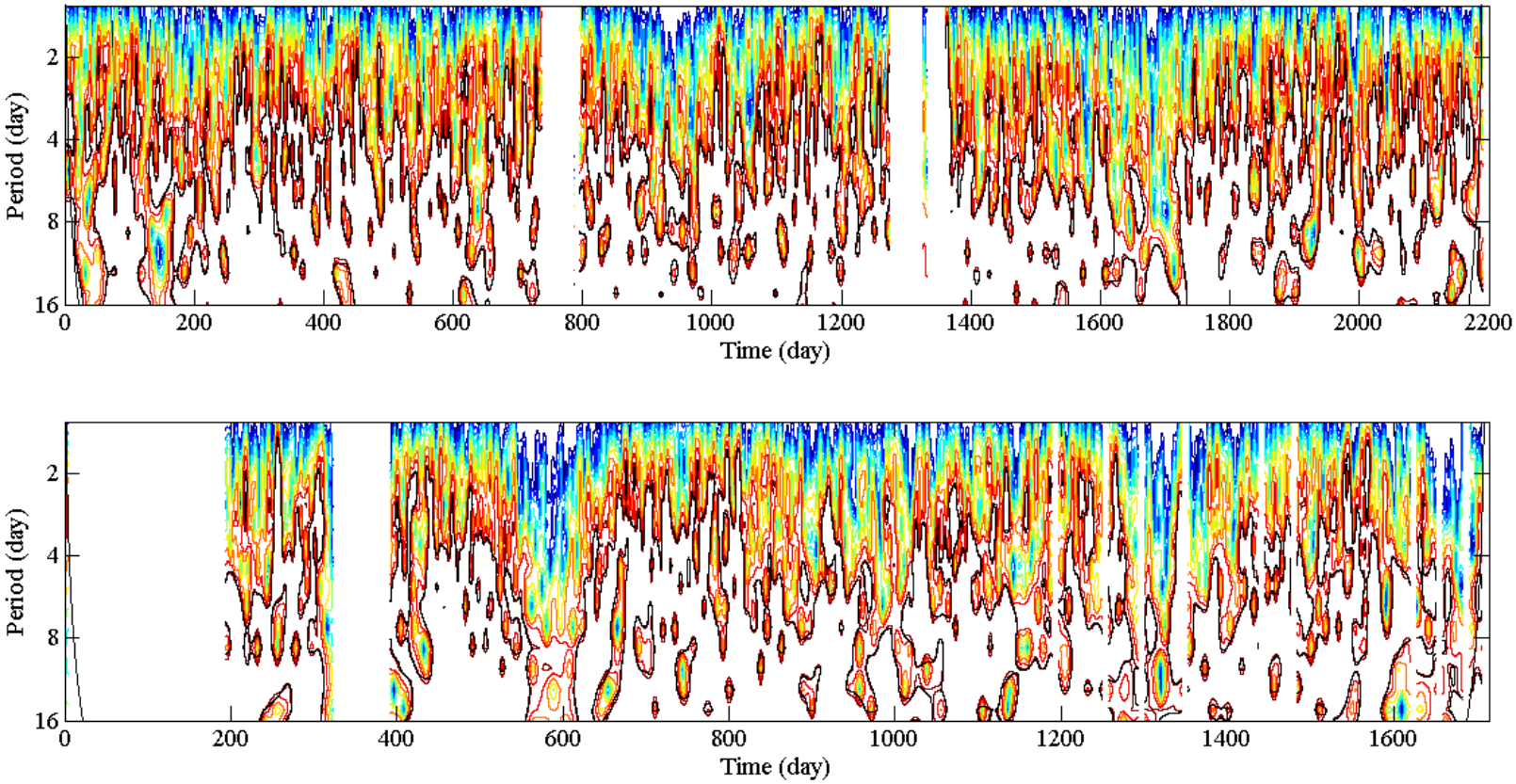

Figure 33. Wavelet spectrum transform for buoy W. Top image displays years 2002-2007 and 2008-2012 are shown in the last figure. Areas where data gaps are present have been masked out. Wavelet spectrum is useful for finding frequency peaks present on certain time scales. Red indicates greatest relative power while blue represents least relative power. Buoy W has most variance present in the 2-8 day time period, with periods of variance present in the 8-16 day time period. This is consistent with the weather band frequencies.

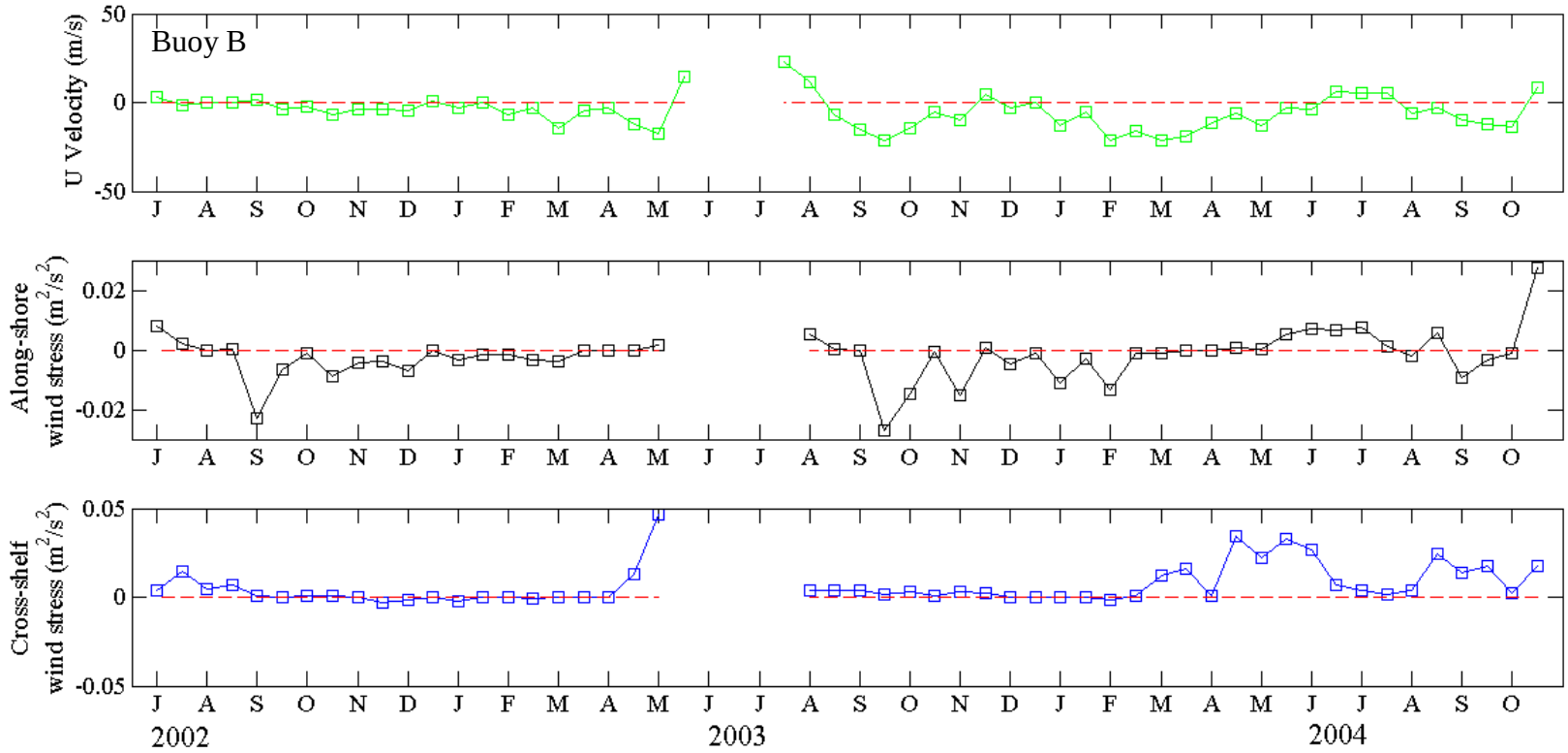

Figure 34. Time series of wind stress and along-shore current velocity at buoy B. The top figure displays the 15-day averaged along-shore current velocity time series while the bottom two figures display the 15-day averaged wind stress is both the along-shore and cross-shelf directions at buoy B. Upcoast forcing is indicated by positive wind stress while negative indicates downcoast in along-shore wind stress. Onshore forcing is indicated by positive cross-shelf wind stress; offshore forcing by negative wind stress. Results show seasonal forcing of the along-shore current velocity by the along-shore wind stress, with upcoast forcing during the summer months and downcoast forcing during the non-summer months.

Further down the Texas coast, there is some evidence of a relationship between the along-shore current flow and along-shore wind stress at buoy D. Figure 35 shows the 15-day averaged time series of the along-shore and cross-shelf wind stress along with the along-shore current. There is an indication of some relationship between the along-shore wind and current, particularly during the non-summer in the beginning of 2007 and during the summer and fall in 2008. In general, this means that the seasonal variability in the along-shore current at coastal locations is related to the along-shore wind.

While seasonal variability is present in the along-shore wind stress at coastal locations, the same is not true for locations further offshore. The 15-day averaged time series of the along-shore and cross-shelf wind stress along with the along-shore current at offshore locations K and N are shown in Figures 36 and 37. While some correlation between the along-shore wind stress and along-shore flow is present at buoy K, no correlation is seen between the along-shore wind stress and current at buoy N. Mesoscale features, such as Loop Current Eddies, provide the forcing for the low-frequency current circulation at locations on the outer shelf. Figures 38-41 show the effect of eddies on the general circulation in the outer shelf area near buoys N and V. From August 10 through August 30, 2008, the position of the anticyclonic eddy to the south results in an eastward-flowing current at buoys N and V. By early September, the cyclonic eddy moves eastward, causing the current flow near buoys N and V to reverse to a westward flow. The time series shown in Figure 36 shows the u-velocity at N during this time period (highlighted by the gray box), confirming the sustained eastward flow through the end of August and the reversal westward in the beginning on September.

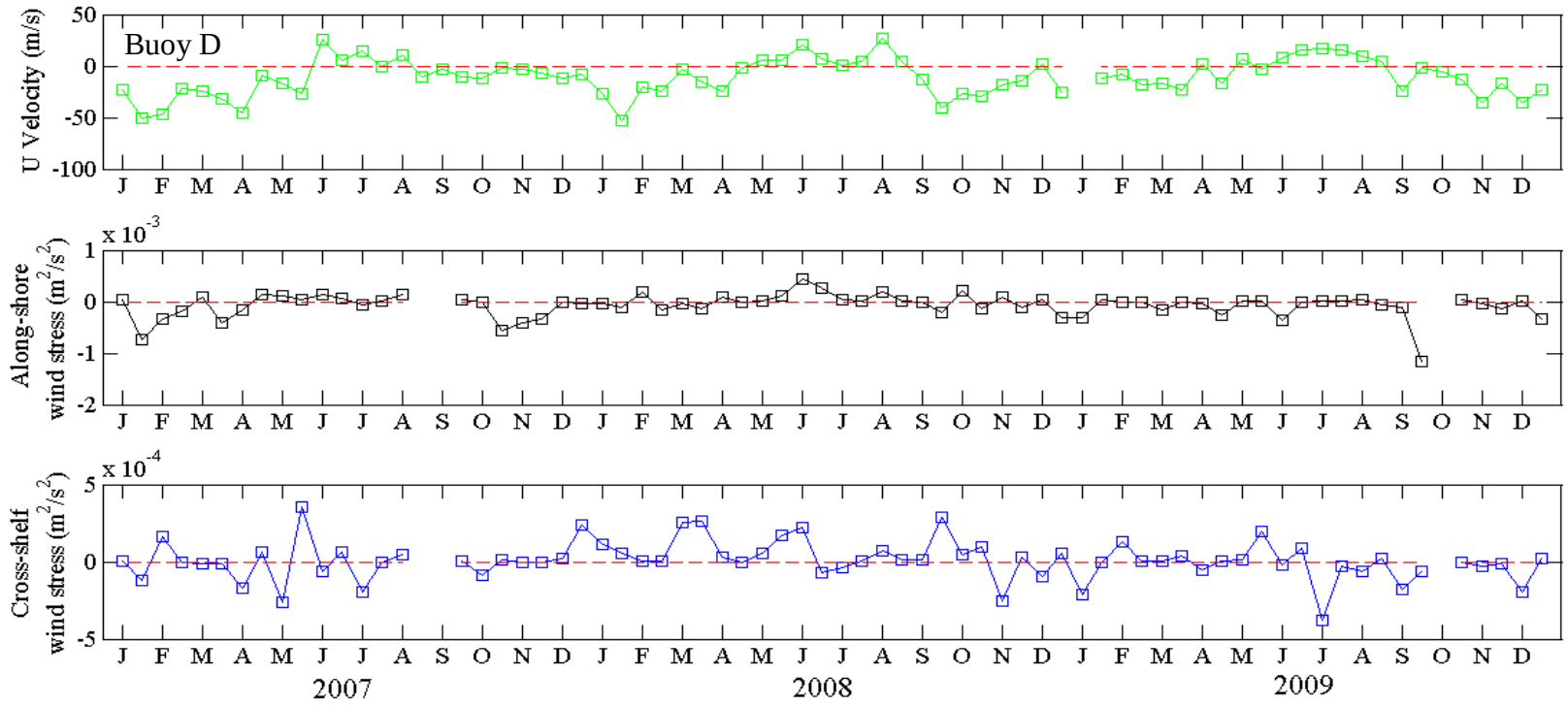

Figure 35. Time series of wind stress and along-shore current velocity at buoy D. The top figure displays the 15-day averaged along-shore current velocity time series at buoy D while the bottom two figures display the 15-day averaged wind stress is both the along-shore and cross-shelf directions measured at nearby NDBC buoy PTAT2. Upcoast forcing is indicated by positive wind stress while negative indicates downcoast in along-shore wind stress. Onshore forcing is indicated by positive cross-shelf wind stress; offshore forcing by negative wind stress. Results show some relationship between the along-shore current velocity and along-shore wind stress, particularly during the first half of 2007 and the second half of 2008.

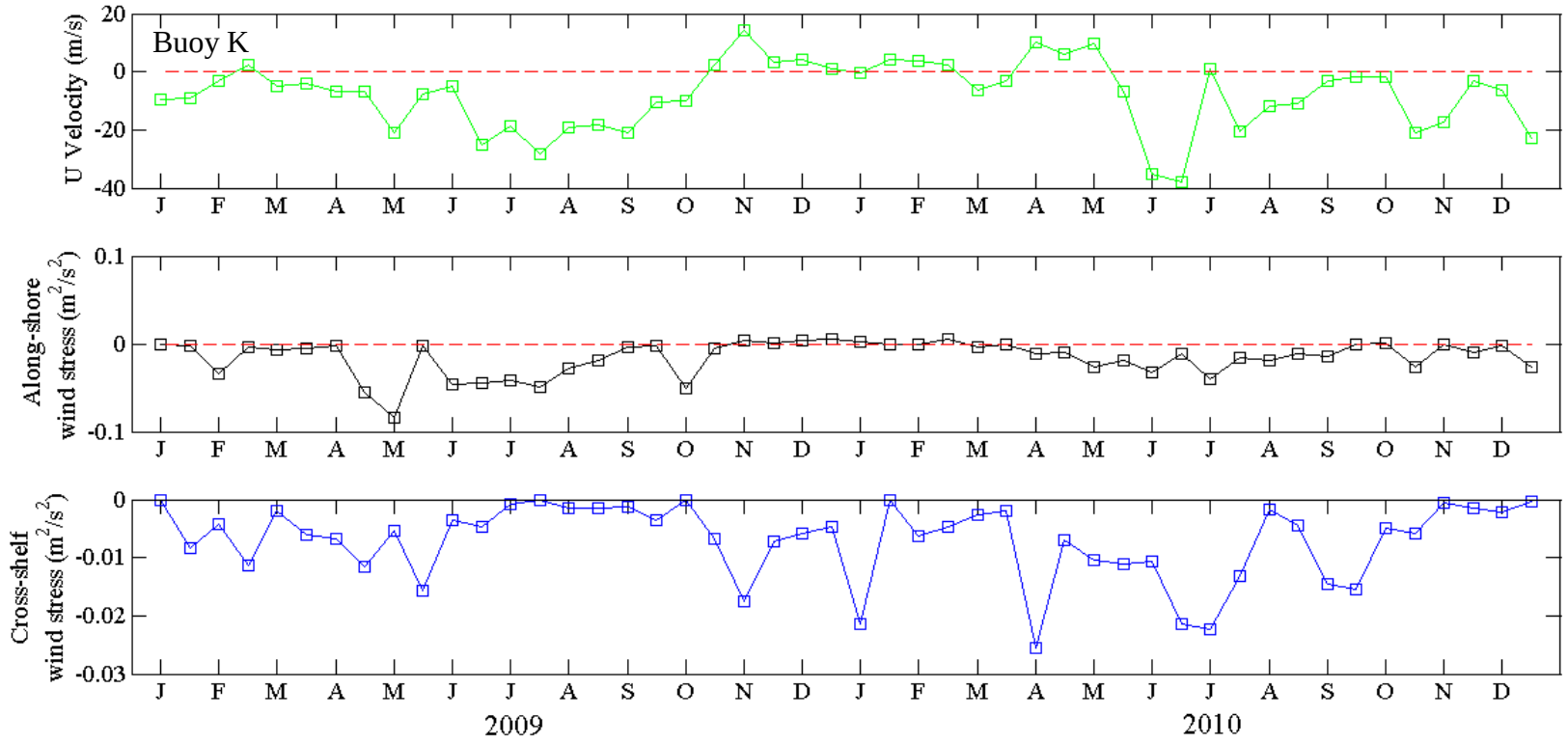

Figure 36. Time series of wind stress and along-shore current velocity at buoy K. The top figure displays the 15-day averaged along-shore current velocity time series while the bottom two figures display the 15-day averaged wind stress is both the along-shore and cross-shelf directions at buoy K. Upcoast forcing is indicated by positive wind stress while negative indicates downcoast in along-shore wind stress. Onshore forcing is indicated by positive cross-shelf wind stress; offshore forcing by negative wind stress. Results show some relationship between the along-shore current velocity and along-shore wind stress. This can be seen from May through August in 2009 and during the winter months of 2009/2010.

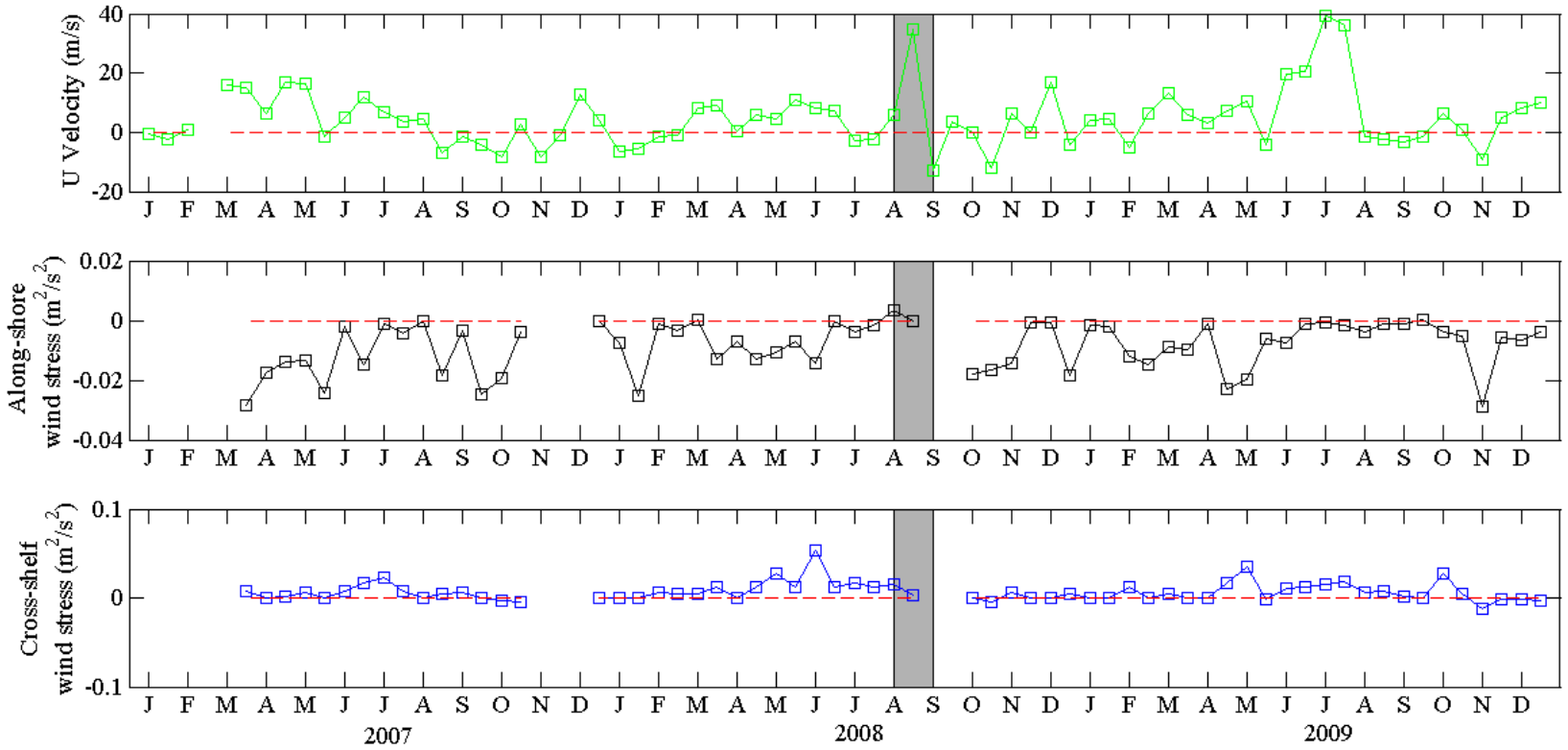

Figure 37. Time series of wind stress and along-shore current velocity at buoy N. The top figure displays the 15-day averaged along-shore current velocity time series while the bottom two figures display the 15-day averaged wind stress is both the along-shore and cross-shelf directions at buoy N. Upcoast forcing is indicated by positive wind stress while negative indicates downcoast in along-shore wind stress. Onshore forcing is indicated by positive cross-shelf wind stress; offshore forcing by negative wind stress. Results show no relationship between the along-shore current velocity and along-shore wind stress. The gray boxes correspond to the dates when an eddy caused prolonged upcoast flow, as shown in figures 38-42.

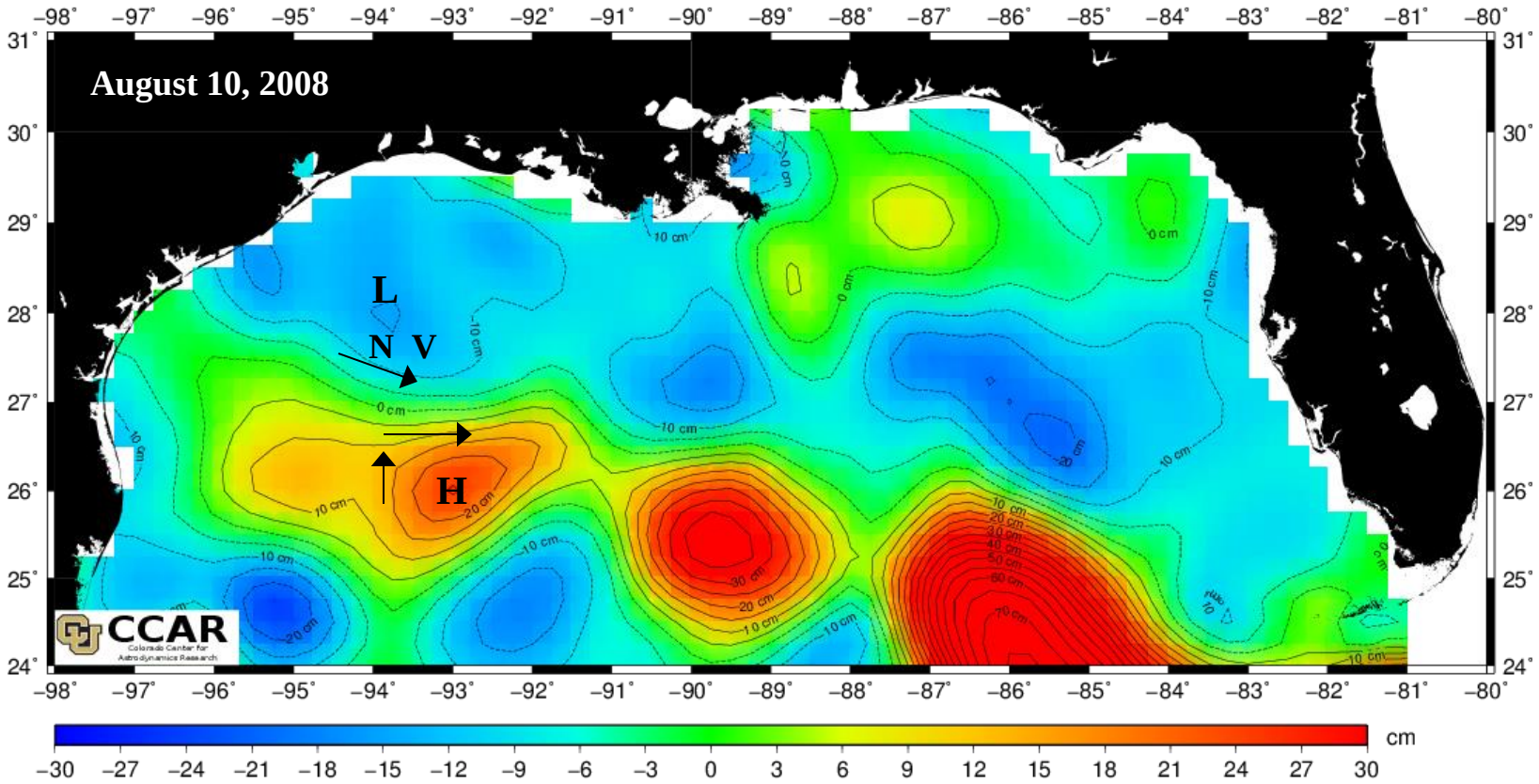

Figure 38. Sea surface height in the Gulf of Mexico on August 10, 2008. Areas of high and low sea surface height are highlighted around the region of buoys N and V. General u-velocity flow is shown by the arrows, moving in an eastward direction in that area. (Figure can be found at http://eddy.colorado.edu/ccar/ssh/hist_gom_grid_viewer).

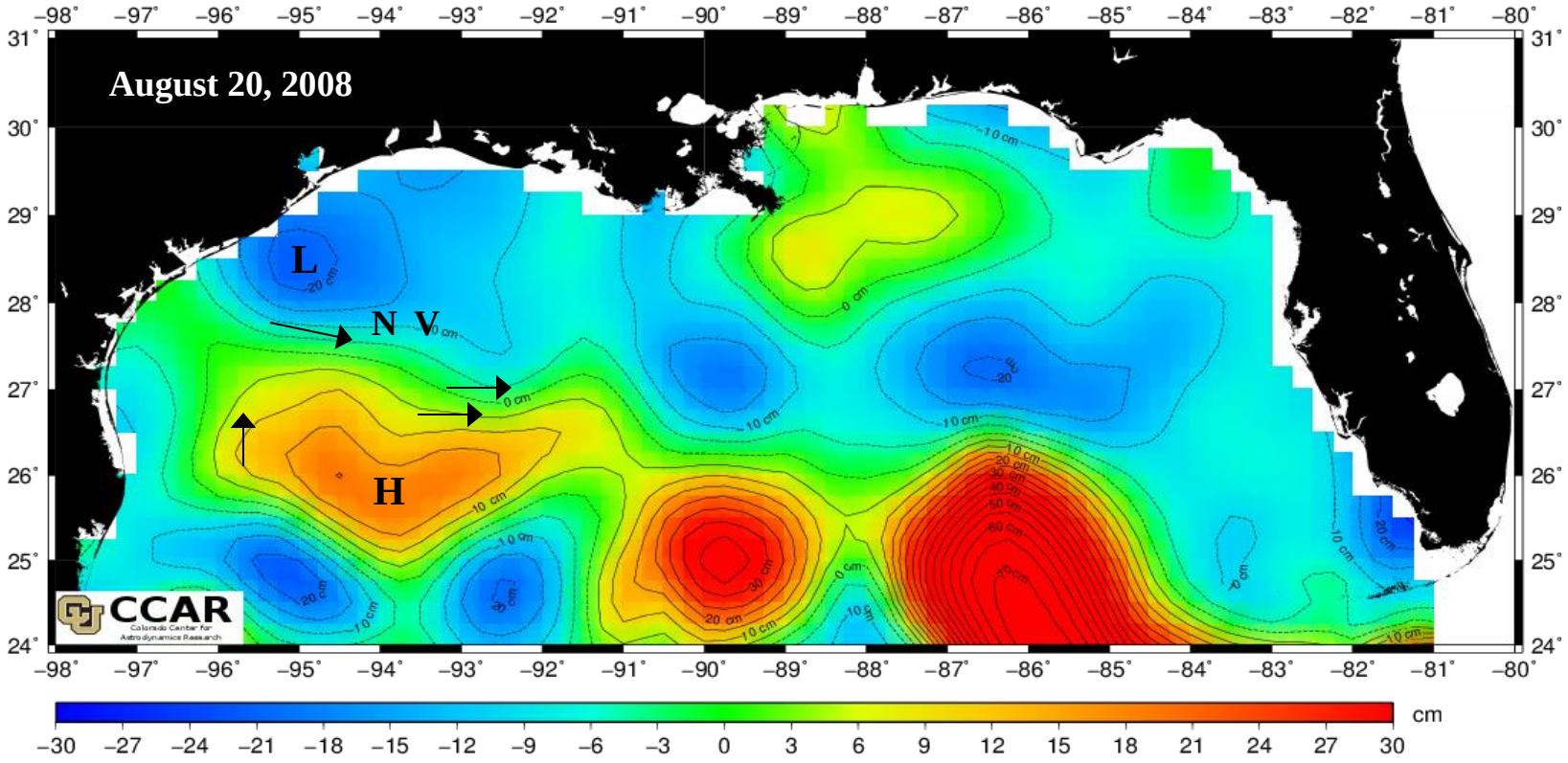

Figure 39. Sea surface height in the Gulf of Mexico on August 20, 2008. Areas of high and low sea surface height are highlighted around the region of buoys N and V. The general u-velocity flow is shown by the arrows, still moving in an eastward direction in that area. (Figure can be found at http://eddy.colorado.edu/ccar/ssh/hist_gom_grid_viewer).

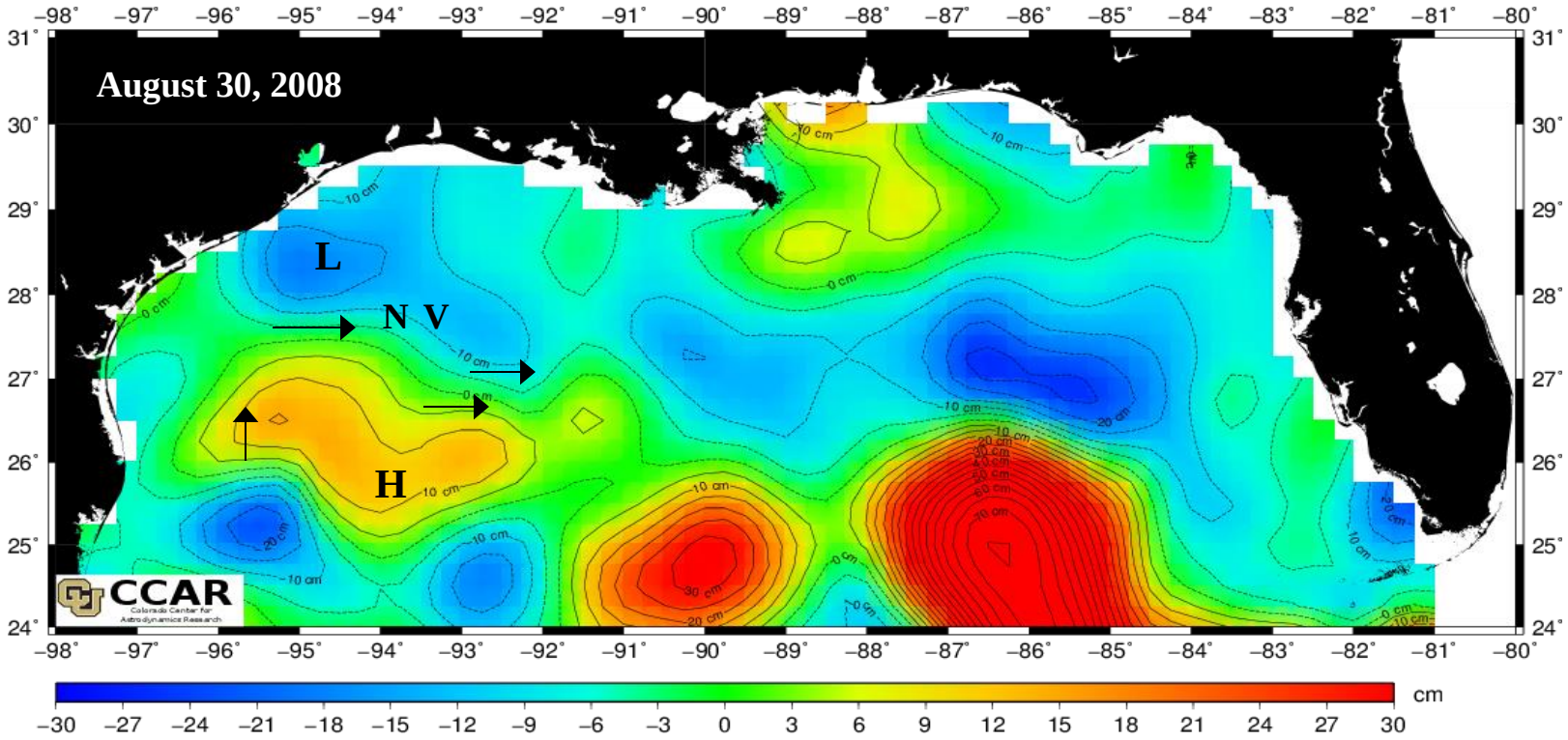

Figure 40. Sea surface height in the Gulf of Mexico on August 30, 2008. Areas of high and low sea surface height are highlighted around the region of buoys N and V. The anticyclonic eddy begins to move further south and weaken, as a cyclonic eddy to the north of buoys N and V moves more westward. The general u-velocity flow is shown by the arrows, moving in an eastward direction in that area. (Figure can be found at http://eddy.colorado.edu/ccar/ssh/hist_gom_grid_viewer).

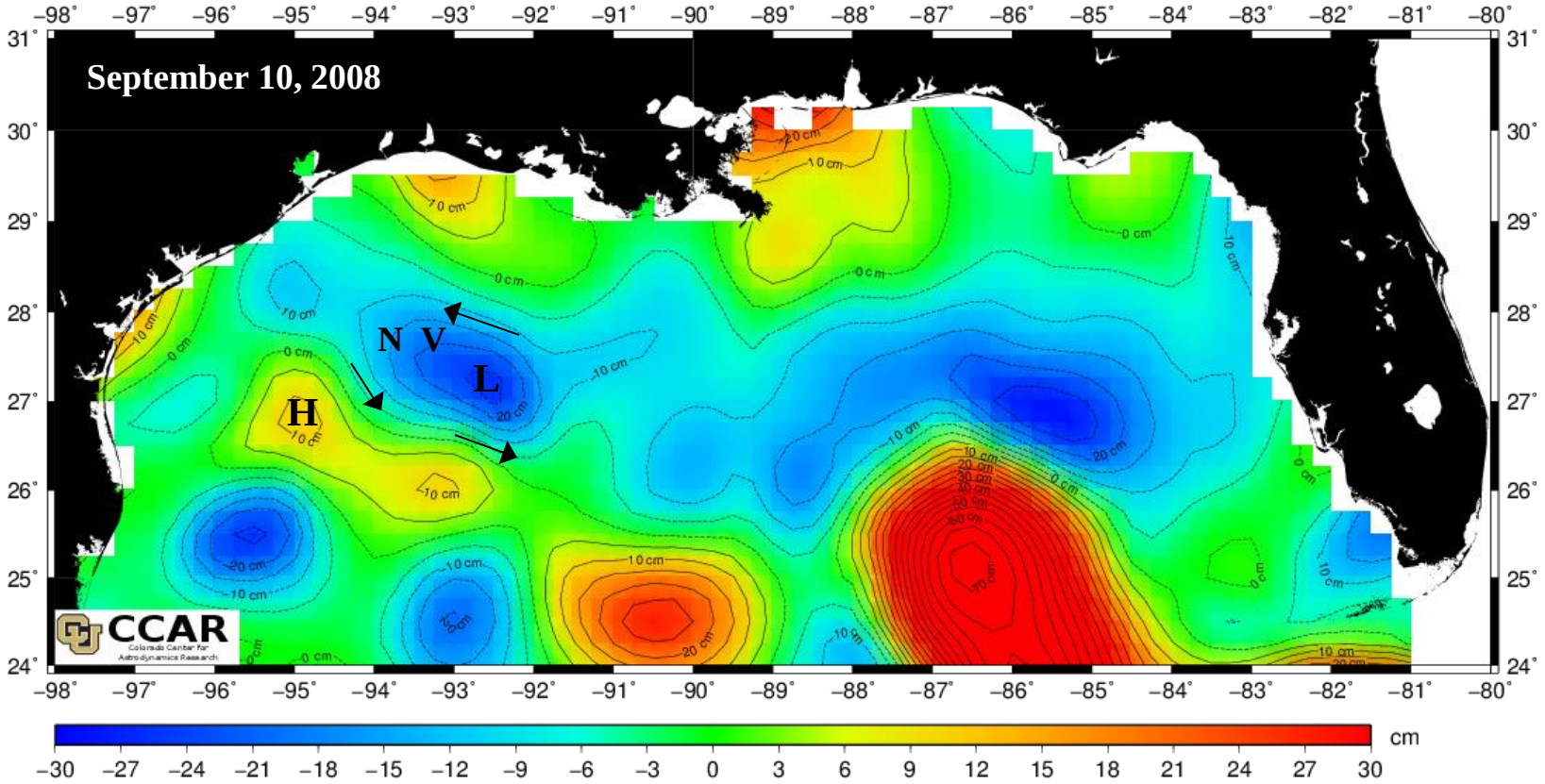

Figure 41. Sea surface height in the Gulf of Mexico on September 10, 2008. Areas of high and low sea surface height are highlighted around the region of buoys N and V. An anticyclonic eddy moved into the area of N and V, causing the general u-velocity to turn more westward. (Figure can be found at http://eddy.colorado.edu/ccar/ssh/hist_gom_grid_viewer).

3.2 Spatial differences

3.2.1 Upper Texas coast

Similarities are present in the general circulation trends at locations near the Upper Texas Coast. Figure 42 shows the upcoast vs. downcoast along-shore velocity trends, with downcoast flow during the non-summer. Both buoys B and F display an overall upcoast flow during the summer. More variability in flow direction is present at buoys R and W. An analysis of mean reversal numbers indicates there are no significant differences between buoys R, F, B, and W. In addition, ANOVAs show no significant differences between normalized reversal numbers at Upper Texas Coast locations are found (Figure 43).

Persistence statistics and ANOVA results indicate similar trends exist in current duration among buoys in the Upper Texas Coast. During non-summer, all four locations have dominant downcoast flow. When flow is upcoast during non-summer, it is relatively slow, with the majority of reversals falling into the 0-5 and 5-10 cm s^{-1} velocity ranges. Downcoast currents tend to be faster, with the majority of velocities being in the 5-10 and 10-15 cm s^{-1} ranges. Buoy B has the highest velocity class of all upper coast buoys in non-summer, with a current recorded between 70-75 cm s^{-1} downcoast. However, this current persisted around 25 hours at that high velocity, meaning that fast currents are generally short-lived.

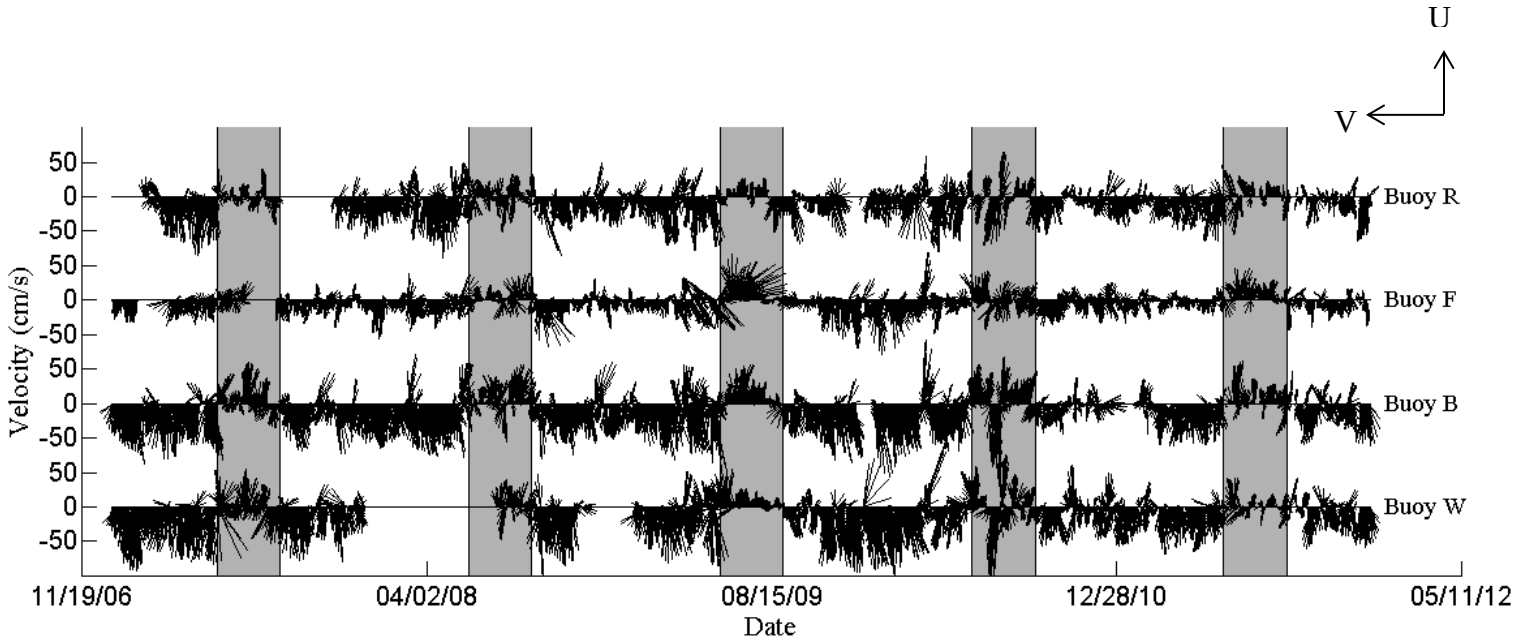

Figure 42. 40-hour low-passed current velocities along Upper Texas Coast. Current velocities are plotted for each Upper Texas Coastal buoy for a 5-year time span, from 2007 through 2011. Data are plotted every six hours and have been rotated in order to show up on the graph as a positive u-velocity (eastward) and down as a negative u-velocity (westward). The gray boxes highlight summer months from June 1 to August 30. Currents are generally upcoast during the summer and transition to dominant downcoast flow during the non-summer months.

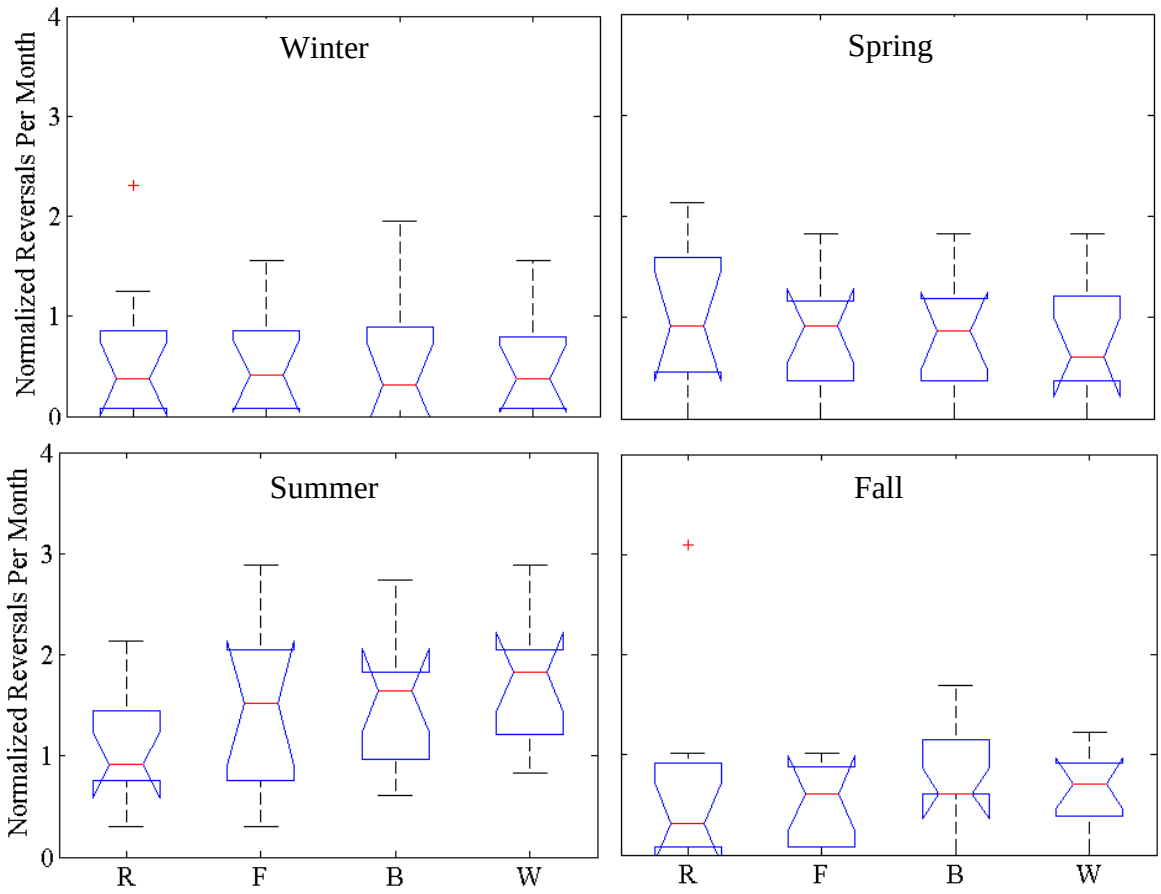

Figure 43. ANOVA of reversal numbers near Upper Texas Coast. The seasonal number of reversals along the Upper Texas Coast are normalized by the number of observations recorded each season. The numbers are then segmented into reversals per month for better interpretation. No statistical differences are found. (Winter – f=.07, probability>f=.977; Spring – f=.4, probability>f=.7542; Summer – f=1.62, probability>f=.2001; Fall – f=.45, probability>f=.7164)

During the summer, buoys B and F have dominant upcoast flow (Table 4). Buoys R and W have slight downcoast dominance present during the summer, with 52.83% and 53.18% of currents flowing downcoast, respectively. Most current reversals fall into the 0-5 and 5-10 cm s^{-1} velocity classes and maximum durations are consistently higher for upcoast flow. Buoy F has the highest number of long-duration currents recorded at 14. These currents last longer than 15 days, but are relatively weak, with velocity ranges of 0-5 and 5-10 cm s^{-1}. In general, while upcoast summer reversals tend to be longer, they are relatively weak. Buoy W has slightly more downcoast reversals than upcoast during the summer. Regardless of direction, currents are generally slow at buoy W, with the majority being in the 0-5 and 5-10 cm s^{-1} velocity classes.

At all buoy locations, including those in the upper coastal area, current duration is centered around 48 hours, meaning that most current reversals are short. The number of currents decreases as both the velocity classes and duration limits increase, as shown in Figure 44, using Buoy B as an example. An overall comparison of current duration at the Upper Texas Coast buoys through ANOVA indicates there are no significant difference at all four locations (Figure 45). This means that each location has similar seasonal trends in current persistence.

A comparison of spectral amplitudes within the weather band frequency shows only one significant difference between the Upper Texas Coastal locations (Figure 46). ANOVA results indicate during the spring, buoy R has significantly higher spectral amplitudes compared to buoys B, F, and W. This means there is more variance present in the weather band frequencies at buoy R compared to the other buoys. However, there

is no significant difference between the spectral amplitudes at these four locations in the weather band frequencies during the winter, summer, and fall. This indicates that there is little variance in the current energy, with fewer oscillations occurring during these seasons at near the Upper Texas coast.

With a distance of about 68.5 km separating buoys B and F, coherency analysis is used to determine the correlation of the along-shore current spectral estimates between the two locations. The outcome shows there is significance in the u-velocity coherency within the weather band frequencies (Figure 47). The average coherence within the weather band frequency is .1476, which is above the 95% confidence level. This means that 14.76% of the u-velocity data between buoys B and F are correlated. Higher coherency exists in the mesoscale frequencies, meaning there is more coherency between the two u-velocity records on seasonal timescale.

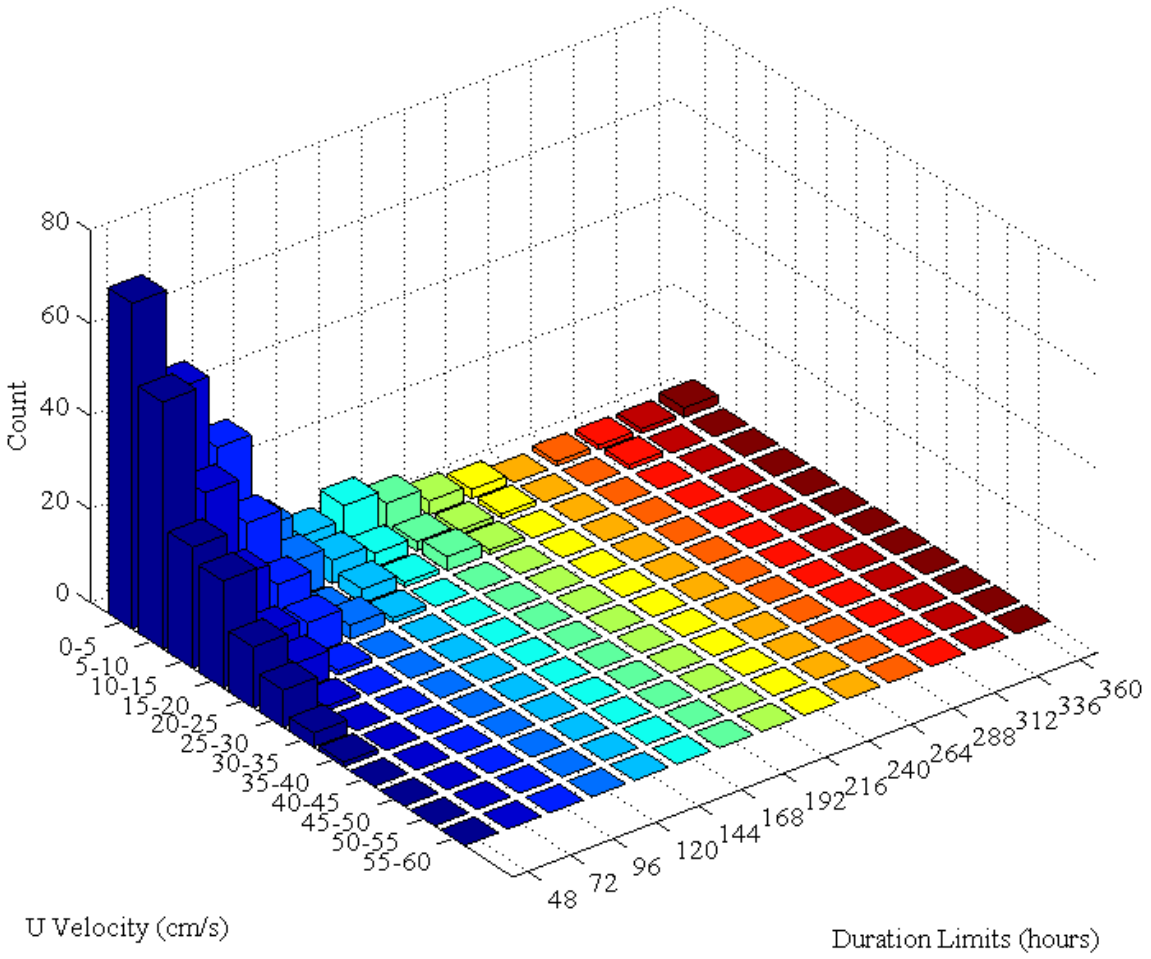

Figure 44. 3D bar graph of upcoast persistence trends at buoy B. Persistence trends at Buoy B show more currents occur in the 0-5 cm s^{-1} velocity class with durations of 48 hours. The general trend shows there are fewer currents that persist as the duration limits and velocity classes increase. This is the general persistence trend is present at all buoys evaluated.

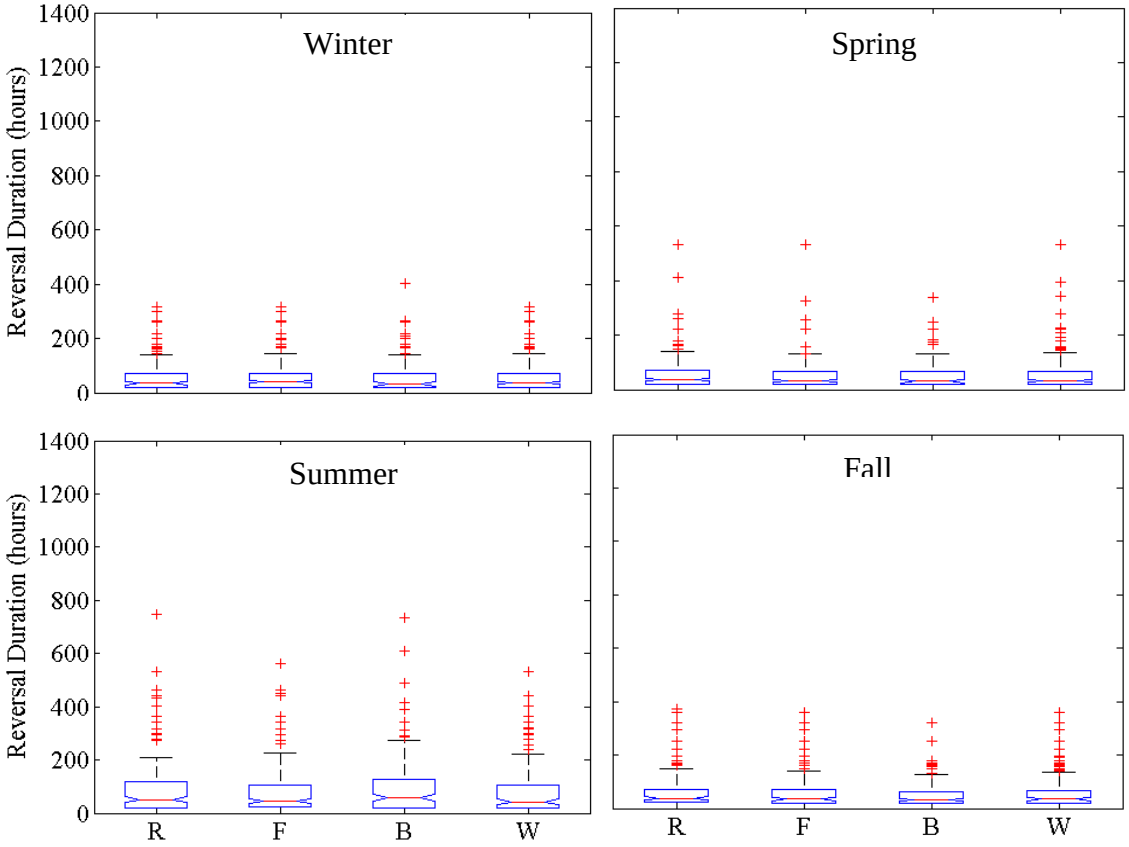

Figure 45. ANOVA of current persistence near Upper Texas Coast. The ANOVAs represent the seasonal current durations at each location near the Upper Texas Coast. No statistical differences are found. (Winter – F=1.15, probability>p=3.29; Spring – F=.21, probability>p=.8904; Summer – F=1.3, probability>p=.2725; Fall – F=.84, probability>p=.4702)

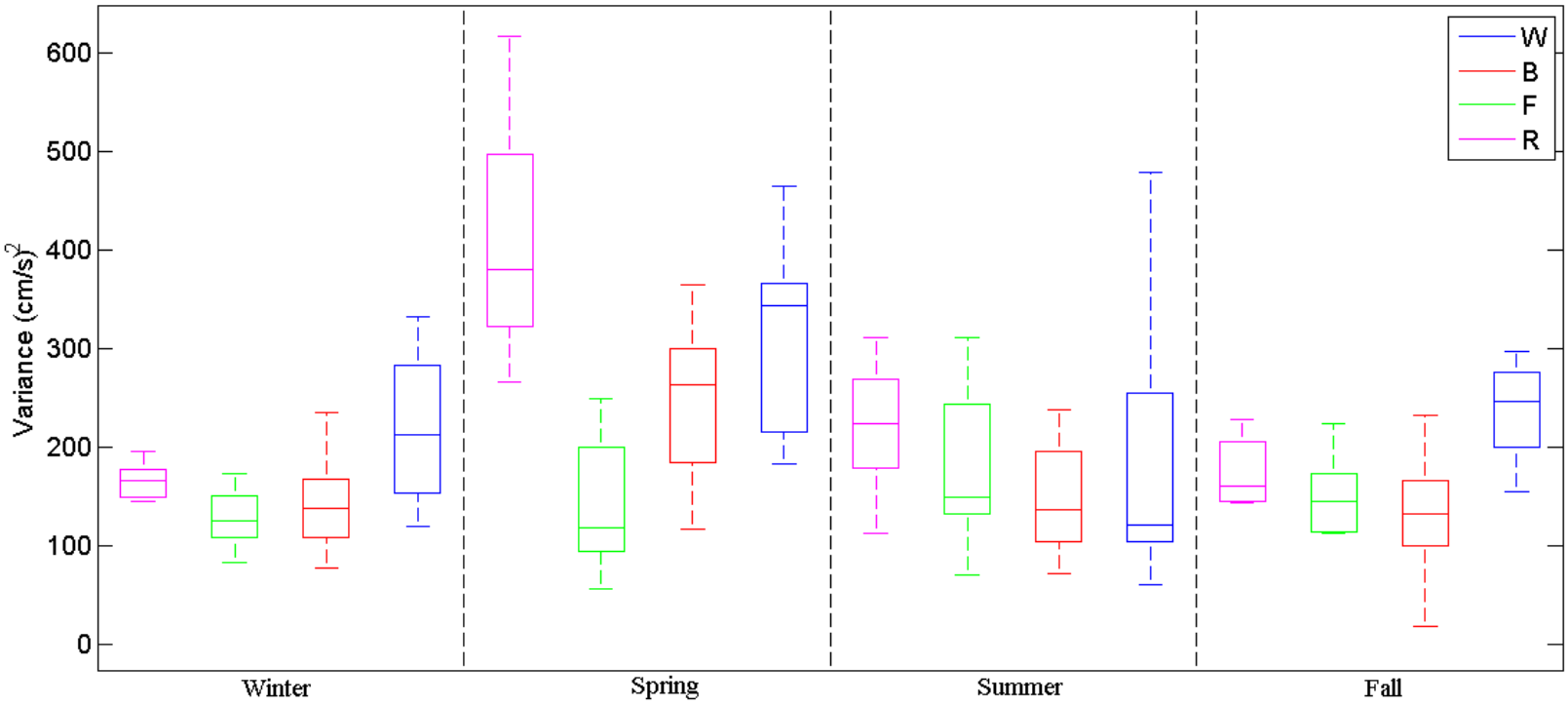

Figure 46. Spectral variance comparison for the Upper Texas Coast. Spectral energy from current velocities within the weather band frequencies for buoys along the Upper Texas Coast are compared. Buoy R has significantly more variance present during the spring compared to buoys F, B, and W. During the other seasons, there is little variation in current energy present.

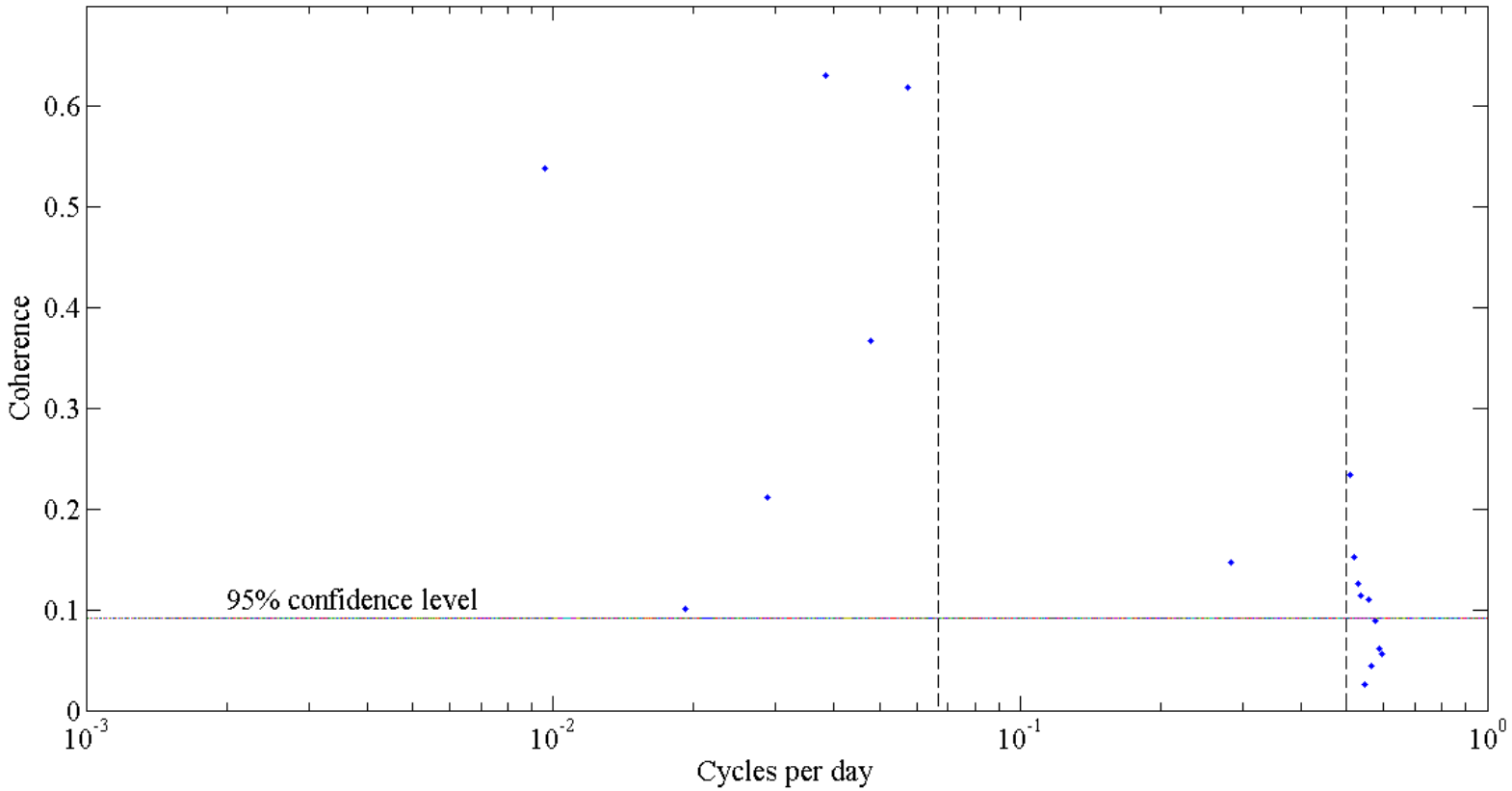

Figure 47. Coherence spectrum for buoys B and F. This display the coherency of the u-velocity for buoys B and F. The dashed vertical lines represent the 2 day and 15 day frequencies, showing the coherence within the weather band frequencies. The coherence within the weather band has been averaged, resulting in a mean coherence of .1476, which is found to be significant.

3.2.2 Lower Texas coast

The Lower Texas Coastal locations show considerable variability in the general circulation. Along-shore flow trends vary within seasons and from year to year. For example, during 2009, summer flow generally moves upcoast, but tends to be more variable in 2010 and 2011 (Figure 48). Results in Table 1 indicate an overall upcoast flow present at buoy D during the non-summer, with a neutral flow (U_{mean}=0) present during the summer. Buoy J has an overall downcoast flow present during the non-summer and summer. This shows that general trends vary between the southern Texas coastal locations.

Analysis of reversal numbers indicates similar trends among buoys on the Lower Texas Coast. Both buoys J and D have fewer reversals during the summer, with more reversals occurring the winter and spring, as displayed in Table 2. An analysis of normalized reversal numbers indicate any differences in the number of seasonal reversals are not significant, as shown in Figure 49.

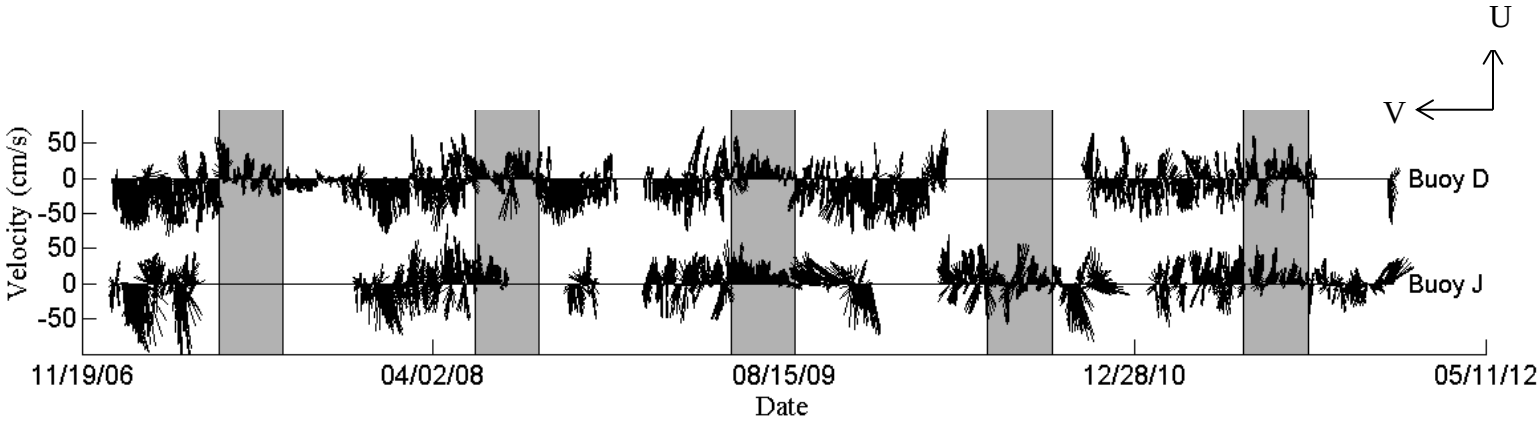

Figure 48. 40-hour low-passed current velocities along Lower Texas Coast. Current velocities are plotted for both Lower Texas Coastal buoys for a 5-year time span, from 2007 through 2011. Data are plotted every six hours and have been rotated in order to show up on the graph as a positive u-velocity (eastward) and down as a negative u-velocity (westward). The gray boxes highlight summer months from June 1 to August 30. Currents are generally upcoast during the summer in 2009 but tend to vary during the other years. Downcoast flow is dominant during the non-summer months but also tends to have variability from year to year.

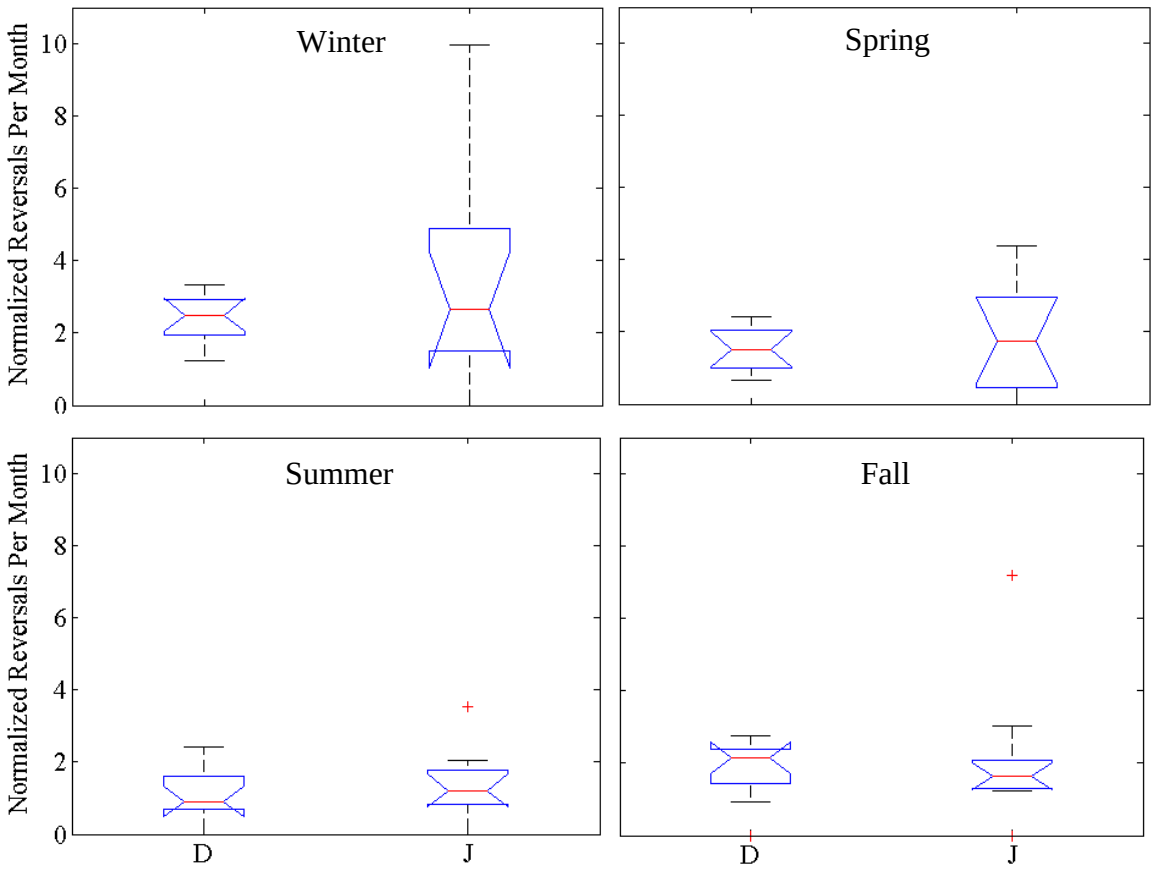

Figure 49. ANOVA of reversal numbers near Lower Texas Coast. The seasonal number of reversals along the Lower Texas Coast are normalized by the number of observations recorded each season. The numbers are then segmented into reversals per month for better interpretation. No statistical differences are found. (Winter – f=1.37, probability>f=.2554; Spring – f=.34, probability>f=.5637; Summer – f=.94, probability>f=.3431; Fall – f=.02, probability>f=.8843)

Spatial variability is present between Lower Texas Coast locations in regards to seasonal flow. During the summer, both buoys have dominant downcoast flow, as shown in Table 4. During the non-summer, both buoys D and J have a general upcoast flow during the non-summer, with 58.54% and 50.68% of currents observed flowing upcoast,

respectively. As shown in Table 5, buoy D has less variability in velocity compared to J during the non-summer. More than 57% of currents observed during the non-summer fall into in the 0-5 cm s^{-1} velocity class for buoy D, while more than 50% of currents recorded at buoy J fall into 0-5, 5-10, or 10-15 cm s^{-1} velocity classes. Longer upcoast persistence is observed at J as well, with some currents flowing upcoast for ~35 days. The longest current recorded at buoy D lasts for ~20 days. Buoy J has the highest observed velocity between the two lower coast buoys in non-summer, with a current recorded between 90-95 cm s^{-1} upcoast. The current only persisted for 25 hours at that high rate, reiterating that fast current flows do not last very long.

During the summer, the prevailing circulation is downcoast at both buoys D and J (Table 4). Table 3 indicates the current flow at buoy D is slow, with a dominant velocity class of 0-5 cm s^{-1}. Buoy J has a faster downcoast flow, with a dominant velocity class of 10-15 cm s^{-1} and several currents persisting at velocities between 15-20 cm s^{-1}. Again, longer downcoast persistence is observed at J, with current durations observed at ~70 days. In addition, buoy J has the highest recorded velocity class during the summer, with a current observed between 55-60 cm s^{-1}, but with duration of less than three days. ANOVA results confirmed that there is no significant difference between both locations in terms of current duration, meaning each location has similar seasonal trends in persistence (Figure 50).

A comparison of the spectral amplitudes within the weather band frequencies reveals significant differences between the two buoys (Figure 51). For all seasons, buoy J has significantly higher spectral amplitudes compared to buoy D. This indicates that

buoy D has less variance in spectral energy compared to buoy J, which has more energy oscillations consistently throughout the year. This is consistent with other analysis results between buoys D and J, indicating there is less variability in both current velocity and energy at buoy D compared to buoy J.

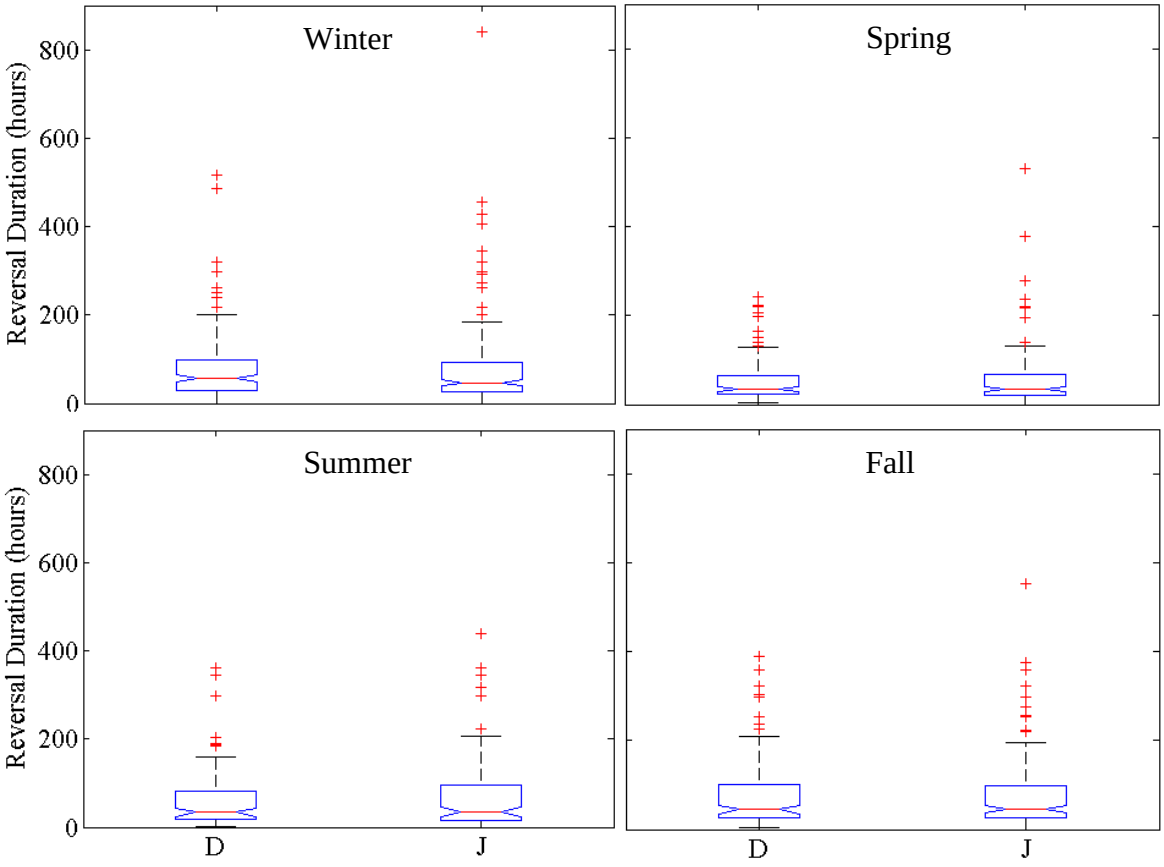

Figure 50. ANOVA of current persistence near Lower Texas Coast. The ANOVAs represent the seasonal current durations at each location near the Lower Texas Coast. No statistical differences are found. (Winter – F=.05, probability>p=.8223; Spring – F=.27, probability>p=.6033; Summer – F=.38, probability>p=.538; Fall – F=.22, probability>p=.6414)

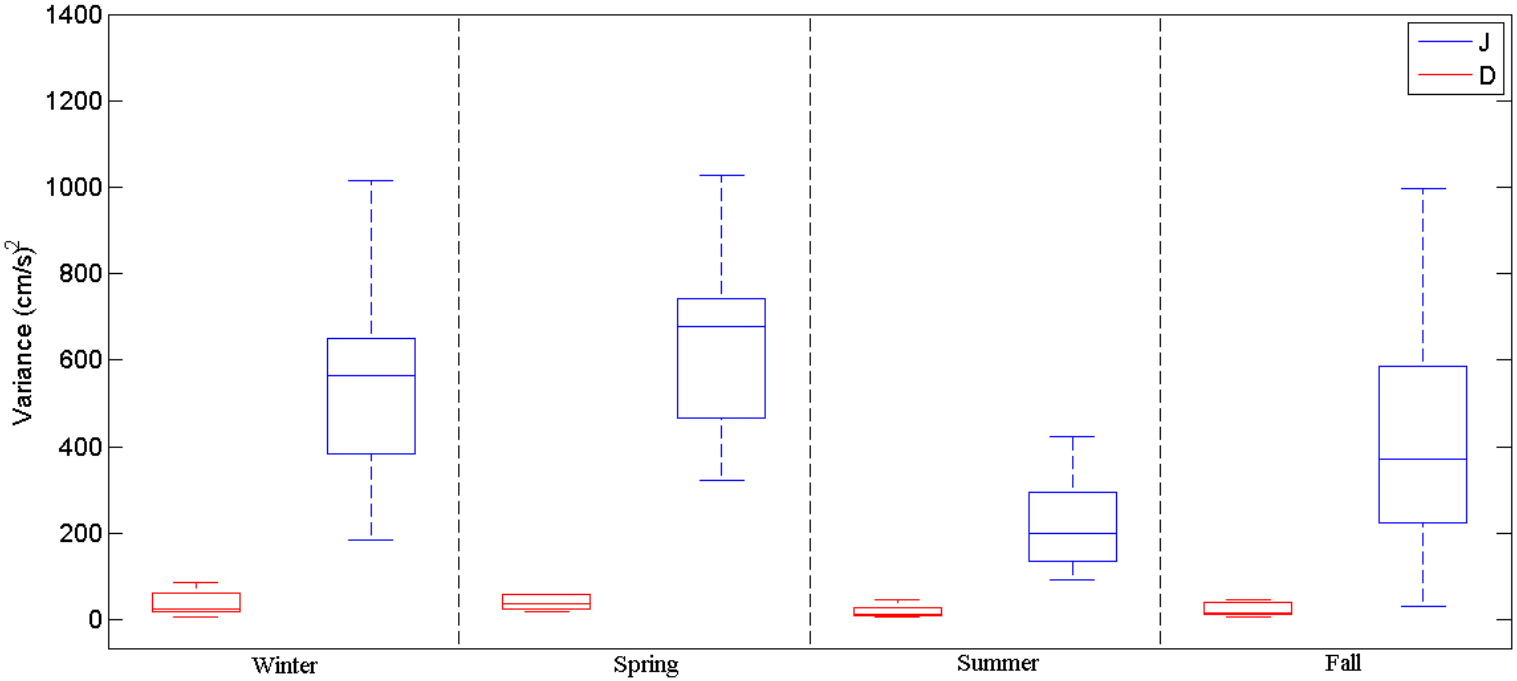

Figure 51. Spectral variance comparison for the Lower Texas Coast. Spectral energy from current velocities within the weather band frequencies for buoys along the Lower Texas Coast are compared. Buoy J consistently has greater variance than buoy D. This means buoy J has more energy oscillations throughout the year while current energy at buoy D is fairly constant.

3.2.3 Offshore

Differences exist in the general circulation trends between the offshore locations. Results in Table 1 and Figure 52 show buoy N has a dominant upcoast flow regardless of season, with average u-velocities of 6.8 cm s^{-1} during the summer and 9.4 cm s^{-1} during the non-summer. Buoy V has a similar upcoast trend, with average u-velocities of 5.7 cm s^{-1} during the summer and 6.4 cm s^{-1} during the non-summer. Unlike buoys N and V, buoy K has an overall downcoast flow during the summer and non-summer, with average u-velocities of -18.2 and -1.9 cm s^{-1}, respectively.

Analysis of reversal numbers indicates similar trends among offshore buoys. Buoys K, N, and V all have fewer reversals during the summer, with more reversals occurring the winter and spring, as displayed in Table 2. An analysis of normalized reversal numbers indicate any differences in the number of seasonal reversals are not significant, as shown in Figure 53.

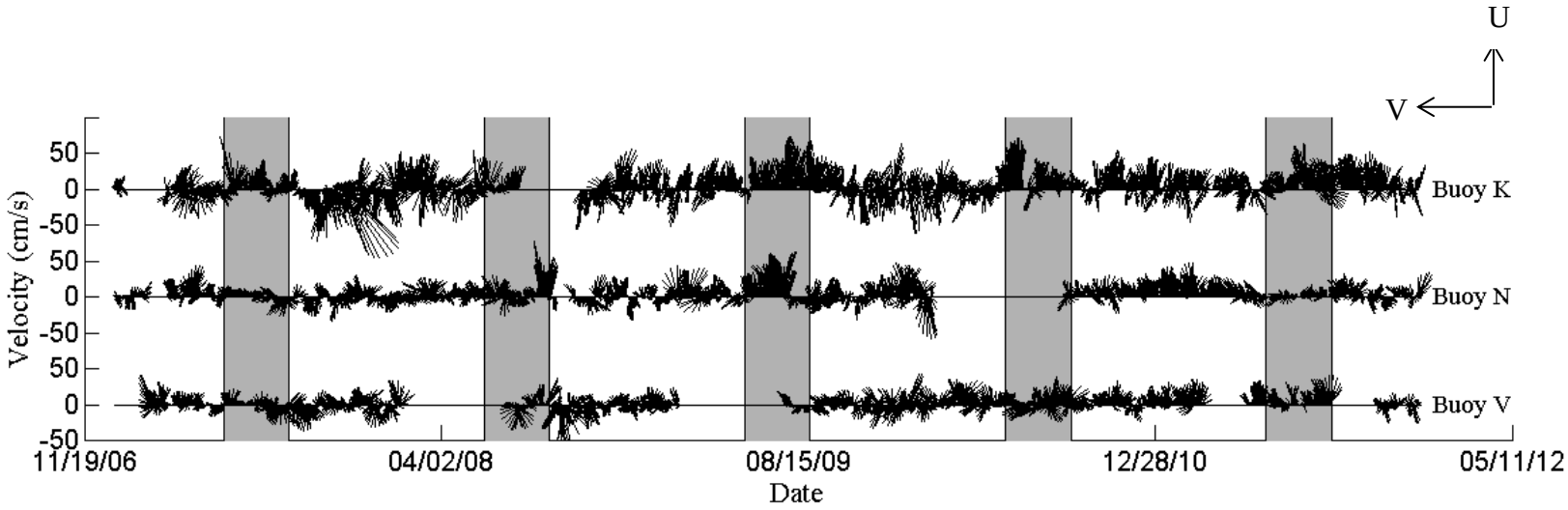

Figure 52. 40-hour low-passed current velocities offshore. Current velocities are plotted for each offshore buoy for a 5-year time span, from 2007 through 2011. Data are plotted every six hours and have been rotated in order to show up on the graph as a positive u-velocity (eastward) and down as a negative u-velocity (westward). The gray boxes highlight summer months from June 1 to August 30. Currents generally flow upcoast at buoy N regardless of season, while buoys K and V have variable flow throughout each record.

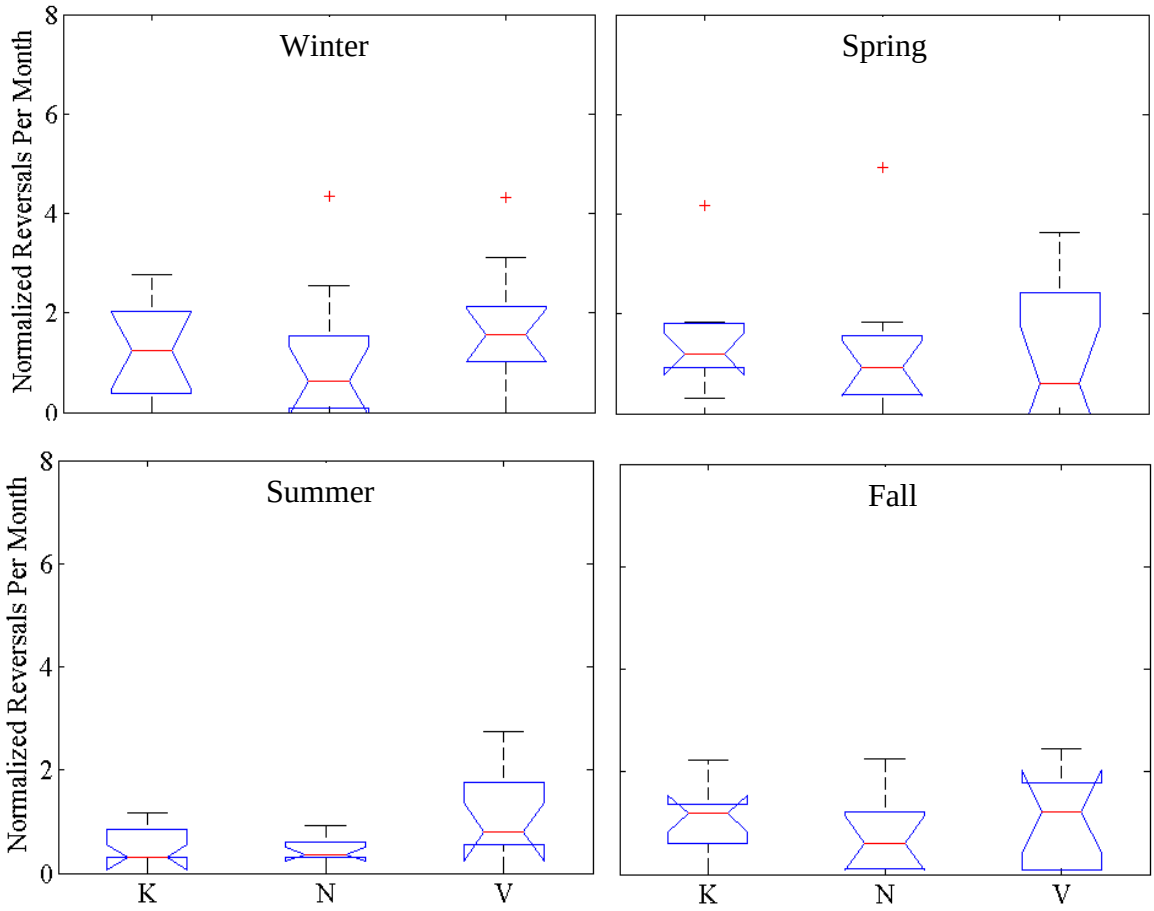

Figure 53. ANOVA of reversal numbers at offshore locations. The seasonal number of reversals at buoys along the outer Texas-Louisiana Shelf are normalized by the number of observations recorded each season. The numbers are then segmented into reversals per month for better interpretation. No statistical differences are found. (Winter – f=.52, probability>f=.5943; Spring – f=.16, probability>f=.8495; Summer – f=.78, probability>f=.4658; Fall – f=.38, probability>f=.6893)

Despite buoys at other locations having seasonal variability, persistence trends are fairly constant at offshore buoys. In the non-summer, all offshore buoys have the same dominant velocity classes regardless of flow direction: 0-5 cm s^{-1} and 5-10 cm s^{-1}

(Table 5). However, non-summer persistence characteristics differ between locations. At buoy K, mean current duration is higher downcoast, with a mean of 97 hours, compared to upcoast flow, which has a mean duration of 76 hours. Both buoys N and V have longer current persistence upcoast, with mean current durations of 191 and 125 hours, respectively. Downcoast currents have shorter durations at both locations, with a mean persistence of 99 hours at buoy N and 93 hours at buoy V. ANOVA results indicate current persistence is significantly higher at buoy N during the spring compared to both buoys V and K, yet there is no significant difference between the offshore locations during fall and winter (Figure 54).

In summer, currents are slower and less persistent when moving upcoast at buoy K, with a dominant velocity class of 0-5 cm s^{-1} and a mean current duration of 65 hours (Table 3). Currents flow faster downcoast and persist longer, with a mean current duration of 186 hours in the dominant velocity class of 10-15 cm s^{-1}. Buoys N and V have similar flow characteristics during the non-summer. Both have faster upcoast currents with longer duration, with a mean current duration of 128 hours at buoy N and 103 hours at buoy V in the dominant velocity class of 5-10 cm s^{-1}. Downcoast currents are slower and less persistent, with average current durations of ~100 hours in the dominant velocity class of 0-5 cm s^{-1}. ANOVA results show that there are significant differences in summer current persistence between buoys K and N, while buoy V shows no significant difference.

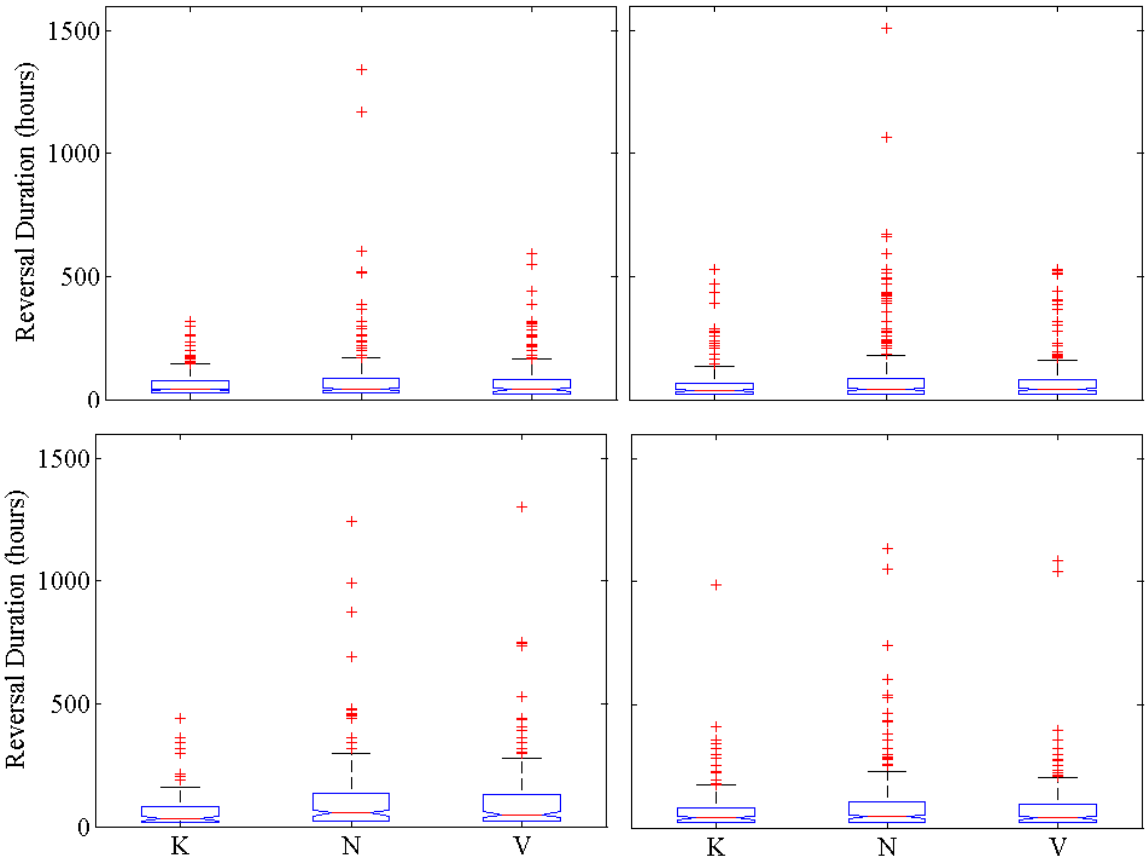

Figure 54. ANOVA of current persistence at offshore locations. The ANOVAs represent the seasonal current durations at each location on the outer Texas-Louisiana shelf. Significant differences are found during the spring, with buoy N having longer current durations compared to buoys V and K. Significant differences are also present during the summer between buoys K and N, with N again having longer current durations. (Winter – F=2.54, probability>p=.0792; Spring – F=7.1, probability>p=.0009; Summer – F=5.54, probability>p=.0042; Fall – F=1.76, probability>p=.1729)

Analysis of the spectral amplitudes shows there are some significant differences in the weather band frequencies between offshore buoys (Figure 55). ANOVA results indicate there are significantly higher spectral amplitudes at buoy K in the fall compared to buoys N and V. This means the current variance is larger at buoy K compared to the other offshore buoys. During the other seasons, there are no significant differences between the three offshore buoys, signifying the variance in spectral energy is more consistent at all three locations.

With only about 42.5 km separating buoys N and V, coherency analysis is used to determine if there is a relationship in the u-velocity spectral estimates between the two locations. Results indicate there is some significant coherency between N and V, as shown in Figure 56. The average coherence within the weather band frequencies is .2357, which is above the 95% significance level. This means that 23.57% of the u-velocity data between buoys N and V are correlated. Some coherency exists in within the mesoscale band, showing there is some correlation between the two buoys on a seasonal scale, but it is less significant compared to the coherency in the weather band frequencies.

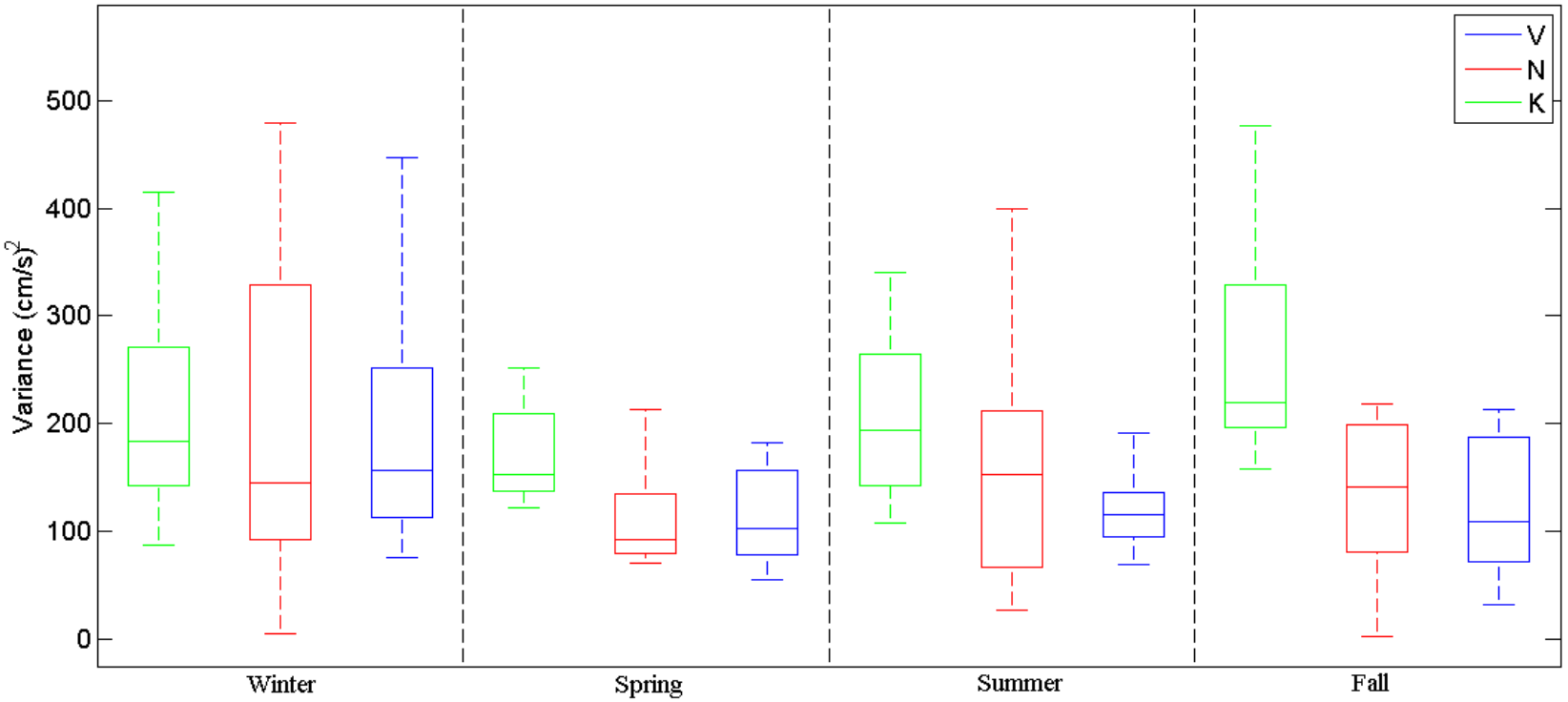

Figure 55. Spectral variance comparison for offshore buoys. Spectral energy from current velocities within the weather band frequencies for buoys located offshore are compared. Buoy K consistently has more variance compared to buoys N and V, particularly in the fall. During the other seasons, all three buoys have more consistent spectral energy, indicating little variance is present in those seasons.

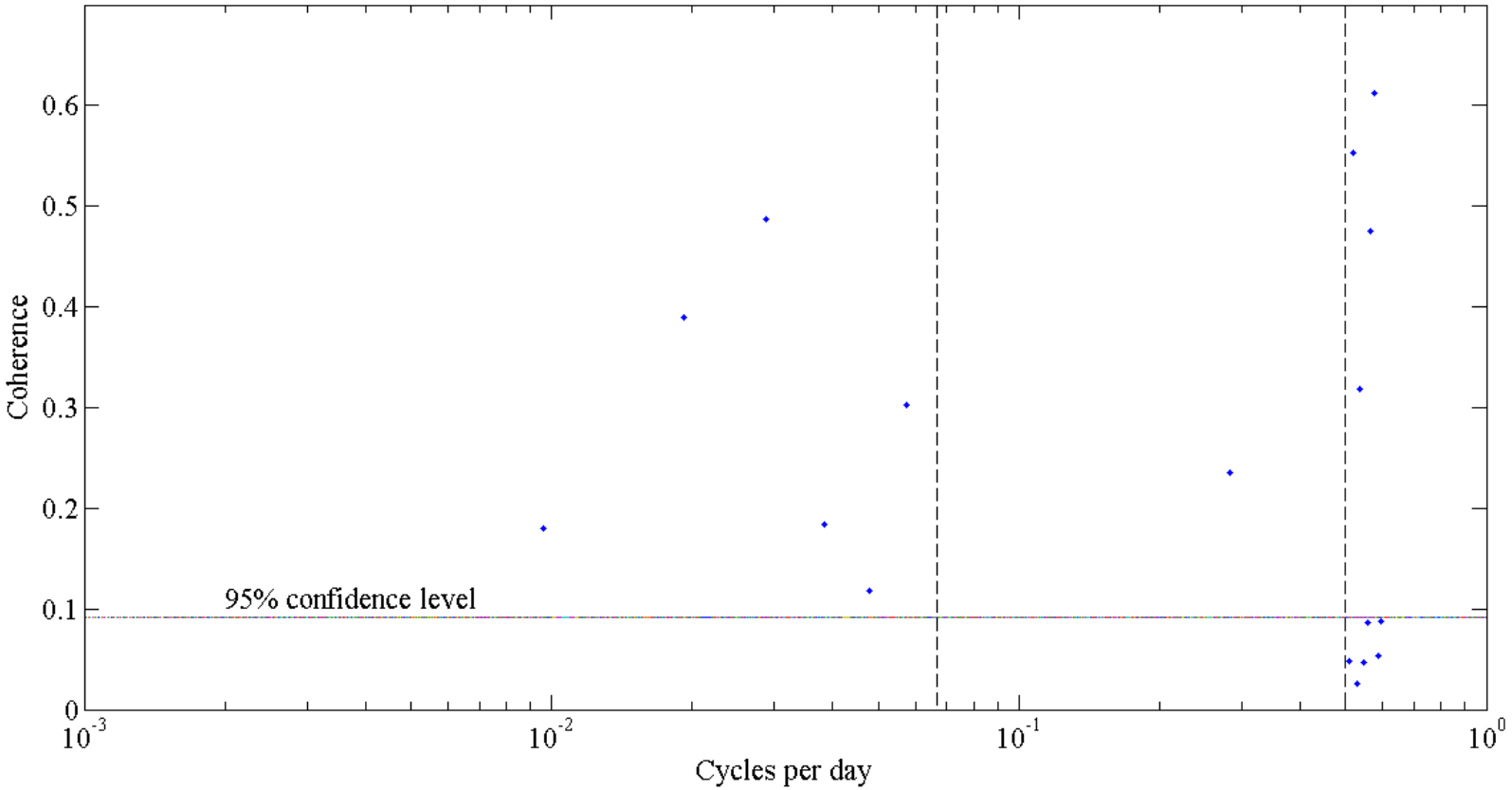

Figure 56. Coherence spectrum for buoys N and V. This displays the coherency of the u-velocity for buoys N and V. The dashed vertical lines represent the 2 day and 15 day frequencies, showing the coherence within the weather band frequencies. The coherence within the weather band has been averaged, resulting in a mean coherence of .2357, which is found to be significant.

4. DISCUSSION

Throughout the Texas-Louisiana Shelf, seasonal and spatial variability is present in the along-shore current flow. Along the Upper Texas Coast, the summer circulation is generally upcoast with relatively slow current velocities and downcoast with faster velocities observed during the non-summer. This is consistent with the shelf circulation findings in Cochrane and Kelly (1986), Cho et al. (1998), and Nowlin et al. (2005). A strong seasonal relationship is observed between the along-shore wind stress and current flow, with southeasterly winds providing the circulation forcing during the summer and northeasterly winds during the non-summer months, as found in Cho et al (1998), Nowlin et al. (1998) and Nowlin et al. (2005). Because the weather band has been a proven forcing mechanism for the coastal circulation, the most variance in current energy is present during the non-summer months due to the frequent passages of fronts (Nowlin et al. 1998; Nowlin et al. 2005). The least variance in current energy is shown during the summer months, due to light upcoast winds and the infrequency of frontal passages.

Compared to the Upper Texas Coast, distinguishable seasonal differences are present along the Lower Texas Coast. Near the region where the Texas coast bends, the current flow is more variable during the summer, transitioning between upcoast and downcoast flow with relatively slow velocities. Further south, downcoast flow is more dominant, with faster velocities compared to other coastal locations. During the non-summer, upcoast flow is present at buoy D near the Texas coastal bend, but with

relatively slow velocities. The flow direction varies between upcoast and downcoast at buoy J along the southern Texas coast, with relatively slow velocities observed as well. A relationship between the along-shore wind stress and along-shore current flow is observed in this region, but to a lesser extent than in the Upper Texas Coast. The wind stress provides some of the forcing for the seasonal current flow, but it is likely that other forcing mechanisms, such as offshore eddies, have an influence on the circulation patterns in the southwestern shelf region (Nowlin et al. 2005). Most variance along the Lower Texas Coast is present during the winter with the frequent passages of fronts and decreases to a minimum during the summer, when frontal passages are infrequent (Nowlin et al. 1998; Nowlin et al. 2005).

The outer shelf region has very little variability on a seasonal scale, with a dominant upcoast flow present during the summer and non-summer, consistent with study findings in Cochrane and Kelly (1986), Nowlin et al. (1998), and Nowlin et al. (2005). Slightly faster velocities are observed during the non-summer in this region compared to the summer. No relationship between the along-shore wind stress and current flow was observed on the outer shelf. The effect of offshore eddies on the circulation in the region is apparent, proving that the mesoscale band provides the major forcing for the current flow on the outer shelf. Again, this is consistent with the results from Cochrane and Kelly (1986), Nowlin et al. (1998), and Nowlin et al. (2005).

While others have generalized the seasonal variability in the circulation on the Texas-Louisiana shelf, there are other variables that are important to look at in order to characterize the circulation not only throughout the continental shelf, but also in the

Texas Coastal Current. Numerous studies (Cho et al., 1998; Chu et al., 2005; Cochrane and Kelly, 1986; Li et al., 1997; Nowlin et al. (1998); Nowlin et al. (2005); Smith, 1980; Wang et al., 1998) have discussed the overall seasonal reversal in the circulation between summer and non-summer, yet no study has quantified the number of reversals that occur on a seasonal basis. Although the quantification of reversals was found to be almost universal regardless of season, it is now known that seasonal reversal numbers are not a good indicator of circulation variability across the shelf.

Additional factors, such as current reversal duration and transport, have also not been previously studied on the Texas-Louisiana shelf and provide an added layer of seasonal variability to the shelf circulation patterns. Most current reversals that occur, regardless of season or location on the shelf, are short-lived, centered around 48 hours. Particularly high velocity currents (>50 cm s^{-1}) are found to consistently have short persistence. Based on the results in Table 5, most very fast currents do not last longer than 3-4 days. While these high velocity currents occur infrequently at Upper Texas Coastal locations, they are found to be more frequent at locations on the southern shelf, especially during the non-summer. The highest velocity current observed is at buoy K, with a current recorded in the 100-105 cm s^{-1} range during the non-summer. The current only lasted 33 hours, reiterating that very fast currents do not persist very long.

Distinctive patterns are also present in the longer persisting currents. Long-lived currents (>15 days) are observed at each buoy location in both the summer and non-summer. During the summer, long-lived currents occur more frequently at buoy J along the southern coast and at offshore locations (Table 3). Long-lived currents occur less

frequently at Upper Texas Coastal locations. Most currents with longer persistence are slow (>10 cm s^{-1}), but occasionally these currents are recorded at faster velocities. During the non-summer, more long-lived currents are observed, particularly in coastal areas in the downcoast direction. The majority of these long-lived currents are also slow, with occasionally faster velocities observed.

Seasonal variability is also present in the quantification of upcoast transport at areas within the continental shelf. Along the Upper Texas Coast, upcoast transport reaches a maximum during the summer and a minimum during the fall and winter. However, this seasonal trend is not consistent throughout the entire Texas Coastal Current. At locations on the Lower Texas Coast, upcoast transport is at maximum during the winter and at a minimum during the summer. Additionally, upcoast transport varies by location further offshore, with buoys K and N reporting maximum upcoast transport during the fall and minimum transport during the summer. Buoy V shows more upcoast transport during the spring with a minimum during the fall.

Understanding the temporal and spatial variability of the coastal current is important for monitoring the surface transport of water and associated coastal hazards, such as oil. Knowing the seasonal variability in the coastal current flow along with the current persistence and upcoast transport trends will allow stakeholders to make quick decisions when oil spills do occur. This can ultimately decrease the environmental impacts on coastal bays, estuaries, and wetlands by limiting the transport of oil from the Texas Coastal Current (Bender et al., 2007; Walpert et al., 2011).

In addition to the monitoring the transport of oil, knowing the temporal and spatial variability of the coastal current can be important for the monitoring of harmful algal blooms (HABs). These events can form along the Texas coast when downwelling conditions are favorable for bloom development. When the coastal current moves upcoast during the summer, this results in conditions that are favorable for upwelling. The downcoast flow of the coastal current during the non-summer results in downwelling favorable conditions (Hetland and Campbell, 2007). This means that knowing the onset of the seasonal reversal and the persistence of the current flow along the Texas coast is important for the prediction of HABs. This information allows managers to make better decisions, which can have impacts on environmental and human health.

Finally, numerous rivers discharge freshwater onto the Texas-Louisiana shelf, causing the Texas Coastal Current to impact the horizontal distribution of surface freshwater throughout the shelf. This, in addition to seasonal conditions present on the continental shelf, can lead to the formation of hypoxia, when coastal waters have dissolved oxygen concentrations less than 2 mg L^{-1}. Decreased wind stress results in slow currents upcoast during the summer, making water conditions conducive to hypoxia, yet faster downcoast currents during the non-summer due to increased wind stress are not favorable for hypoxia formation (DiMarco et al., 2012). Because both the transport of oil and freshwater distribution can have potentially harmful implications on coastal ecosystems, knowing the temporal and spatial variability of the Texas Coastal

Current can be vital for stakeholders in the mitigation of and preparedness for such potential hazards.

5. CONCLUSION

Significant seasonal and spatial differences in the current circulation have been observed on the Texas-Louisiana Shelf, particularly within the Texas Coastal Current. Several factors have been evaluated in order to characterize the Texas Coastal Current in two sections; the Upper Texas Coast and the Lower Texas Coast. First, the onset of the well-known wind-driven summer upcoast reversal is confirmed with a transition to a general downcoast flow in the non-summer along the Upper Texas Coast. Other reversals are present throughout the seasons, but they tend to be short-lived. Second, current velocities are found to be faster downcoast during the non-summer with a slower upcoast flow during the summer in this region. Finally, longer upcoast durations are present during the summer along with maximum upcoast transport at upper coastal locations.

On the other hand, the general circulation trend is opposite along the Lower Texas Coast. First, downcoast flow is present during the summer only at the southernmost location, while currents around the coastal bend tend to be more neutral. An upcoast flow is observed during the non-summer along the coastal bend, while the flow direction varies more at the southernmost location. Again, other reversals are present throughout the seasons in this region, but they tend to be short-lived. Second, slower current velocities are present year-round near the Texas coastal bend, with faster velocities present in the upcoast direction during the non-summer at the southernmost location. Third, longer current persistence is observed in the downcoast direction during

the summer at the southernmost location, but in the upcoast direction during the non-summer at the coastal bend. Lastly, maximum upcoast transport occurs during the winter, reaching a minimum during the summer along the Lower Texas Coast. Outside of the coastal circulation, less seasonal variability is present on the outer shelf with dominant upcoast flow present year-round due to the influence of mesoscale eddies. Overall, very few seasonal differences in the frequency of current reversals were observed regardless of location, indicating reversal numbers are not a good means of characterizing interannual variability within the Texas Coastal Current.

It has been shown that understanding both the seasonal and spatial variability present within the Texas Coastal Current is important for the monitoring and mitigation of coastal hazards. Results from this study prove that characterizing the flow of the Texas Coastal Current is not just as simple as a seasonal reversal; various other factors, such as current duration and transport, must be considered when evaluating its seasonal trends. Considering all these factors as a whole will allow stakeholders to make better decisions when potentially hazardous situations do arise along the Texas coast.

REFERENCES

Bender III, L.C., Guinasso Jr., N.L., Walpert, J.N., *et al.* (2007) Development, operation, and results from the Texas Automated Buoy System, *Gulf of Mexico Science*, 1, 33-60.

Chen, C., Reid, R.O. and Nowlin Jr., W.D. (1996) Near-inertial oscillations over the Texas-Louisiana Shelf, *J. Geophy. Res.*, 101 (C2), 3509-3024.

Cho, K., Reid, R.O. and Nowlin Jr., W.D. (1998) Objectively mapped stream function fields on the Texas-Louisiana shelf based on 32 months of moored current meter data, *J. Geophys. Res.*, 103, 10,377-10,390.

Chu, P.P., Ivanov, L.M. and Melnichenko, O.V. (2005) Fall-Winter current reversals on the Texas-Louisiana Continental Shelf, *J. Phys. Ocean.*, 902-910.

Cochrane, J.D., and Kelly, F.J. (1986) Low-frequency circulation on the Texas-Louisiana continental shelf, *J. Geophys. Res.*, 91 (C9), 10,645-10,659.

De Velasco, G.G., and Winant, C.D. (1996) Seasonal patterns of wind stress and wind stress curl over the Gulf of Mexico, *J. Geophys. Res.*, 101(C8), 18,127-18,140.

DiMarco, S.F., Jochens, A.E. and Howard, M.K. (1997) LATEX shelf data report: Current meter moorings, April 1992 to December 1994, Texas A&M University Dept. of Oceanography, College Station, TX.

DiMarco, S.F., and Reid, R.O. (1998) Characterization of the principal tidal current constituents on the Texas-Louisiana Shelf, *J. Geophys. Res.*, 103(C2), 3093-3109.

DiMarco, S.F., Strauss, J., May, N., *et al.* (2012) Texas coastal hypoxia linked to Brazos River discharge as revealed by oxygen isotopes, *Aquat. Geochem.*, 18, 159-181.

Duchon, C.E. (1979) Lanczos filtering in one and two dimensions, *J. Appl. Meteorol.*, 18(8), 1016-1022.

Emery, W.J., and Thomson, R.E. (2001) *Data Analysis Methods in Physical Oceanography*, Amsterdam: Elsevier.

Garrison, L.E.. and Martin, Jr., R.G. (1973) Geologic Structures in the Gulf of Mexico Basin, in *Geological Survey Professional Paper Volume 773*. Washington D.C., United States Government Printing Office, 1-29.

Guinasso Jr., N.L., Lee III, L.L., Yip, J *et al.* (2001) Observing and forecasting coastal currents: Texas Automated Buoy System (TABS). In Oceans 2001 MTS/IEEE Conference Committee (eds) *OCEANS 2001 MTS/IEEE Proceedings*, November 5-8 2001 Honolulu, HI. Washington, DC: The Marine Technology Society, 1318-1322.

Hetland, R.D., and Campbell, L. (2007) Convergent blooms of *Karenia brevis* along the Texas coast, *J. Geophys. Res*., 102 (C9), 1027-1049.

Jarosz, E. and Murray, S.P. (2005) Velocity and transport characteristics of the Louisiana-Texas Coastal Current, in Sturges, W. and Lugo-Fernandez, A. (eds) *Circulation in the Gulf of Mexico: Observations and Models*. Washington, DC: American Geophysical Union, 143-156.

Kelly, F.J., Guinasso, N.L., Lee III, L.L. *et al.*, (1998) Texas Automated Buoy System (TABS): A public resource. In Oceanology International Conference Committee (eds) *Oceanology International 98 Conference Proceedings*, March 10-13 1998, Brighton, UK. Surrey, UK: Oceanology International, 103-112.

Leben, R. (2005) Altimeter-derived Loop Current metrics, in Sturges, W. and Lugo-Fernandez, A. (eds) *Circulation in the Gulf of Mexico: Observations and Models*. Washington, DC: American Geophysical Union, 181-201.

Li, Y., Nowlin Jr., W.D. and Reid, R.O. (1997) Mean hydrographic fields and their interannual variability over the Texas-Louisiana continental shelf in spring, summer, and fall, *J. Geophys. Res*., 102 (C9), 1027-1049.

Li, Y., Nowlin Jr., W.D. and Reid, R.O. (1996) Spatial-scale analysis of hydrographic data over the Texas-Louisiana continental shelf, *J. Geophys. Res.*, 101 (C9), 20,595-20,605.

Liu, Y., Liang, X.S. and Weisberg, R.H. (2007) Rectification of the bias in the wavelet power spectrum, *Journal of Atmospheric and Oceanic Technology*, 24(12), 2093-2102.

Nowlin Jr., W.D., Jochens, A.E., DiMarco, S.F. *et al.* (2005) Low-frequency circulation over the Texas-Louisiana continental shelf, in Sturges, W. and Lugo-Fernandez,

A. (eds) *Circulation in the Gulf of Mexico: Observations and Models*. Washington, DC: American Geophysical Union, 219-240.

Nowlin Jr., W.D., Jochens, A.E., Reid, R.O. *et al.* (1998) *Texas-Louisiana Shelf Circulation and Transport Processes Study: Synthesis report, Volume 1: Technical report*, New Orleans, LA: U.S. Dept. of the Interior, MMS 98-0035.

Pearce, S.M. (2011) *Coastal trapped waves generated by Hurricane Andrew on the Texas-Louisiana Shelf*. Thesis, (M.S. Oceanography). Texas A&M University.

Smith, N.P. (1975) Seasonal variations in nearshore circulation in the northwestern Gulf of Mexico, *Cont. Mar. Sci.*, 19, 49-65.

Smith, N.P. (1978) Low-frequency reversals of nearshore currents in the northwestern Gulf of Mexico, *Cont. Mar. Sci.*, 21, 103-115.

Smith, N.P. (1980) Temporal and spatial variability in longshore motion along the Texas Gulf Coast, *J. Geophy. Res.*, 1531-1536.

Thompson, R.O.R.Y. (1979) Coherence significance levels, *J. Atmo. Sci.*, 36, 2020-2021.

Torrence, C., and Compo, G.P. (1998) A practical guide to wavelet analysis, *Bull. Amer. Meteor. Soc.*, 79(1), 61-78.

Vastano, A.C., and Barron Jr., C.N. (1994) Comparison of Satellite and Drifter Surface Flow Estimates in the Northwestern Gulf of Mexico, *Cont. Shelf Res.*, 14,589-14,605.

Vastano, A.C., Barron Jr., C.N. and Shaar Jr., E.W. (1995) Satellite observations of the Texas Current, *Cont. Shelf Res.*, 15(6), 729-754.

Walpert, J., Guinasso Jr., N.L., Lee, L.L. *et al.* (2011) Texas Automated Buoy System: Sustainable ocean observations to help protect the environment, in Oceans 2011 MTS/IEEE Conference Committee (eds) *OCEANS 2011 MTS/IEEE Proceedings*, September 19-22 2011, Kona, HI. Washington, DC: The Marine Technology Society, 1-7.

Wang, W., Nowlin Jr., W.D. and Reid, R.O. (1998) Analyzed Surface Meteorological Fields over the Northwestern Gulf of Mexico for 1992–94: Mean, Seasonal, and Monthly Patterns, *Mon. Wea. Rev.*, 126, 2864–2883.

Wiseman, Jr., W.J. and Kelly, F.J. (1994) Salinity variability within the Louisiana coastal current during the 1982 flood season, *Estuaries*, 17(4), 732-739.

Zhang, Z., and Hetland, R. (2012) A numerical study on convergence of along-shore flows over the Texas-Louisiana shelf, *J. Geophys. Res.*, 117 (C11